Negative Surface Ionization

and

Electron Affinity

By Mass Spectrometry

A thesis submitted for the degree of

DOCTOR OF PHILOSOPHY

by

Ghassan Mohammad Ibrahim YOUNES

of

The University of Aston in Birmingham

May 1980

SUMMARY

Negative Surface Ionization and Electron Affinity by Mass Spectrometry

Ghassan Mohammad Ibrahim Younes, Ph.D, 1980.

The negative surface ionizations of some halogens, metal hexafluorides, carbon tetrachloride, benzene and dime thyl mercury have been studied over polycrystalline platinum, tungsten and tantalum filaments by mass spectrometry.

A description is given of the construction and operation of the V. G. Micromass Q9 quadrupole mass spectrometer. A negative surface ionization source and suitable detection system has been designed.

The kinetic methods of Page were applied to the results, and from non-zero gradients of the plots of the ratio the electron to ion current E', the apparent electron affinity was evaluated. The values of E, the actual electron affinity were then calculated from Page's relationship:

$$E'(O) = E + Qr - D$$

Although this study shows that some of the ions assumed to be present in the magnetron were not observed in the quadrupole mass spectrometer, yet the electron affinity of the ions observed were found to be in good agreement with those obtained in magnetron and by optical methods.

Thus a valid estimate of the electron affinity of an observed species may be determined from the temperature coefficient of the ratio of the electron to total ion current, provided the mechanism of the rate determining process is known and the criteria of surface ionization (temperature dependence) is applied.

Key words:

Negative Surface Ionization
Electron Affinity
Electron Work Function
Negative Ions

TABLE OF CONTENTS

CHAPTER 1

Negative Ions and Electron Affinity

		Page NO.
1.1	Introduction ...	(1)
1.2	Importance of Negative Ions ...	(2)
1.3	The Determination of the Stability of Negative Ions ...	(4)
1.4	Electron Affinity, Definition ...	(4)
1.5	Electron Affinity Determinations ...	(5)
1.5.1	Theoretical Calculations ...	(5)
1.5.2	Empirical Fitting ...	(7)
1.5.2.1	The Extrapolation method of Glockler ...	(7)
1.5.3	Experimental Methods ...	(8)
1.5.3.1	Photodetachment and Radiative Attachment ...	(8)
1.5.3.1.1	The Crossed Beam Method ...	(10)
1.5.3.1.2	The Shock Tube Method ...	(14)
1.5.3.1.3	Ion Cyclotron Resonance (ICR) ...	(15)
1.5.3.2	Photoionization ...	(17)
1.5.3.3	Charge Transfer Between Neutrals and Hyper Thermal Energies ...	(17)
1.5.3.4	Charge Transfer in Ion-Molecule Collisions ...	(17)

1.5.3.5 The Polarographic Method ... (18)

1.5.3.6 The Method of Charge Transfer Complexes CT ... (20)

1.5.3.7 The Potentiometric Method ... (21)

1.6 Electron Affinities by a Variation-Perturbation Approach ... (22)

CHAPTER 2

Negative Surface Ionization

2.1 Introduction ... (24)

2.2 Saha-Langmuir Equation ... (24)

2.2.1 The Determination of Electron Affinity by the Absolute Method ... (27)

2.2.2 Determination of the Electron Affinity by the Method of Magnetic Separation of Electrons and Negative Ions ... (27)

2.2.3 Electron Affinity: Difference Method ... (28)

2.2.4 The Method of the Comparison of the Currents of Positive and Negative Ions of Two Elements (The Twofold Comparison Method) ... (29)

2.3 Methods Concerned with Direct Measurement of the Equilibrium Constant ... (30)

2.3.1 The Method of the Shift in the Volt-Ampere Characteristics ... (31)

2.4 Electron Work Function Measurement ... (35)

CHAPTER 3

The Magnetron Technique

3.1	The Statistical Theory	... (39)
3.2	The Magnetron Technique and Page	... (40)
3.3	The Kinetic Method of Page and Page's Equation	... (41)
3.4	The Mechanism of Ion Formation	... (42)
3.4.1	Type I. Direct Capture	... (43)
3.4.2	Type II. Weak Bond	... (43)
3.4.3	Type III. Strong Bond	... (44)
3.4.4	Type IV. Dissociation with Adsorption	... (45)
3.5	Temperature Correction of Experimental Electron Affinity to $0^{o}K$	... (47)
3.6	A Critique of the Surface Ionization Systems for the Determination of the Electron Affinity of Atoms, Molecules and Radicals	... (49)
3.6.1	Temperature Dependance of the Pre-exponential Function	... (49)
3.6.2	Surface Ionization and Thermal Equilibrium	... (49)
3.6.3	Subsidiary Process and Surface Ionization	... (50)
3.6.4	The Attainment of Equilibrium at the Surface	... (50)
3.6.5	The Indirect Identification of the Charge Carriers in the Magnetron	... (51)

CHAPTER 4

The Quadrupole Mass Filter System

4.1	Introduction	... (52)
4.2	The Source System	... (57)
4.2.1	The Ion Source	... (57)
4.2.2	Temperature Measurement	... (60)
4.3	The Mass Filter System	... (69)
4.3.1	The Detector System	... (71)
4.4	The Vacuum System	... (72)
4.5	The Sample Introduction System	... (75)
4.6	Negative-Ion Mass Spectrometry	... (77)
4.6.1	Introduction	... (77)
4.6.2	Modes of Negative Ion Formation	... (77)

CHAPTER 5

Electron Work Function Measurement

5.1	Introduction	... (90)
5.2	The Apparent Electron Work Function	... (91)
5.3	Experimental	... (93)
5.3.1	Platinum Filaments	... (94)
5.3.2	Tantalum Filaments	... (98)
5.3.3	Tungsten Filaments	... (98)
5.4	Measurement of Apparent Electron Affinity (Calculation of $E^{-}(T)$)	... (104)
5.4.1	Method of Page and Goode	... (104)
5.4.2	Method of Gaines and Page	... (107)

5.5 Transmission of Electrons through the Mass Filter ... (107)
5.6 Electron Affinity of CCl_4 ... (111)
5.6.1 Composite Spectra ... (114)
5.7 Surface Ionization of Iodine and Bromine ... (115)
5.7.1 Introduction ... (115)
5.7.2 Electron Affinity of Iodine ... (115)
5.7.3 Electron Affinity of Bromine ... (118)
5.8 Electron Affinity Determination ... (120)
5.8.1 Introduction ... (120)
5.8.2 Carbon Tetrachloride CCl_4 ... (122)
5.8.3 Sulphur Hexafluoride SF_6 ... (129)
5.8.4 Uranium Hexafluoride UF_6 ... (131)
5.8.5 Molybdenum Hexafluoride MoF_6 ... (134)
5.8.6 Dimethyl Mercury $Hg(CH_3)_2$ ... (134)
5.8.7 Benzene C_6H_6 ... (135)
5.9 General Discussion ... (140)
5.10 Conclusion ... (143)

List of Figures vi
List of Plates ix
List of Tables ix
Summary a
Declaration x
Acknowledgements xi

LIST OF FIGURES

Figure No.			Page
1.1	Vertical and Thermodynamic Electron Affinities	...	(6)
1.2	Level Diagram of Au and Au^-	...	(12)
1.3	Photodetachment of Au^-	...	(12)
4.2	The Negative Surface Ionization Source	...	(58)
4.3	Details of the Filament Assembly	...	(59)
4.4	Negative Surface Ionization Accelerating Voltage	...	(61)
4.5	Transmission of Electrons through Quadrupole Rods	...	(62)
4.6	Emissivity and Absorption Temperature Correction for Tantalum Ta	...	(64)
4.7	Emissivity and Absorption Temperature Correction for Platinum Pt	...	(65)
4.8	Emissivity and Absorption Temperature Correction for Tungsten W	...	(66)
4.9	Filament Current as a Function of T^2 (Tungsten)	...	(68)
4.10	RF/DC Voltages Applied to Filter Rods	...	(70)
4.11	The Vacuum System Arrangement	...	(73)
4.12	The Sampling System	...	(76)
4.13	Potential Energy Curve Showing Formation of Negative Ion from a diatomic Molecule by Resonance Capture	...	(80/81)

4.14	Potential Energy Curves Showing the Formation of a Negative Ion from a Diatomic Molecule by Dissociative Resonance Capture	...	(82/83)
4.15	Potential Energy curves Showing the Formation of a Negative Ion from a Diatomic Molecule by Ion-Pair Production	...	(84)
4.16	Positive and Negative Ion Spectra of Copper Hexafluoroacetylacetonate	...	(89)
5.1	True Temperature and Brightness Temperature (Ta)	...	(95)
5.2	Filament Current as a Function of Temperature	...	(96)
5.3	Filament Current as a Function of T^2	...	(97)
5.4	Electron Work Function of "Clean" Platinum	...	(99)
5.5	Electron Work Function of Platinum in the Presence of Sample Gas	...	(100)
5.6	Electron Work Function of Tantalum	...	(101)
5.7	Electron Work Function of Tantalum Carbide	...	(102)
5.8	Electron Work Function of Tungsten	...	(103)
5.9	Electron Work Function of Tungsten Carbide	...	(105)
5.10	Constancy of Transmission Efficiency	...	(109)
5.11	Transmission Characteristic Plot	...	(110)
5.12	Ion Accelerating Potential	...	(113)

5.13	Composite Spectra Cl_2	...	(116)
5.14	Composite Spectra CH_4	...	(117)
5.15	Log j_e/j_i Against Reciprocal Temperature for I^-	...	(119)
5.16	Log j_e/j_i Against Reciprocal Temperature for Br^-	...	(121)
5.17	The Variation of Ionic and Electronic Current with Temperature	...	(124)
5.18a	Variation of Ionic Current With Temperature (Cl^-)	...	(125)
5.18b	Typical Spectrum obtained at Constant Temperature	...	(126)
5.19	Ionic Current/Electronic Current Against Heating Current	...	(127)
5.20	Log j_e/j_i Against Reciprocal Temperature	...	(128)
5.21	Ratio $j_e/j_i = f(T)$ for Ionization of SF_6	...	(130)
5.22	Ratio $j_e/j_i = f(T)$ for Ionization of UF_6	...	(132)
5.23	Log j_e/j_i Against Reciprocal Temperature for UF_6	...	(133)
5.24	Mass Scan of Benzene in the Negative Ion Mode Obtained by Joyce	...	(137)
5.25	Negative Surface Ionization of Benzene at 1.8×10^{-4} torr	...	(138)
5.26	Positive Ion Mass Spectra of Benzene	...	(141)

LIST OF TABLES

Table No.			Page
1.1	Comparison of Calculated and Observed Electron Affinities	...	(23)
2.1	Electron Affinity Determination Based on the Saha-Langmuir Equation	...	(33)
3.1	Electron Affinities by the Space-Charge and Magnetron Technique	...	(46)
5.1	Practical Electron Work Function	...	(106)

LIST OF PLATES

Plate No.			Page
4.1a	The General Layout of the Mass Spectrometer (rear view)	...	(54)
4.1(1b)	The General Layout of the Mass Spectrometer (front view)	...	(55)
4.1(b2)	The General Layout of the Mass Spectrometer (front view)	...	(56)

Preface

This thesis, which is being submitted for the degree of Doctor of Philosophy in the University of Aston in Birmingham, is an account of the work done under the supervision of Professor F M Page, B.A., Ph.D., Sc.D in the Department of Chemistry of the University of Aston in Birmingham from October 1976 to May 1980. Except where references are given in the text, the work described herein is original and has not been nor is being submitted for a degree at any other university.

Gh. M. I. Younes

May 1980

ACKNOWLEDGEMENT

I wish to express my gratitude to Professor F M Page for his guidance and encouragement during the last four years. I should also like to thank my accomplices, Gordon Pool, Gary Boxley, Peter Bott and Muneer Morsy for many helpful discussions and suggestions.

Last, but by no means least, I should like to thank Jenny for typing this thesis.

"I often say that if you can measure that of which you speak, and can express it by a number, you know something of your subject; but if you cannot measure it, your knowledge is meagre and unsatisfactory."

Lord Kelvin

To my Parents

and my Brother Bassam.

CHAPTER 1

Negative Ions and Electron Affinity

1.1 Introduction

Chemistry involves a systematic study of the substances of the universe, of their properties and their reactions with each other to form new substances with different properties, and of the conditions governing their reactions.

It is also concerned with condensing the acquired information into a series of precise generalisation called laws.

So in the scientific approach to matter, the chemists role is to describe and understand nature at the molecular level, that is to say is primarily concerned with the study of the properties of the outermost electrons of atoms and molecules. It is well known that bonds are usually formed by sharing of these electrons, and ions are produced when their number in a given system is increased or decreased. It is of a fundamental importance to have a knowledge of their binding energy in any chemical investigation. Nowadays there are several methods of measuring the binding energy of the outermost electrons in neutral atoms or molecules, most of these methods are well established[1], and compilation of such data are available in most chemistry text books[2,3].

The reverse is true for the corresponding electron in negative ions, and this lack of general reference accurately reflects the paucity of the quantitative experimental data.

The stability of a negative ion is usually given in terms of the electron affinity of the parent molecule. This is defined as the work done in bringing an electron up to the molecule from infinity and adding it to the lowest vacant orbital of the isolated gas molecule.

1.2 Importance of Negative Ions

An understanding of the stability of negative ions is most important in many fields of research, particularly in flame chemistry[4], due mainly to the interest in rocket propulsion and magneto hydrodynamic generation.

In rocket propulsion a problem arises in the control of the rocket due to attenuation of the electro-magnetic signals by the electrons in the rocket flame.

An electromagnetic wave, in passing through a partially ionized medium, excites the ions into sympathetic oscillation. The ions rapidly lose the directed momentum thus acquired at subsequent collisions with gas molecules, so that the energy of the wave is degraded into thermal energy of the gas.

The attenuation may easily be controlled if the electrons are removed, which is done by introducing species into the flame that readily capture electrons, that is with high electron affinities.

The inverse of this problem occurs in magnetohydrodynamic generators, where electricity is generated directly from a high velocity flame between the poles of a magnet.

Since the flame is here equivalent to the armature of a dynamo, and the electrical energy of the output is obtained at the expense of the thermal and kinetic energy of the flame gases, it is of vital importance that the conductivity of the flame be high, which implies a high concentration of free electrons.

Heavy negative ions are undesirable parasites here, and knowledge of the stabilities of those negative ions which can be formed from the flame gases or from impurities is required, properly to assess the performance of an M.H.D. generator.

Physicists have been interested in the properties and composition of the ionized layers in the upper atmosphere. Massey[5] drew

attention to the absorption of light by the hydrogen negative ions in the solar photosphere, thus determining the spectral distribution in the visible region. Berkowitz et al[6] emphasized the need for a better knowledge of the electron affinities of the atmospheric gases to help establish the reaction sequence in the D and E layers of the ionosphere, and hence the electron concentrations that determines radio transmission.

Lovelock et al[7] raised the question of the likely link between the ability of certain materials to capture electrons and their high biological activity.

Mulliken[8] defined electronegativity as the average of the first ionization energy and electron affinity of an atom ($\frac{1}{2}(I + E)$), hence it is very important to know the electron affinity in order to measure the strengths of chemical bonds.

Christophorou[9] reported the importance of the interaction of ionizing radiation with living tissue to form negative ions. Briegleb[10] asserted the necessity of accurate electron affinity in the discussion of ionic-covalent resonance.

Lange[11] and Hedges et al[12] demonstrated the importance of the knowledge of the stabilities of negatively charged species produced in the study of electro-chemical reactions both at ordinary and highly polarised electrodes, such as in the polarograph.

Page and Goode[4] discussed the importance of an understanding of the stability of negative ions in chemistry with reference to three principal fields; reaction mechanisms, electrode processes, and solvation.

For example: Surface catalysed rearrangement of hydrocarbons is thought to involve the intermediate formation of negative ions where the relative ease of transfer of an electron to and from a surface favours ionic reactions generally.

A recent article[13] has presented evidence that the free negative ions in the air (about 20 ions per cm^3) have a profound psychological effect upon human beings. A reduction in the level of negative ion concentration in the air has been related to the alertness of human subjects who breathe it.

The implications of this discovery are wide ranging and further work is proceeding in this area of research.

1.3 The Determination of the Stability of Negative Ions

A measure of the stability of a negative ion A^- is given by the quantity known as the electron affinity of the parent molecule, radical or atom A, which is defined to be

$$E(A) = E_0 - E_-$$

where E_0 and E_- are the energies of the ground states of the molecule, radical or atom and the negative ion, respectively. For a stable negative ion the electron affinity must be positive.

1.4 Electron Affinity, Definition.

It is customary to define adiabatic electron affinity, E, of a species as the difference in the energies of the ground states of the gaseous neutral species and its negative ions.

As the energy of a diatomic molecule and its ion depend on its internuclear distance, it is necessary to differentiate between two types of electron affinity; a thermodynamic electron affinity and vertical ionization energy.

The difference of the energies of the molecule and molecular ion at their equilibrium positions is the thermodynamic or adiabatic electron affinity.

The vertical processes, one of electron attachment and the other of electron detachment, occur with no change in intermolecul distance.

The vertical electron affinity of a molecule AB is the energy

given up in the process of attaching a zero-energy electron to the molecule when at its equilib rium nuclear separation.

The vertical detachment energy of AB^- is the minimum energy required to remove an electron from AB^- when at its equilibrium nuclear separation. Fig. (1.1).

The earliest attempts to evaluate electron affinities followed the development of the Born-Haber[14,15] cycle, and were confined to a refinement of the calculation of lattice energies on which this cycle is based.

Some of the values obtained by the more accurate photodetachment studies[16,17], especially those carried out by Cubicciotti[18], who using the best available data for the dissociation energy, heat of sublimation and ionization energy gave the values of the electron affinities for F, Cl, Br and I as 3.45 ev, 3.62 ev, 3.49 ev and 3.19 ev respectively.

1.5 Electron Affinity Determinations

There are several methods to determine the electron affinity, these could be classified into the following:

1. Theoretical Calculations
2. Empirical Fitting
3. Experiment

1.5.1 Theoretical Calculations

These theoretical calculations are based on the quantum mechanical approach to estimate the electron affinity, two types of calculation could be distinguished.

(1) The variational method of Pekeri s[19]

(2) Hartree-Fock self consistent field calculation

The first method was applied to hydrogen to give a value E(H) of 0.75421 ev, thought to be several orders of magnitude more accurate

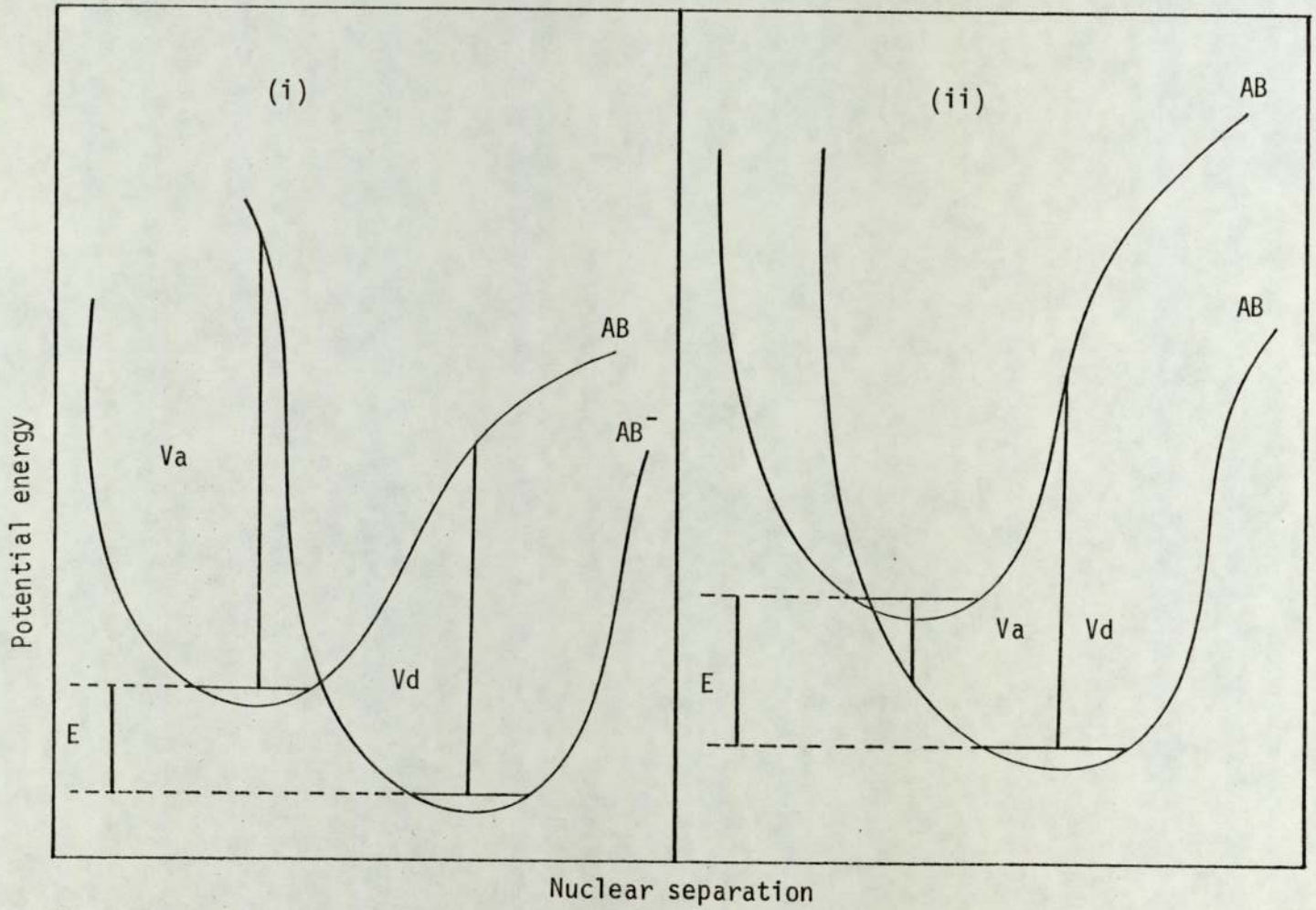

Figure (1.1) Va Vertical electron affinity -ve in (i), +ve in (ii)
Vd vertical detachment energy -ve in (i) and (ii)
E thermodynamic electron affinity, +re in (i) and (ii)

than any a priori electron affinity. However this approach is not applicable to heavier ions.

Hartree-Fock calculations which make allowances for electron correlation and relativistic effects have proved satisfactory.

Clementi and Mclean[20] and Clementi[21] et al have used isoelectronic extrapolation and experimental affinities in estimating correlations for their Hartree-Fock calculations.

Recent work by Weiss[22,23] Sinanoglu and Oksuz[24,25] and Schaefer et al[26,27] have refined the corrections still further.

Although the electron affinity values of most atoms and molecules are so small (less than 4 ev) that their accurate calculations is difficult, most of the recently enlarged table of affinities is due to the stimulus of theoretical methods.

Cade[28,29] has calculated E for a number of diatomic molecules. His value E(OH) = 1.91 ev compares favourably with Branscomb E(OH) = 1.83 ev.

1.5.2 Empirical Fitting

A variety of empirical approaches have been used to estimate the electron affinity because of the difficulties encountered in the theoretical calculations and experiments.

1.5.2.1 The extrapolation method of Glockler[30]

Glockler (1934) proposed the ionization energy relationship

$$E(Z) = I(Z_-) = 3I(Z_0) - 3I(Z_1) + I(Z_2) \ldots \qquad (1.1)$$

where I is the ionization energy of each member of the series and Z_0, Z_1, Z_2 are the atomic numbers of the neutral atom and the singly and doubly charged positive ions of the isoelectronic sequence.

So equation (1.1) provides the ionization or electron affinity of nitrogen in the isoelectronic series N^-, O, F^+, Ne^{++}. Empirical

constants a, b and c were used to calculate the appropriate ionization energies through an equation of the type

$$I(Z) = a + bZ + cZ^2 \ldots \quad (1.2)$$

where Z is the nuclear charge.

Johnson and Rohrlich[31], Edlen[32] and Kaufman[33] developed the equation of Glockler using more elaborate series forms with negative powers of ionic charge.

Comparisons with experimental results shows that the Glockler formula works very well for atomic hydrogen and it does not work well for other atomic ions. In general the stabilities of molecular ions are of greatest interest, hence many experimental techniques have been developed to measure this quantity.

The majority of experimental methods fall into one of the three main groups:

(1) Determination of the energy threshold for destruction of the ion

(2) Determination of the energy threshold for formation of the ion

(3) The study of the equilibrium between atoms, electrons and negative ions.

1.5.3.1 Photo detachment and Radiative Attachment

Despite considerable interest in recent years in determining electron affinities, few reliable values have been measured experimentally.

Accurate data (accurate within 10-20 meV) are available only for about a dozen atoms, including the halogens, H, C, O, S, Se[34a], Recently Hotop and Lineberger[34b] have reported the precise determination of the electron affinities of Au and Pt in a dye laser photodetachment experiment.

So the development of optical methods for the study of photodetachment has lead to the measurement of several precise and unambiguous electron affinity values. Typical of photodetachment studies are those of Branscomb and co.-workers[35], where the determination of the limiting frequency, at which the incident light falling upon a beam of ions is sufficiently energetic to cause detachment of an electron, allows the activation energy of the detachment process to be evaluated.

This method,being spectroscopic, is capable of extreme accuracy.

The detachment of an electron from a gaseous negative ion, A^-, may be caused by a photon of absorbed energy

$$A^- + h\nu = A + e^-$$

The reverse of this process, radiative attachment, may be an important mechanism in forming negative ions in arc and shock-heated gases.

The measured photodetachment threshold corresponds to a vertical detachment energy, which for atomic systems is exactly equal to electron affinity.

On the other hand, for a molecular species the adiabatic electron affinity of the neutral will be the same as the vertical detachment energy of the negative ion only when the equilibrium geometries of the neutral and ion are identical.

In any case, the vertical detachment energy provides an upper limit for the molecular electron affinity provided that the negative ion is initially in its ground electronic and vibrational state.

There are three principal techniques for exploiting this concept

(i) Crossed Beams

(ii) The Shock-Tube

(iii) Ion Cyclotron Resonance (ICR)

1.5.3.1.1 The Crossed Beam Method

In this crossed beam method, a mass selected beam of negative ions formed in an arc discharge intersects a perpendicular beam of light whose frequency is selected by means of a high intensity monochromator. More recently, the light beam has been produced by a tunable dye laser based on the dye Rhodamine B [36] with a band width of about 1A°.

It is necessary to measure the ion and electron currents as functions of the light energy, and, in addition, to monitor the light intensity with a thermopile.

Kuyatt and Simpson[37] used a beta-spectrometer to measure the energies of the detached electrons.

The energy of photodetachment may be readily deduced from these electron energies and the corresponding electron currents.

Both the photon energy and the electron energy systems of analysis are complementary.

The requirements for crossed beams, then, are a suitable ion source for negative ions (from a discharge constricted electrically and / or magnetically), an intense stable light source and suitable detection techniques.

To distinguish electrons formed by collisional processes from photodetachment electrons, it is necessary to employ a chopped beam with phase-sensitive detection devices.

To obtain an experimental photodetachment threshold using photon energy analysis one must plot experimental cross section (either absolute or relative) against photon energy and extrapolate the curve to zero cross section (either absolute or relative).

The cross section probability that a photon has detached an

electron is related to the other parameters by the expression

$$J_e = KJ_i \left(1/h\nu \right) \sigma(1/V_i) \ldots \quad (1.3)$$

where K is a geometrical constant, J_e and J_i the electron and ion currents respectively.

I is the intensity of the light or $1/h\nu$ the photon flux, σ is the photodetachment cross section, and V_i is the ion speed in the reaction chamber.

While theoretical cross sections have been developed it is easier to extrapolate an experimental curve to determine the threshold energy.

Wigner[38] suggested that in the case of atoms, photodetachment cross section σ_D will go as $K^{2\ell + 1}$, where K is proportional to the square root of the energy above threshold and ℓ is the angular momentum of the electron in its final free state.

O'Malley[39], derived the relationship

$$\sigma_D \propto (E_i - E_{thresh})^{\ell + \frac{1}{2}} \ldots \quad (1.4)$$

where E_i and E_{thresh} are, respectively, the energies of the incident light near threshold and at threshold.

This has included the long range forces between the atom and electron. When the electron is photodetached, the selection rule, $\Delta\ell = \pm 1$, applies. On the loss of a p electron from an atom as a free s electron (l=0), equation (1.4) becomes

$$\sigma_\Delta \propto (E_i - E_{thresh})^{\frac{1}{2}}$$

and this predicts an infinite slope at threshold.

The photodetachment of Au^- [43] would be a typical example; Fig. (1.2) shows the level diagrams of Au and Au^-, Au has a $5d^{10} 6S^2\ S_{1/2}$ ground state, the first excited state being more than 1 ev above and not accessible in the photon energy range of the described

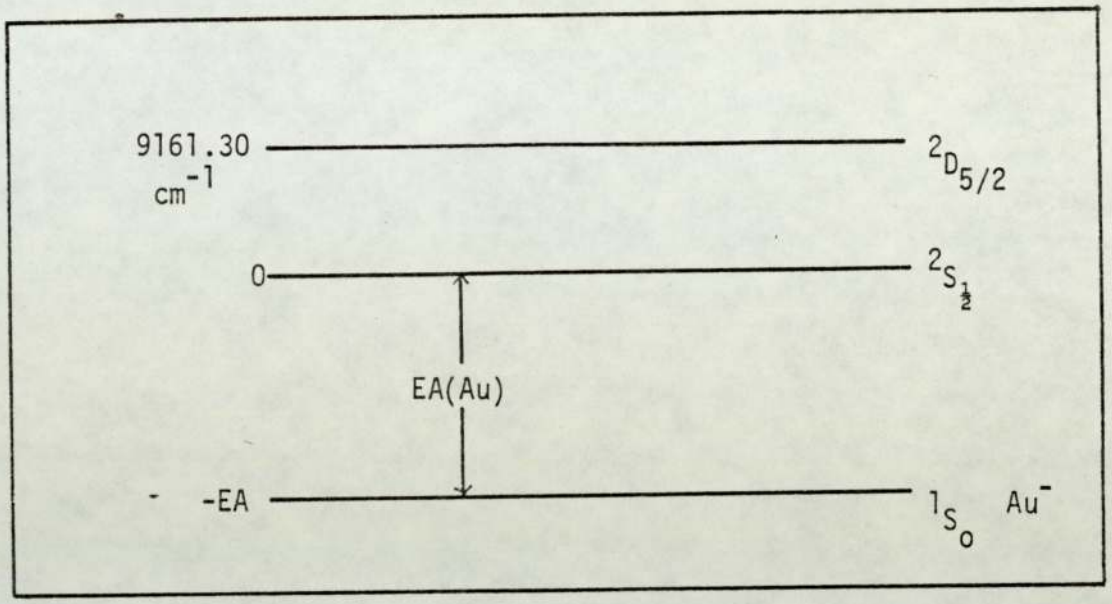

Figure (1.2) Level diagram of Au and Au^-

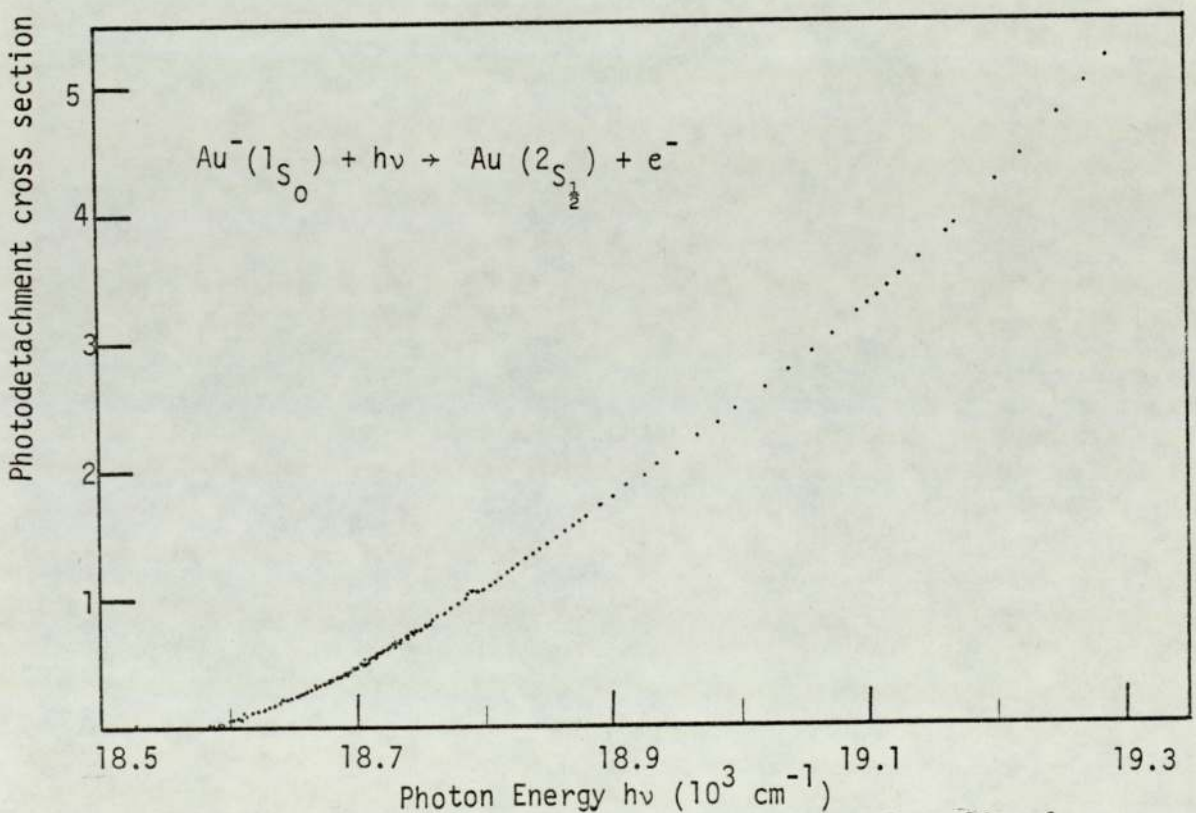

Figure (1.3) Absolute cross section in units of 10^{-18} cm^2 for photodetachment of Au^- in the photon energy range 18500 -19500 cm^{-1} (eV = 8065.466 cm^{-1})

experiment.

The ground state of Au^- should be $5d^{10}\ 6S^1\ ^1S$ with no other stable negative ion state being likely.

In a measurement of the photodetachment cross section, which, near threshold E_{Thresh}, will exhibit the p-wave behaviour

Since an S electron is detached, the first onset will correspond to $Au^-(1S_0) \longrightarrow Au\ (^2S_{1/2})$ or electron affinity transitions. Fig. (1.3) shows the threshold behaviour of Au^- during photodetachment.

There is zero apparent cross section below 18620 cm^{-1} (2.3086 eV); above that energy one finds a cross section behaviour compatible with Wigner's law for p-wave electrons $\sigma \propto K^3$.

Geltman[40] showed that cross section behaviour for photodetachment from negative diatomic ions was dependent on molecular symmetry, for which he derived the expression

$$\sigma = \nu K^m (1 + a_1 K^2 + a_2 K^4 + \ldots) \qquad \ldots \qquad (1.5)$$

where ν is the photon frequency, K is proportional to the square root of energy above threshold and m is a threshold exponent.

The value of m depends on the electrons axial angular momentum quantum number, λ_0, on whether the diatomic molecule is heteronuclear or homonuclear, and, if it is the latter, on the U, g symme try of the orbital from which the electron is detached.

For non-linear polyatomic ions, the absence of symmetry precludes the description of molecular orbitals in terms of integral orbital angular momentum quantum numbers, and a theoretical treatment of cross section behaviour at threshold has not been put forward.

Berry[41] reviews the position with respect to multiple threshold energy determination in some photodetachment experiments due to the fact that a neutral atom can have more than one bound state.

He remarks that while virtually all negative ions have only one bound electronic state some may have two or more states, e.g. C^- ions.

There may be many excited rotational and vibrational levels in molecular negative ions, depending on whether the extra electron is bonding or non bonding.

The problem of extracting E, the adiabatic electron affinity, from molecular photodetachment data is difficult because E may differ from V_d, the vertical detachment energy and because the populations of vibrational and rotational states may not be known.

1.5.3.1.2 The Shock Tube Method

Direct spectroscopic observation is characteristic of the shock tube technique.

To observe photodetachment in the form of an absorption spectrum it is necessary to have the alkali halide vapour at about 3000 K^o in a concentration of about 10^{16} dissociated molecules/cm^3 in a cell 10-50 cm long. A heat bath of shock-heated argon is sufficient to vaporize the salt, and a flash lamp will serve as the absorption source, the spectra being recorded photographically. The spectra are taken in emission with O^-, which, because of its smaller equilibrium concentration, must be subjected to higher temperatures ($\simeq 4000^oK$).

Alkali oxides are used as the source of oxygen and electrons. Berry[42] et al discusses the two photodetachment thresholds obtained in the case of Cl^- from a plot based on the Beer's law expression in terms of the photodetachment cross section $\sigma_{det}(\nu)$, the incident

and transmitted intensities $I_o(\nu)$ and $I(\nu)$, the path length ℓ(cm) and $n(x^-)$, the concentration of absorbers, x^- ions per cm^3

$$\ell n \ I_o(\nu)/I(\nu) = \sigma_{det}(\nu) n(x^-)\ell \ldots \quad (1.6)$$

The threshold are identified with $^2p_{\frac{1}{2}}$ and $^2p_{3/2}$ states of Cl^o.

Berry et al identified the three thresholds ob served in the emission spectrum during the radiative capture of electrons by oxygen atoms to correspond to the reactions:

$$O^o(^3p_2) + e^- \rightarrow O^-(^2p_{\frac{1}{2}}) \ldots \quad (1.7)$$

$$O^o(^3p_2) + e^- \rightarrow O^-(^2p_{3/2}) \ldots \quad (1.8)$$

$$O^o(^3p_1) + e^- \rightarrow O^-(^2p_{3/2}) \ldots \quad (1.9$$

processes (1.8) gave the most intense spectrum and corresponds to the electron affinity transition.

From this, E(0) = 1.478 ± 0.002 eV. This compares favourably with the value due to Branscomb[35] of 1.465 ± 0.005 eV. The advantages of these techniques are the spectroscopic precision available and the freedom from interaction with other systems.

On the other hand, because of lack of definition of the spectral states at times, it is necessary to confirm the transitions by other experiments or by theory.

Relatively few photodetachment experiments have been done because of their experimental complexity.

1.5.3.1.3 Ion Cyclotron Resonance (ICR)

Another photodetachment technique involves direct spectroscopic observation, either of the absorption spectrum of the negative ions or of the emission spectrum arising from radiative attachment.

Recently[43] ion cyclotron resonance (ICR) spectroscopy has

been used with conventional light sources as well as with the tunable dye laser to perform photodetachment experiments.

This technique may be classified as a third method for studying photodetachment, since it differs distinctly from the two approaches described above.

Negative ions generated by an electron beam in the resonance cell are allowed to drift slowly by means of crossed magnetic and electric dc fields.

The negative ion concentration is monitored as a function of the frequency of light which is directed into the cell.

Thus direct confirmation of the detachment process is provided.

This technique offers a number of unique advantages:

(1) conventional means of mass selection are not needed, since ICR spectrometer allows observation of any given ion under appropriate conditions.

(2) Since the negative ions are moving at low velocity, collisional detachment does not occur and the ions can be trapped efficiently for long periods of time.

(3) High negative ion densities or fluxes are not needed, and a wide variety of negative ions can be generated by dissociative electron capture.

(4) By monitoring the negative ion concentration, the detection efficiency for observing photodetachment exhibits no angular or wavelength dependence, whereas detection efficiency can be a problem in monitoring detached electrons.

1.5.3.2 Photoionization [44]

By measuring the threshold photon energy, $h\nu$, in the resonant process

$$AB + h\nu = A^+ + B^-$$

Estimating the kinetic energy (K.E), of the ions from the efficiency function, and knowing the bond dissociation energy, D(AB), the ionization potential of A, I(A), the electron affinity of B,E(B), in the diatomic molecule AB is determined from expression

$$h\nu = D(AB) + I(A) - E(B) + K.E$$

Accurate determination of electron affinity was possible by this process, for example,the value obtained for hydrogen E(H) = 0.754 ± 0.002 eV[45] is in a good agreement with the variational value of Pekeris[19] E(H) = 0.75421 eV.

1.5.3.3 Charge Transfer Between Neutrals at Hyper Thermal Energies [46,47]

From studies of colliding beams of alkali metal atoms and molecules, values of molecular electron affinity have been deduced through measurements of threshold for the formation of positive and negative ion pairs.

This technique has contributed considerably to a knowledge of molecular electron affinity.

There is a good agreement between electron affinities determined by this technique and other techniques, especially for the halogens and oxygen.

1.5.3.4 Charge Transfer in Ion-Molecule Collisions

This method was used by Chupka et al[48] to determine the electron affinity of each of the halogen molecules.

The atomic halogen negative ions were prepared through ion formation by photon absorption at threshold wavelengths with room temperature thermal energies , for example

$$X_2 + h\nu = X^- + X^+$$

The X^- ions are accelerated to undergo endoergic reactions with the halogen molecule Y_2 to produce Y_2^- and XY^-

$$X^- + Y_2 = X + Y_2^-$$

$$X^- + Y_2 = XY^- + Y$$

By measuring energy thresholds, $E_{threshold}$, for the reaction the electron affinity of Y_2 and possibly XY^- may be determined from the relationships

$$E(Y_2) = E(X) - E_{threshold} \cdots \quad (1.10)$$

The method yields results in fair agreement with those derived from some other methods.

1.5.3.5 The Polarographic Method

The reversible one-electron reduction of the acceptor A is determined by the following process:

$$A_{solv} + e = A^-_{solv}$$

The half-wave potential is given by the expression[49]

$$E_{\frac{1}{2}} = E_o - \frac{RT}{F} \ln \frac{D1}{D_2} \ldots \quad (1.11)$$

Where E_o is the formal or standard potential, R the gas constant, F the Faraday, and D1 and D_2 are the diffusion coefficients of the oxidised and reduced forms in the layer near the electrode.

E_o is determined by the energetic characteristics of many processes[50], including the electron affinity of the acceptor

$$E.A = E_{1/2} - \Delta E_{solv} - 5.07 + \frac{RT}{F} \ell n\, D_1/D_2 \ldots. \qquad (1.12)$$

where ΔE_{solv} is the difference between the solution energies of $A^{\cdot-}$ and A.

Since the diffusion coefficients D_1 and D_2 cannot differ by more than 1-2 orders of magnitude, the last term of this equation is negligibly small and can be neglected.

Consequently the relation between the electron affinity in the gas phase and the half-wave potential of the reversible one-electron reduction is given by the equation

$$EA = E_{\frac{1}{2}} - \Delta E_{solv} + 5.07\ (eV) \ldots. \qquad (1.13)$$

Since the solvation energies of neutral molecules are small, the quantity ΔE_{solv} is determined mainly by the solvation energy of the corresponding radical-anion, i.e. $\Delta E_{solv} \simeq EA$. The study of the radical-anions of aromatic hydrocarbons[51], and of other electron acceptors[50] has shown that the solvation energies of radical-anions do not vary significantly with the structure of the delocalised radical-ion.

The following equation was used with an adequate degree of approximation to calculate the electron affinities of acceptors forming delocalised radical - ions

$$EA \simeq E_{\frac{1}{2}} + C$$

$$EA \simeq E_{\frac{1}{2}}$$

where C is a constant and $E_{\frac{1}{2}}$ the half-wave potential for polarographic reduction under the same condition.

1.5.3.6 The Method of Charge-Transfer Complexes CT

It is based on the determination of the charge-transfer (CT) energy for complexes of a series of donors with the electron acceptor investigated[50].

The CTC energy is usually determined from the CT band maximum. According to Mulliken's theory[52] the CT energy for a weak interaction between the donor and the acceptor can be expressed by the following equation:

$$h\nu_{CT} = IP - EA + G_o - C + x_1 + x_o \ldots. \qquad (1.14)$$

where G_o is the energy of all types of interactions between the donor and the acceptor in the ground CTC state, , with the exception of the donor-acceptor interaction, C is the energy of the coloumbic interaction between the components in the excited CTC state, and x_o and x_1 are the energies of the resonance interaction between ψ (D,A) and ψ $(D^{+}.,A^{-}.)$ in the ground and excited CTC states. Using the expressions for x_o and x_1, it is possible to obtain the following equation:

$$h\nu_{CT} = IP - EA - C - G_o + \frac{B_o^2 + B_1^2}{IP - EA - C - G_o} \ldots. \qquad (1.15)$$

where $B_o = H_o + S_{o1}W_o$ and $B_1 = H_{o1} - S_{o1}W_1$

After simplification we obtain[53]

$$h\nu_{CT} = IP - EA + E + \frac{Cl}{IP - (EA + E)} \ldots \qquad (1.16)$$

For small values of Cl and fairly high-ionisation potentials, this equation acquires an even simpler form, which is frequently used in investigations:

$$h\nu_{CT} = IP - EA - W$$

where W is an approximately constant quantity for the given class of CTC.

In principle eqn (1.16) can be used directly to calculate the

electron affinities of acceptors, provided that W is known. Since its exact value is not known, one usually starts with Eqn.(1.16) obtaining in this way the following expression for complexes of a common donor with a series

$$h\nu_{CT}^{X} - h\nu_{CT}^{O} = EA^{O} - EA^{X} + W^{O} - W^{X} \ldots \quad (1.17)$$

where EA^{O} and EA^{X} are the electron affinities of the reference acceptor and the test acceptor respectively.

1.5.3.7 The Potentiometric Method[54]

The method is based on the measurement of the potential arising in the A/A^{-} redox system. A modified method, resembling potentiometric titration, has found the most extensive applications. Measurements are made of the potential between two platinum electrodes, one of which is immersed in a standard redox system A_o/A_o^{-} and the other in a solution containing the test redox system A_x/A_x^{-}.

The redox sytem investigated is obtained from the titration curve. According to Jaguar - Crodzinski et al[55], it is given by the expression

$$\varepsilon = \varepsilon_o + 0.03 \ln (KA_o/KA_x) + 0.03 \ln \frac{(A_x, K^+)_t}{(A_o, K^+)_t} \ldots \quad (1.18)$$

when ε_o is the standard potential of the reaction

$A_o^{-} + A_x = A_x^{-} + A_o$, KA_o and KA_x are the dissociation constants of the corresponding ion pairs, and $(A^{-}, K^+)_t$ is the sum of (A_o^{-}, K^+) and $A_x^{-}, K^+)$.

The standard potential ε_o is equal to the difference between the electron affinities of A_x and A_o i.e. the method yields the relative electron affinities.

There are many other methods for electron affinity determinations.

(1) Dissociative electron attachment to form x and y^- from collisions of electrons with the molecule xy.

(2) Field detachment

(3) Thermal electron capture

(4) Surface Ionization: Typical of third group studies of equilibrium in flames and at heated metal surface, the energy changes involved are computed either from the temperature dependence of the equilibrium constant (second law methods) or by the methods of statistical mechanics (third law methods). Because of the importance of surface ionization method in electron affinity determination, the next chapter is devoted to this method.

1.6 Electron affinities by a variation-perturbation approach[56]

A simple variation-perturbation method recently developed was applied to the calculation of electron affinities.

In this method a common basis was used for both the ion and the neutral system.

This method has been applied to calculate the EA's of the atoms Li, Na, F and Cl and of the molecule OH. For Li, Na and Cl the errors in the computed EA's were about 0.04 eV and for the other systems about 0.2 - 0.3 eV. The values obtained by this method are listed in the following table.

Table 1.1

Comparison of calculated and observed electron affinities

System	EA calculated eV	EA observed eV
Li	0.577	0.620[57]
Na	0.578	0.548[58]
F	3.68	3.448[17]
Cl	3.66	3.613[17]
OH	2.07	1.825[59]

CHAPTER 2

Negative Surface Ionization

2.1 Introduction

Neutral species adsorbed on an incandescent metal surface may evaporate partly as neutrals and partly as ions. This phenomenon, first discovered by Kingdon and Langmuir[60], has been called surface ionization.

This phenomenon received a great interest by Scientists and research workers because of its important application in various instruments and techniques, such as mass spectrometers, ion sources and neutral particle detectors, ion engines and the thermo electric conversion of thermal energy into electrical energy. Nowadays the study and use of surface ionization is quite widespread. Its applications in physicochemical investigation are enormous, for example:

1 - Determination of the first ionization potentials of atoms and molecules.
2 - Determination of the electron affinity of atoms and radicals (which is our main concern in this thesis).
3 - Measurement of heats of evaporation and desorption.
4 - Measurement of the vapour pressure of materials.
5 - Study of the thermionic emission properties of emitters.
6 - Study of adsorption and heterogenous reactions by the surface ionization method.

When the electron affinity of the species is sufficiently high, negative ions may be observed; this process is described as negative surface ionization.

2.2 Saha-Langmuir Equation[61,62]

The degree of surface ionization is defined as the ratio

$$\alpha = \frac{\nu+}{\nu o} \quad \text{for positive ions} \qquad \ldots (2.1)$$

and

$$\alpha = \frac{\nu-}{\nu o} \quad \text{for negative ions} \qquad \ldots (2.2)$$

where νo, $\nu+$, $\nu-$ are the fluxes of neutral, positive and negative particles desorbing from the surface. The positive ion current from a polycrystalline surface is expressed in the Saha-Langmuir equation

$$j_+ = e\nu A_+^* \exp\left[(\phi_+^* + \sqrt{e\varepsilon} - V)e/KT\right] \qquad \ldots (2.3)$$

where $A_+^* = (A/S \sum_k S_k \exp\left[(\phi_k - \phi_+^*)e/KT\right]$

ϕ_+^* = effective work function in producing positive ions.

A^* = effective pre-exponential function.

A^+ = pre-exponential function of homogenous surface.

S = ion-emitting surface area.

S_k = area occupied by patches of the k kind with work function ϕ_k.

e = electronic charge

ν = flux of particles adsorbing on the surface from the surrounding space

ε = accelerating electronic field

T = Kelvin temperature

V = ionization potential of the species where

$V - \phi_{max} - \sqrt{e\varepsilon} >> KT.$

ϕ_+^* may be determined by plotting $Lnj_+/T^2 = f(1/T)$.

The analogous equation for negative ions from a polycrystalline surface

$$j_- = e\nu A_-^* \exp\left[(E - \phi_-^* + \sqrt{e\varepsilon})\, e/KT\right] \qquad \ldots (2.4)$$

where $A_-^* = S^{-1}\sum_k Sk\, A\left(\frac{1 - R_-}{1 - R_o}\right)_k \exp\left[(\phi_-^* - \phi_k)\, e/KT\right]$

R_o and R_- are reflection coefficients of neutral particles and negative ions from the surface.

The equation for electron emission from a polycrystalline surface (Richardson -Dushman equation)[109] completes the equations which are necessary for deriving electron affinity from surface ionization in a mass spectrometer.

$$j_e = SA_R^* T^2 \exp\left[-(\phi_R^* - \sqrt{e\varepsilon})\, e/KT\right] \qquad \ldots (2.5)$$

where $A_R^* = S^{-1}\sum_k S_k A_{Rk} \exp\left[-(\phi_k - \phi_R^*)\, e/KT\right]$

and ϕ_R^* = effective Richardson work function

A_R^* = effective pre-exponential function of thermionic emission

A_{Rk} = pre-exponential function of thermionic emission in patch of k - kind.

By using equations (2.3), (2.4) and (2.5) in different combinations, a number of different approaches to electron affinity determinations have been developed.

2.2.1 The Determination of Electron Affinity By the Absolute Method

By dividing equation (2.5) over (2.4) we obtain

$$j_e/j_- = (T^2/e\nu)(A_R^*/A_-^*) \exp\left[(-E-\phi_R^* - \phi_-^*)e/KT\right]$$

$$= (A_R^*/e\nu A_-^*)\, T^2 \exp\left[-eE/KT\right] \qquad \ldots (2.6)$$

or

$$E = -K/e\; d(\ell n\; j_e/j_-)\; d\,(1/T) \qquad \ldots (2.7)$$

This equation was used by Ionov (1947) to determine E(I) in the magnetron.

The mode of calculation, therefore differed from that of Sutton and Mayer[63] in the use of a Richardson-type plot, but was the same as that employed by Page[64]. It has been shown by Zandberg that this method is able to determine the electron affinity with a good agreement of photodetachment methods.

2.2.2 Determination of the Electron Affinity by the Method of Magnetic Separation of Electrons and Negative Ions

By comparing equation (2.3) and (2.4) one may obtain the ratio of the currents j_+/j_- for the simultaneous surface ionization of fluxes of particles ν_1 and ν_2

$$j_+/j_- = (\nu_1 A_+^*)/(\nu_2 A_-^*) \exp\left[(\phi_+^* + \phi_R^* - V - E)e/KT\right] \ldots (2.8)$$

The negative ions were separated from the thermoelectrons by a magnetic field.

Dukel'skii and Ionov[65] assumed that the production of negative ions in the surface ionization of a well - collimated beam of MX molecules of alkali halide salts was governed by the Saha-Langmuir equations (2.3). Hendricks et al[66] and Johnson and Phipps[67] had already demonstrated it to be true for positive ions.

2.2.3 Electron Affinity: Difference Method

Ionov (1948)[68] used a mass spectrometer for the first time in the study of the surface ionization of alkali halide molecules on polycrystalline tungsten.

It was shown that positive atomic ions M^+ of the alkali metal and negative atomic ions X^- of the halogens were the only ions adsorbed, and that equation (2.2) was correct for the temperature dependence of the negative ion current. If fluxes ν_1 and ν_2 of particles 1 and 2, respectively are ionized simultaneously on the same surface, the ratio of the two negative ion currents, may be expressed as:

$$j_{-1}/j_{-2} = \nu_1 A^*_{-1}/\nu_2 A^*_{-2} \exp[e(E_1 - E_2)/KT] \qquad \ldots (2.9)$$

So ΔE could be obtained by plotting

$$\ell n\, j_{-1}/j_{-2} = f(1/T)$$

This method was used to determine the electron affinity of halogen atoms by Bakulina and Ionov[69] and Bailey[70].

2.2.4 The Method of the Comparison of The Currents of Positive and Negative Ions of Two Elements (The Twofold Comparison Method)

The j_+/j_- current ratio of atomic ions for two elements formed simultaneously was expressed in the following equation:

$$(j_-/j_+)1(j_+/j_-)2 = (A^*_-/A^*_+)1(A^*_+/A^*_-)2 \exp[(E_1 - E_2 + V_1 + V_2)e/KT] \quad \ldots (2.10)$$

Zandberg et al[71] examined the following ions desorbed from a tungsten surface Sb^-, Sb_2^-, Bi^-, Bi_2^-.
Zandberg et al[81] determined E(Cu, Sn, Pb) by the same method as did Zandberg et al[71] for E(Si, Ge).

2.3 Methods Concerned with Direct Measurement of the Equilibrium Constant

These methods were based on measuring the equilibrium constant K of the following reaction[72]

$$X_{(g)} + e_{(g)} = X^-_{(g)} \qquad \ldots (2.11)$$

occurring at a hot filament.

Regard any surface in temperature equilibrium at a temperature Ts with a gas phase containing atoms X, ions X^- and electrons e, then at equilibrium the number of each atom species a striking on its surface per unit time from the gas phase must be equal to the numbers leaving the surface = Za which have a simple relation (2.12) to the equilibrium pressure Pa in the gas phase and therefore to the equilibrium constant K and to the standard free energy change ΔF of reaction

$$Za = Pa/(2\pi mak\ Ts)^{\frac{1}{2}} \qquad \ldots (2.12)$$

$$K = e^{-\Delta F/RT} = \frac{Px^-}{Px\ Pe} = \frac{Zx^-}{Zx\ Ze}\ (2\pi\ me^-R\ Ts)^{\frac{1}{2}} \qquad \ldots (2.13)$$

where Ts = Temperature at equilibrium

ma = Mass of particle "a"

R = Boltzman constant

It may be shown by methods of statistical mechanics that

$$e^{-\Delta F/RT} = \frac{Zx^-}{Ze^-} \quad \frac{1}{Px} \left(\frac{TG \; mx^-}{2Ts \; me^-} \right)^{\frac{1}{2}} \qquad \ldots (2.14)$$

$$= \frac{jx^-}{je^-} \quad \frac{1}{Px_2} \left(\frac{TG \; mx^-}{2Ts \; me^-} \right)^{\frac{1}{2}} \qquad \ldots (2.15)$$

Where jx^-/je^- is the ion to electron current ratio, TG is the temperature of the gas x_2 and mx^- and me^- are the ion and electron masses respectively.

From the measurements of Px, je^- and jx^-, ΔF may be evaluated (equation (2.15)), and from this by the simple calculation indicated in equation (2.16) the electron affinity $-\Delta Eo$ may be found.

$$\Delta F = \Delta H - T\Delta S = \Delta Eo + \int_o^{Ts} \Delta Cp \; dT - Ts\Delta S \qquad \ldots (2.16)$$

Where ΔH, ΔS and ΔCp have the usual significance.

2.3.1 The Method of the Shift in the Volt-Ampere Characteristics

The space- charge method is based on the Langmuir - Childs relationship.

$$\text{Log } j = \text{Log } C \; (e/m)^{\frac{1}{2}} + 3/2 \text{ log } V \qquad \ldots (2.17)$$

where V = electrodes potential difference

C = geometrical constant

e/m= the specific charge to mass ratio of the current carriers.

In the presence of a gas like I_2, the following equation applies

$$je/ji = (M^{\frac{1}{2}} - m^{\frac{1}{2}})/(m^{\frac{1}{2}} - m_e^{\frac{1}{2}}) \qquad \ldots (2.18)$$

Where M, m_e are the mass of iodine atom and the electron respectively.

Thus a plot of log ji against log V for different gas pressures would give a straight line, so je/j- is determined.

This method is limited to ions which contributes considerably to the total current.

It also assumes complete dissociation of the molecules on the filament and the absence of reflection of molecules from the surface during adsorption.

Because of the low accuracy in the determination of the current ratio je/j- and consequently, also the values of E this method is no longer used. Electron affinity determinations by the methods discussed above are set out in table (2.1).

Table 2.1

Electron Affinity Determination Based on the Saha-Langmuir Equation

Atom	E, eV	Method	Reference
H	0.8	MS*	Khvostenko and Dukel' Skii (73)
Li	0.65<E>1.05	MS	Scheer and Fine (74)
F	3.62	MAG*	Dukel'Skii and Ionov (65)
	3.36	MS	Bakulina and Ionov (75,76)
	3.57	MS	Bailey (70)
S	2.11	MS	Bakulina and Ionov (69)
Cl	3.71	MAG	Dukel'Skii and Ionov (65)
	3.70	MS	Ionov (77)
	3.60	MS	Bakulina and Ionov (75,76,78)
	3.77	MS	Bailey (70)
Cu	1.5±0.5	MS	Bakalina and Ionov (79)
As	≤2	MS	Bakalina and Ionov (76,78)
Se	≈2	MS	Bakulina and Ionov (76,78)
Br	3.64	MAG	Dukel'Skii and Ionov (65)
	3.34	MS	Ionov, Bakulina Ionov (68,75,76,78)
	3.52	MS	Bailey (70)
Ag	2.0	MS	Bakalina and Ionov (79)
	1.90±0.15	MS	Zandberg and Paleev (80)
Sb	1.50±0.17	MS	Zandberg and Paleev (80)
Te	≈2	MS	Bakalina and Ionov (76,78)
I	3.31	MAG	Dukel'skii and Ionov (65)
	3.12	MS	Ionov (77)

Table 2.1 (continued)

Atom	E, eV	Method	Reference	
	3.07	MS	Bakulina and Ionov	(76,78)
Au	2.8±0.1	MS	Bakulina and Ionov	(79)
Bi	1.76±0.16	MS	Zandberg and Paleev	(80)
Si	1.84±0.15	MS	Zandberg et al	(71)
Ge	1.74±0.15	MS	Zandberg et al	(71)
Pb	1.65±0.17	MS	Zandberg et al	(81)
Sn	1.76±0.16	MS	Zandberg et al	(81)
Cu	1.78±0.16	MS	Zandberg et al	(81)
Mo	1.0± 0.2	MS	Fine and Scheer	(82)
Ta	0.8±0.3	MS	Scheer	(83)
W	0.5±0.3	MS	Scheer and Fine	(84)
Re	0.15±0.10	MS	Scheer and Fine	(84)

* MS mass spectrometer

MAG magnetic separation of electron and negative ion currents.

2.4 Electron Work Function Measurement

Using the phenomenon of surface ionization, the work function of emitters can be determined by many methods.

The values of Φ determined for homogenous emitters and of ϕ^* for heterogenous emitters represent values of the work function obtainable by extrapolations from the interval of measurement temperatures to T = 0. Using a constant value of the temperature coefficient of the work function γ (corresponding to the measurement interval of the ion current).

The work function of a material is defined as the work necessary to remove an electron from the highest occupied energy level inside that material to a point in vacuo which is outside the surface and free of surface interactions[89,90].

The importance of measuring work functions of solid materials and the effect of this property on the interpretation of observed data is exemplified in the development of flame chemistry[91].

The general understanding of ionization in flames has been developed from a simple equilibrium description based on Saha's equation[92].

Work functions of materials in the form of ribbons, wires, etc., have usually been determined under high vacuum conditions and the importance of using clean surfaces was realised at a very early stage. Kingdon[93] demonstrated that the work function of tungsten was raised to approximately twice its clean surface value when subjected to low pressures of oxygen.

The importance of the experimental determination of work function changes is reflected not only in the theoretical

analysis of many problems but also in the valuable information which can be obtained concerning a number of "quantities" important to both the technologist and the scientist[94].

The following examples indicate some of the data which can be obtained. Since the chemisorption involves the transfer of electrons between adsorbent and adsorbate, the nature of the bonding between the adsorbing species can be investigated. The surface concentration of adsorbate can often be determined[95] and hence a knowledge of desorption energies and energies of migration can be obtained[96].

The elucidation of catalytic reactions[97], details relating to precursor states and the formation of surface complexes in the mixed adsorption of two or more gases[98] also serve as examples of the importance of such studies.

The methods available for determining work functions and work function changes of surfaces are:-

(1) The thermionic method[99,100,101,102,103], in which the work function is found from the temperature behaviour of the emission current appearing in response to heating of the filament.

(2) The photoelectronic method[104], in which the work function is determined by the long wavelength edge of the photo-electric effect.

(3) The field-emission method[105], in which the work function is determined by the current flowing when a high accelerating field is set up at the surface of the filament.

(4) The contact potential difference method[106], in which the work function is determined by measuring the contact

potential difference between the filament (cathode) and a second electrode having a known work function.

(5) The calorimetric method[107], in which the work function is computed by using the relationship between the quantity of heat supplied to heat the filament and the quantity of heat carried off by the electrons participating in the emission process.

(6) The flame method[108].

(7) Empirical relationships linking the work function to various physical characteristics are utilised in the theoretical computation of the work function.

The application of thermodynamics and statistical mechanics to the calculation of the saturated current density, js, for electrons emitted from a conductor at temperature, T, leads to the well known Richardson - Laue - Dushman equation

$$js = AT^2 (1 - \bar{r}_e) \exp -x/KT \qquad \ldots (2.19)$$

where A = thermionic constant

$\bar{r}_e$ = zero field reflection coefficient

x = work function

Several assumptions have been made in the derivation of this equation, the most important of which are that the surface of the conductor is uniform (i.e. a single crystal) and that the field necessary to produce saturation of the electron current is negligibly small (and maybe set equal to zero). Metals usually contain not only absorbed gases (hydrogen, oxygen, nitrogen, SO_2), but also carbon, sulphur, phosphorus alkali metals and other impurities.

In polycrystalline metals the impurities are found not only

in solution but are also concentrated at the grain boundaries. Therefore, when metals are heated, not only lattice atoms of the metal but also the impurity elements evaporate in the form of atoms and ions. The ion current of alkali metal impurity elements can reach high densities (the effect of this will be discussed later).

The evaporation of atoms and ions of the base metal proceeds from its visible surface and does not change the concentration of particles on the surface. To evaporate impurity elements from the metal volume it is necessary to transport them to the metal surface.

Therefore, the law of ion emission of the metal proper differs substantially from the laws of ion emission of impurity elements.

Usually W, Ta and Pt are used as metal substrates. The first two metals are frequently employed. Since they permit an increase in the efficiency of ionization when the operating temperature is raised- the formation of an oxide with a high work function on their surface also leads to an increase in the ionization efficiency. However the contamination of the platinum surface leads to substantial lowering of its work function[109].

CHAPTER 3

The Magnetron Technique

3.1. The Statistical Theory

The first successful theory correlating the emission current from a hot filament in a substrate at low pressure, with the electron affinity of the ions produced on the surface of the filament was that of Mayer[72].

He assumed that atoms, electrons and ions were in equilibrium at this surface, which therefore made it possible to compute the equilibrium constant and hence the energy change for the reaction

$$X(g) + e(g) = X^{-}(g) \qquad \ldots (3.1)$$

Sutton and Mayer used a Magnetron-type device (a thermionic vacuum tube provided with a uniform magnetic field at right-angles to its electric field) to measure j_- and j_e separately.

A magnetic field parallel to the cathode was generated by a solenoid and a specially designed grid, placed coaxially between the cathode and cylindrical anode, provided a complete separation of electron and ion currents. In the absence of the magnetic field the current due to the electrons and negative ions can be measured, and in the presence of the magnetic field the electrons are constrained into helical paths and are captured by the grid whereas the heavier negative ions are virtually unaffected and pass through to the anode.

Then, knowing the current due to the electrons and negative ions, the pressure of the substrate and the filament temperature,

the equilibrium constant and, therefore, the free energy change for the reaction at that filament temperature, can be calculated.

The combination of this with the entropies and specific heats of the reaction, gives the electron affinity of the reactant.

3.2 The Magnetron Technique and Page[4]

Mayer interpeted his observations in terms of an equilibrium set-up at an inert surface (the filament). It is implicit that the total current should be independent of the pressure of the substrate under these conditions.

Page[64], however, found this was not true. He noticed that the total current of electrons and ions in the magnetron was inversely proportional to the gas pressure.

So he suggested that adsorption was occurring on the filament surface with a consequent increase in its work function.

The arguments developed lead to essentially the same results as Mayers in the case of fission homonuclear diatomic molecules of low bond energy, but a very different interpretation with other substrates.

3.3 The Kinetic Method of Page and Page's Equation

Page argued that an equilibrium constant could be derived assuming equilibrium conditions at the filament, once the filament temperature and electron to ion current ratio are measured.

The rate of desorption of ions under equilibrium conditions would be proportional to the ion concentration at the filament, and the rate at which the electron acceptors reach the filament may be found from the kinetic theory[64,65,110].

Here, the main features of Page's approach is to be described briefly.

Considering the steady-state adsorption of the parent gas the fraction of surface covered θ may be related to the rate of adsorption K_1 and of desorption K_2 and to the pressure P of adsorbate by the following equation

$$\theta = K_1 P/(K_2 + K_1 P) \qquad \ldots (3.2)$$

Page suggested that the process of desorbing a negative ion, may be considered as equivalent to three steps.

(1) desorption of the electron acceptor involving an energy Qa, heat of desorption

(2) removal of an electron from the interior of metal to free space involving the work function of the metal surface X,

(3) addition of the free electron to the acceptor in the gas phase involving the electron affinity E of the acceptor -E.

The electron emission is described by the familiar equation

$$je = BA(1 - \theta)T^2 \exp[- X/RT] \qquad \ldots (3.3)$$

where A is the area of the filament, B = 120 amp cm^{-2} deg^{-2}. Then the effective heat of desorption is

$$Qa + X - E \qquad \ldots (3.4)$$

A similar equation may be written for the rate of desorption of negative ions, that is for the ion current

$$je = CA\theta \exp[E - Qa - X/RT] \qquad \ldots (3.5)$$

then by dividing equation (3.3) over (3.5) we obtain the following

$$je/ji = BT^2 (1 - \theta)/C\theta \exp[Qa - E/RT] \quad \ldots (3.6)$$

By inserting the value of θ in the equation (3.5) it leads to:

$$je/ji = BT^2 K_2/CK_1 P \exp[Qa - E/RT] \quad \ldots (3.7)$$

but $K_2 = B \exp[D - Qa - Qr/RT]$

where Qr is the heat of adsorption of the residue of the molecule. Finally the following equation would be obtained

$$jeP/ji = BT^2/CK_1 \exp[-(E + Qr - D/RT] \quad \ldots (3.8)$$

Thus the apparent or experimental electron affinity obtained from a plot of log jeP/ji against 1/T will lead to a straight line whose slope the apparent electron affinity E' is given by

$$E' = E + Qr - D + nRT \quad \ldots (3.9)$$

Where D is the energy of dissociation of the molecule. The term n is introduced in connection with the correction of the observed values to $0K^o$, and its value will depend on the temperature dependence of the pre-exponential term.

3.4 The Mechanism of Ion Formation

Page[4] has noted four cases under which some simplification of the expression for E' can be made.

3.4.1 Type I - Direct Capture

In this case the acceptors are adsorbed or desorbed as atoms or molecules, that is there is no dissociation of the substrate molecule.

In this case, D and Qr are zero and we have

$$E' = E \qquad \ldots (3.10)$$

for example

$$SF_6 + e^- = SF_6^- \qquad \ldots (3.11)$$

where the compound (SF_6) consists of electronegative elements (F)

Other examples are $C_2(CN)_4 + e^- = C_2(CN)_4^-$ ... (3.12)

$$C_6H_3FO_2 + e^- = C_6H_3FO_2^- \qquad \ldots (3.13)$$

where the compounds may contain pi-bond systems, such as tetracyano ethylene in the first and fluorobenzoquinone in the second.

3.4.2 Type II Weak Bond

This case involves molecules of low bond energy, which are completely dissociated into acceptors at the filament temperature

Here again D and Qr are zero and we have

$$E' = E \qquad \ldots (3.14)$$

Page distinguished between

(i) Symmetrical fission e.g. Hydrazine

$$N_2H_4 + 2e^- = 2NH_2^- \qquad \ldots (3.15)$$

(ii) Unsymmetrical fission, dimethyl mercury

$$(CH_3)_2Hg + 2e^- = 2CH_3^- + Hg \quad \ldots (3.16)$$

Generally, this type is characteristic of radicals capturing an electron to form negative ions.

Page argued that it is possible to omit the bond energy term, if the equilibrium lies toward the side of the free radicals so that the degree of dissociation is over 50%, and increasing temperature will have only a slight effect on the number of radicals reaching the filament, so that no significant error is introduced in assuming that dissociation is complete.

3.4.3 Type III Strong Bond

In this case the bond energy is very high, so a small fraction is dissociated.

Here Qr is zero, but D is now 1/n times the bond energy, in most cases n is found to be equal to two (n = 2) for example

(i) Symmetrical fission

$$O_2 + 2e^- = 2O^- \quad \ldots (3.17)$$

$$E' = E - D/2 \quad \ldots (3.18)$$

where D is the dissociation energy of oxygen

$$D \equiv D(O - O) \quad \ldots (3.19)$$

(ii) Unsymmetrical fission

$$CCl_4 + e^- = CCl_3 + Cl^- \quad \ldots (3.20)$$

$$E' = E - D$$

Where D is the energy of the CCl_3 - Cl bond

$$D \equiv D(CCl_3 - Cl) \quad \ldots (3.21)$$

3.4.4 Type IV Dissociation with Adsorption

In this case the bond energy is high, and both the bond dissociation energy and the heat of adsorption contribute to the observed results and the apparent electron affinity is given by:

$$E' = E - Q - D \quad \ldots (3.22)$$

For example

$$CCl_4 + e = CCl_3^- + Cl_{ads} \quad \ldots (3.23)$$

$$D \equiv D(CCl_3 - Cl) \quad \ldots (3.24)$$

$$Q \equiv Q(Cl/Filament) \quad \ldots (3.25)$$

Page and co-workers[4] investigated the ion formation by a wide range of substrate and confirmed the essential validity of the kinetic method.

The results obtained show the kinetic approach to be far more flexible than the statistical one and represents a considerable advance in the interpretation of the mode of ion formation in the magnetron.

Table 3.1 sets out the measurements of electron affinity made by Mayer and his co-workers.

Table 3.1

Electron Affinities by the Space-Charge and Magnetron Technique

Atom	Substrate	Electron Affinity eV	Reference
O	O_2	3.07±0.07	Vier and Mayer[111]
	N_2O	2.33	Metley and Kimball[112]
	H_2O	1.35	Page[113]
	NO_2	1.42	Farragher,Page and Wheeler[114]
	N_2O	1.37	Farragher and Page[115]
	O_2	1.38	Farragher and Page[115]
F	$C_6H_3O_2F$	3.45± 0.04	Farragher and Page [115]
S	H_2S'	2.09± 0.07	Ansdell and Page[116]
Cl	HCl	3.48	Page[64]
	CCl_4	3.70± 0.03	Gaines, Kay and Page[117]
	$SnCl_4$,Cl_2	3.73	McCallum and Mayer[118]
	Cl_2	4.02	Mitchell and Mayer[119]
Br	HBr	3.00	Page[64]
	Br_2	3.82	Glockler and Calvin[120]
I	I_2	3.17	Page[64]
	I_2	3.14	Sutton and Mayer[72]
	I_2	3.26	Glockler and Calvin[122]
	CH_3I	3.24	Ritchie and Wheeler[123]
	Br_2	3.52	Doty and Mayer[121]

3.5 Temperature Correction of Experimental Electron Affinity to $0^{o}K$

The experimental values for the apparent electron affinity (E') are obtained at various temperatures. Since few results lead directly to electron affinities, and most have to be combined with other data, obtained by other techniques at different temperatures, it is necessary to carry out a correction to the standard conditions at some point during the calculations.

The main weakness of the kinetic approach to the determination of electron affinity by the magnetron method lies in the uncertainty of the procedure to correct the measured values to $0^{o}K$.

In an attempt to obtain more information about the rate of emission of electrons and ions from heated surfaces the theory of rate processes of Glasstone et al[124] was applied by Farragher[110] and Goode[125] to the calculation of the emission currents and the correction of the experimental electron affinity.

The rate of emission of electrons (Richardson's equation) was deduced in the form:

$$je = [\bar{d}\ (4\pi m_e (KT)^2 e)(1/h^3)] \exp[-X/RT] \qquad \ldots (3.26)$$

where je is the current of electrons, $\bar{d}$ the transmission coefficient for electron emission, m_e the mass of the electron, T the filament temperature, X the work function for electron emission, and other terms have their usual significance.

The rate of emission of negative ions was deduced in the form

$$j_i = (\bar{d}pe)(1/2\ MKTg)^{\frac{1}{2}}(Q_i/Q_m)\exp\frac{-X-E}{RT} \quad \ldots (3.27)$$

where j_i is the current of the ions, Tg and p the temperature and pressure of the substrate vapour, respectively, M the mass of the ions, $\bar{d}$ the transmission coefficent of ion emission, Qi and Q_m the internal partition functions of the transition state ion and gas molecule, respectively, E the electron affinity of the ion precursor.

The electron to ion current ratio, j_e/j_i, is then expressed as

$$j_e/j_i = 4\pi me(KT)^2(2\ MKTg)^{\frac{1}{2}}(1/ph^3)\ (Q_m/Q_i\ \exp -E/RT \quad \ldots (3.28)$$

if the transmission coefficients may be assumed to cancel.

Since the apparent electron affinity at the temperature of the experiment E'(T), is evaluated

$$E'(T) = -R\left[d\ \log\ (j_e/j_i)/d(I/T)\ \right] \quad \ldots (3.29)$$

The value of the derivative of (3.28) with respect to (I/T) will rely on the temperature dependence of Q_e/Q_i.

Farragher and Goode developed the following equations to correct experimental electron affinity to 0^oK;

(i) direct capture, $E'(T) = E + 2RT$ ... (3.30)

(ii) dissociative capture without adsorption, $E(T) =$

$$E - D + 2RT \quad \ldots (3.31)$$

(iii) dissociative capture with adsorption, $E'(T) =$

$$E - D + Q + 3RT \qquad \ldots (3.32)$$

The validity of the equations depends on the vibration frequencies in the molecule for which certain assumptions are made.

3.6 A critique of the Surface Ionization Systems for the Determination of the Electron Affinity of Atoms, Molecules and Radicals

3.61 Temperature Dependence of the Pre-exponential Function

It was pointed out by Zandberg and Ionov[109] that in the surface ionization of electron affinity determination by use of the expression:

$$j_e/j_- = A_R^*/e\upsilon A^* - T \exp[-eE/KT] \qquad \ldots (3.33)$$

as a basis of plots of $\ell n\, j_e/j_- T^2 = f(1/T)$, then the greatest error incurred in the measurement of the electron affinity, E, will be due to the temperature dependence of the pre-exponential term A_R^*/A_-^*

3.6.2 Surface Ionization and Thermal Equilibrium

Hotop et al[34] questioned whether the condition of thermal equilibrium, a key assumption for surface ionization was fulfilled especially when beams of atoms or complex vapour impinge on a heated metal surface and interact with atoms of the surface for an average time which is difficult to estimate.

He emphasizes that what one actually measures in surface ionization is an average over many small surface areas of quite different constitution and work function, and that the assumption that these local differences cancel out over the whole surface, if the two atom beams being compared impinge on the surface simultaneously, is only true if the two beams interact with exactly the same surface area.

Hotop maintains that this condition is not easy to establish experimentally especially when two locally separated evaporators are used.

3.6.3 Subsidiary Processes and Surface Ionization

Zandberg and Paleev[126] have shown that negative ions may be also produced in surface ionization by secondary processes such as dissociative electron capture.

It is claimed by Paleev and Zandberg[127] that many complex organic molecules in surface ionization form mass spectra of negative ions due to bombardment of adsorbed films by positive ions, and that the energy distributions are not homogeneous.

3.6.4 The Attainment of Equilibrium at the Surface

Both the theoretical methods (thermodynamic and kinetic) for obtaining expressions to determine the electron affinity include the assumption that the particles incident from the gas phase on the surface of the ion emitter are adsorbed on this surface and, during adsorption, reach thermal and electrical equilibrium with the adsorbent.

This may be justified indirectly by the experimental values

obtained by other methods (e.g. photodetachment[128] and shock tube studies[129]) and directly by the demonstration that the initial energy distribution of the emitted particles is Maxwellian and corresponds to the filament temperature.

The ionic energy distribution may be determined using the retarding field technique[130].

Experiments for both the ion[131,132] and electron[133] emission have shown that the initial energy distribution of the particles is Maxwellian.

In experiments using a high resolution analyser both alone[134] and linked to a mass spectrometer[135] a similar result was obtained for the initial energy distribution of thermoelectrons, K^+, Li^+, Cs^+ and Cl^- ions (both from Cl_2 and KCl).

3.6.5 The Indirect Identification of the Charge Carriers in the Magnetron

Experimentally, the magnetron technique can only resolve electrons from negative ions, no characterisation of the negative ions being possible.

In consequence of this, the deductions drawn about the identity of the charge carriers on energetic grounds may be in error.

It is possible that impurity currents may derive from the material of the filament.

Herron et al[136] and Zandberg[126] demonstrated that ions predicted in the magnetron were not always observed in the mass spectrometer.

CHAPTER 4

The Quadrupole Mass Filter System*

4.1 Introduction

In order to advance the investigation of negative ions formed by surface ionization, a negative surface ionization source was built (the details of which will be described later).

Most of the magnetron critiques were based on the fact that only indirect identification of ions produced by surface ionization was possible, and therefore complex reactions which give rise to similar numbers of ions of the same masses may be misinterpreted in terms of a simple reaction. The negative surface ionization source was connected to a quadrupole type mass spectrometer where positive identification of ions under investigation is possible.

Although there have been countless routine applications of quadrupole mass spectrometers, particularly in residual gas analysis, there are an unusual number of individualized applications in both science and technology which require the construction of specially designed or modified instruments with particular combinations of properties.

Thus for many users, not primarily interested in quadrupole mass spectrometers as such, the instrument cannot remain merely a "black box", it is the characteristic qualities leading to these specialised applications which justify the consideration

---

* The work has been presented at the 8th International Mass Spectrometry Conference, Oslo, Norway, August 12-18 (1979).

of quadrupole use separately,from general mass spectrometric applications[85] although there is obviously a considerable overlap.

The more recent applications of quadrupole mass spectrometry include chemical kinetics and surface chemistry studies, gas chromatography, the study of free radicals and ion neutral collision investigations.

The promising characteristics of the quadrupole as a mass analyser which spurred development were sensitivity and moderate resolution in compact devices, the apparent mechanical simplicity, the light weight and absence of a cumbersome magnet, high-speed electronic scanning, the linear mass scale, and the possibility of trading off sensitivity against resolution by a simple adjustment of the circuitry.

The availability of these features coincided with a leap forward in the routine application of high and ultra-high vacuum techniques.

The ions formed at the filaments were accelerated toward the anode in which there was a small hole in line with the axis of the quadrupole field. This enabled the ions to be further accelerated and focussed into the quadrupole field, where they were mass analysed.

The general layout is shown in plates (4.1). The following sections describe the various components and also the mode of operation of the quadrupole mass filter system used in this work.

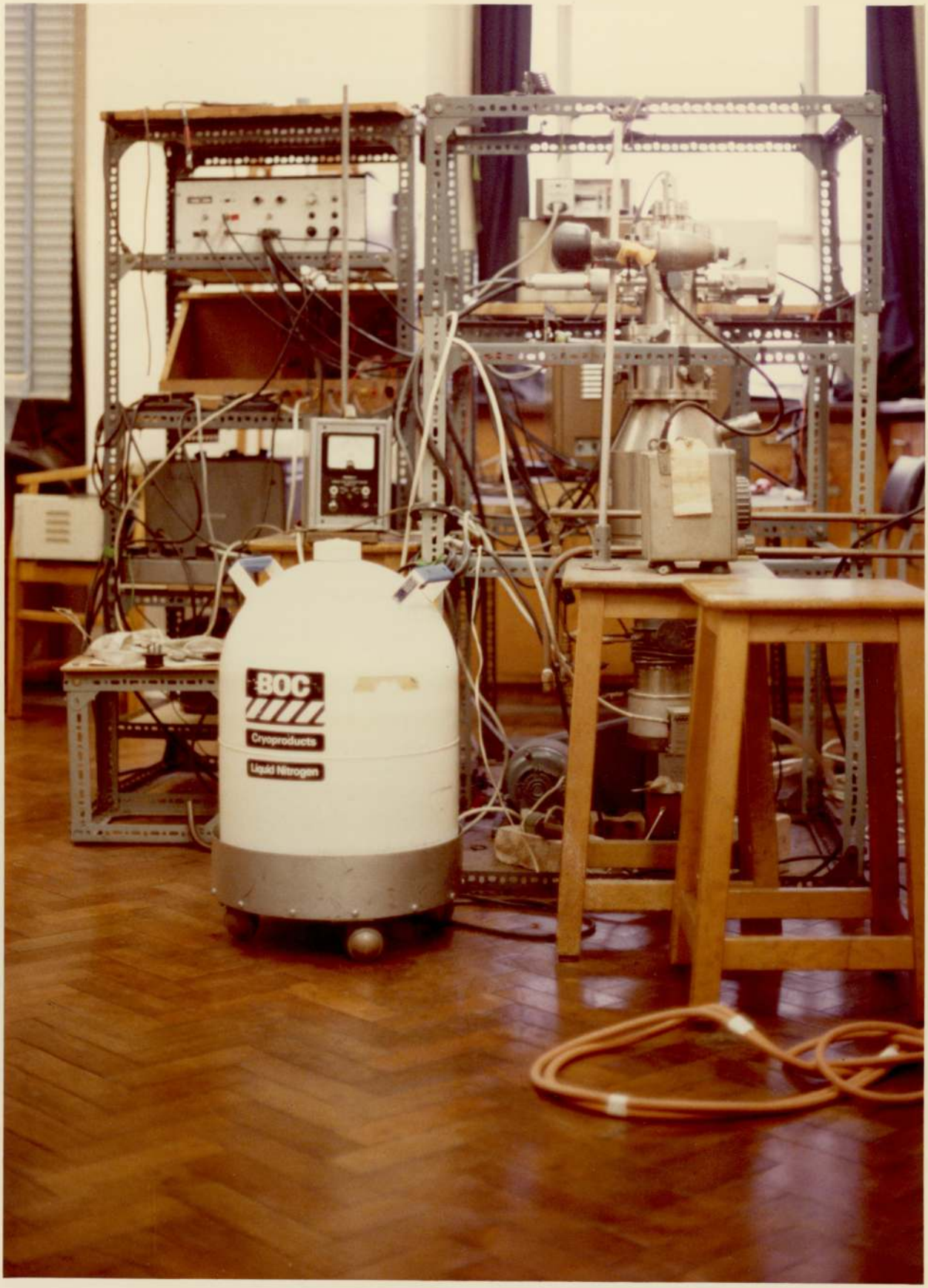

4.1a The general layout of the Mass Spectrometer (rear view)

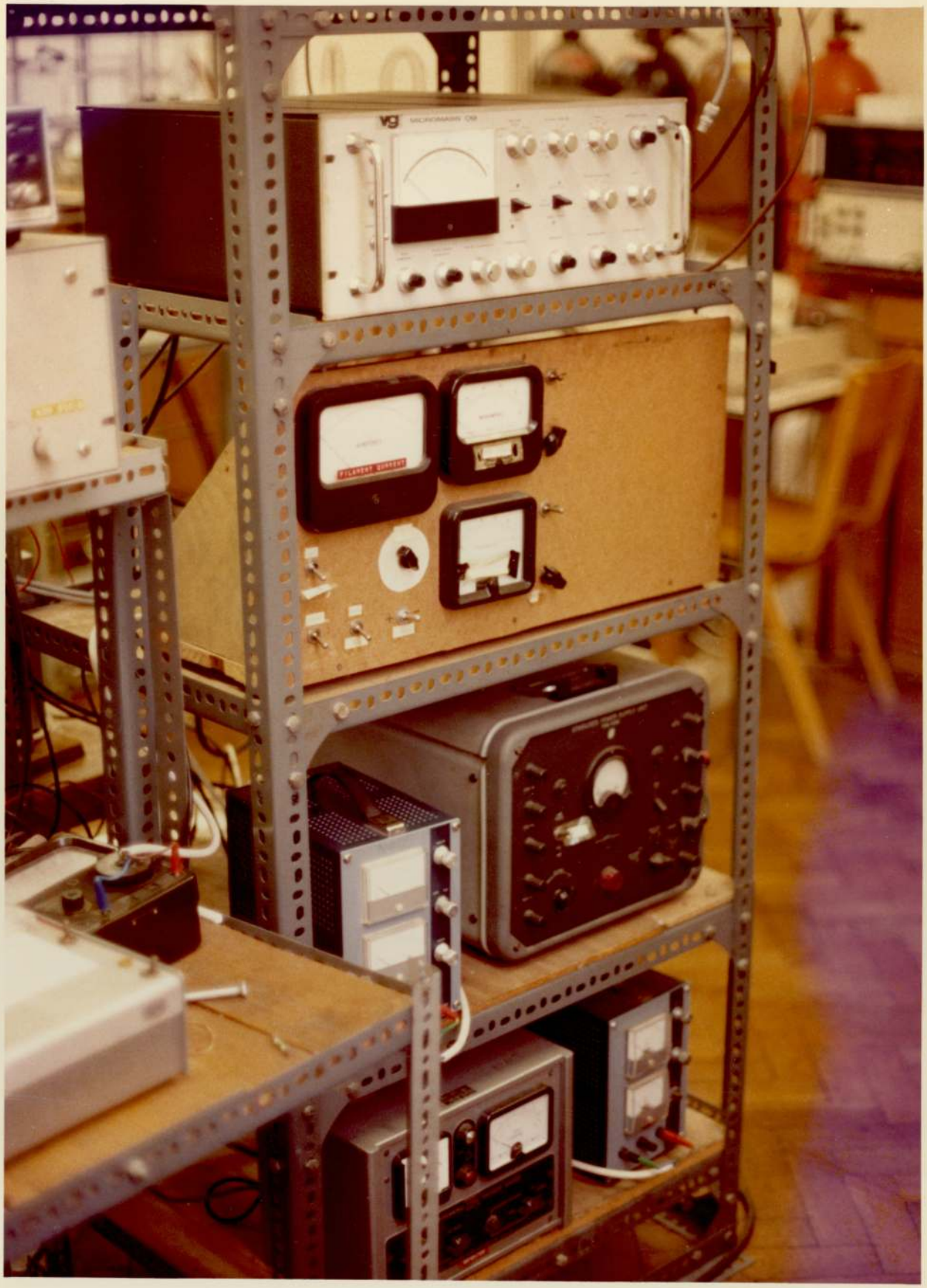

4.1 1b The general layout of the Mass Spectrometer (front view)

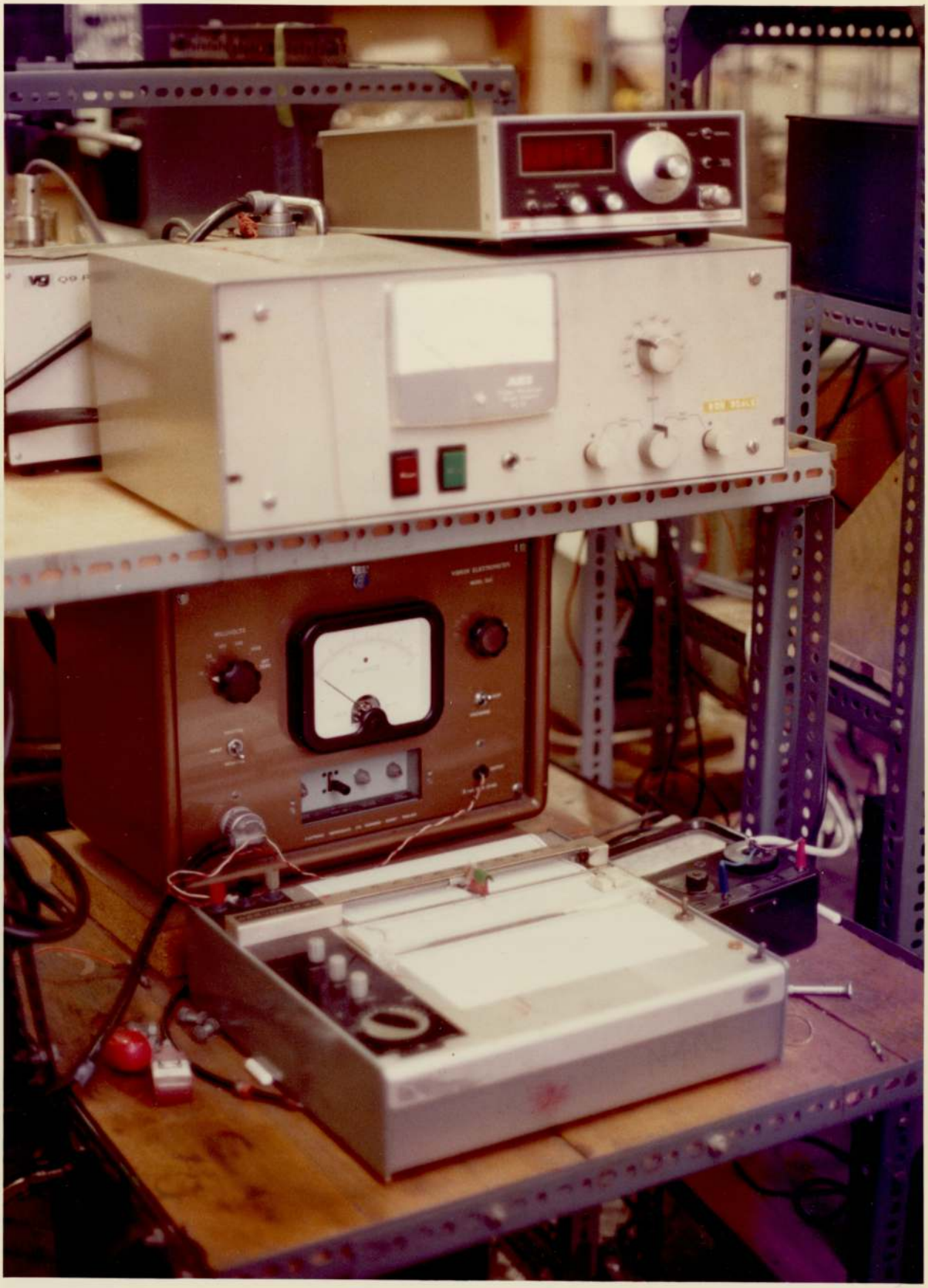

4.1 b2 The general layout of the Mass Spectrometer (front view)

4.2 The Source System

4.2.1 The Ion Source

The main features of the ion source assembly are shown in Figure (4.2).

It consists of a simple triode design, cathode (filament) coaxial wire grid and a perforated anode, the three parts were connected together over stainless steel studs and separated by means of pyrex spacers 5.00 mm thick. The ion source was rested over three studs welded to the upper flange of the vacuum system. A hole of 5.00 mm in diameter was made in the anode facing the entrance aperture of the quadrupole analyser chamber.

For practical purposes, the filament was introduced to the ion source without spot welding.

Two molybdenum springs were used to support the filament and were fitted around two iron rods Figure (4.3).

The filament was usually fitted to the two springs "O" terminals by "knitting", this was found to be very practical when there was a need to change the filament or to clean the ion source.

It was difficult to select the exact length of the filament which when held taut enough to prevent twisting occurring at high temperatures (>2500^{o}K) would not undergo breakdown.

After several trials, an "experimental" length was found, under which the above mentioned requirements were satisfied.

It was found experimentally to be more convenient to mount the filament in two steps, in the first one the filament was mounted "knitted" as described earlier, it was stretched to slightly less than "experimental" length.

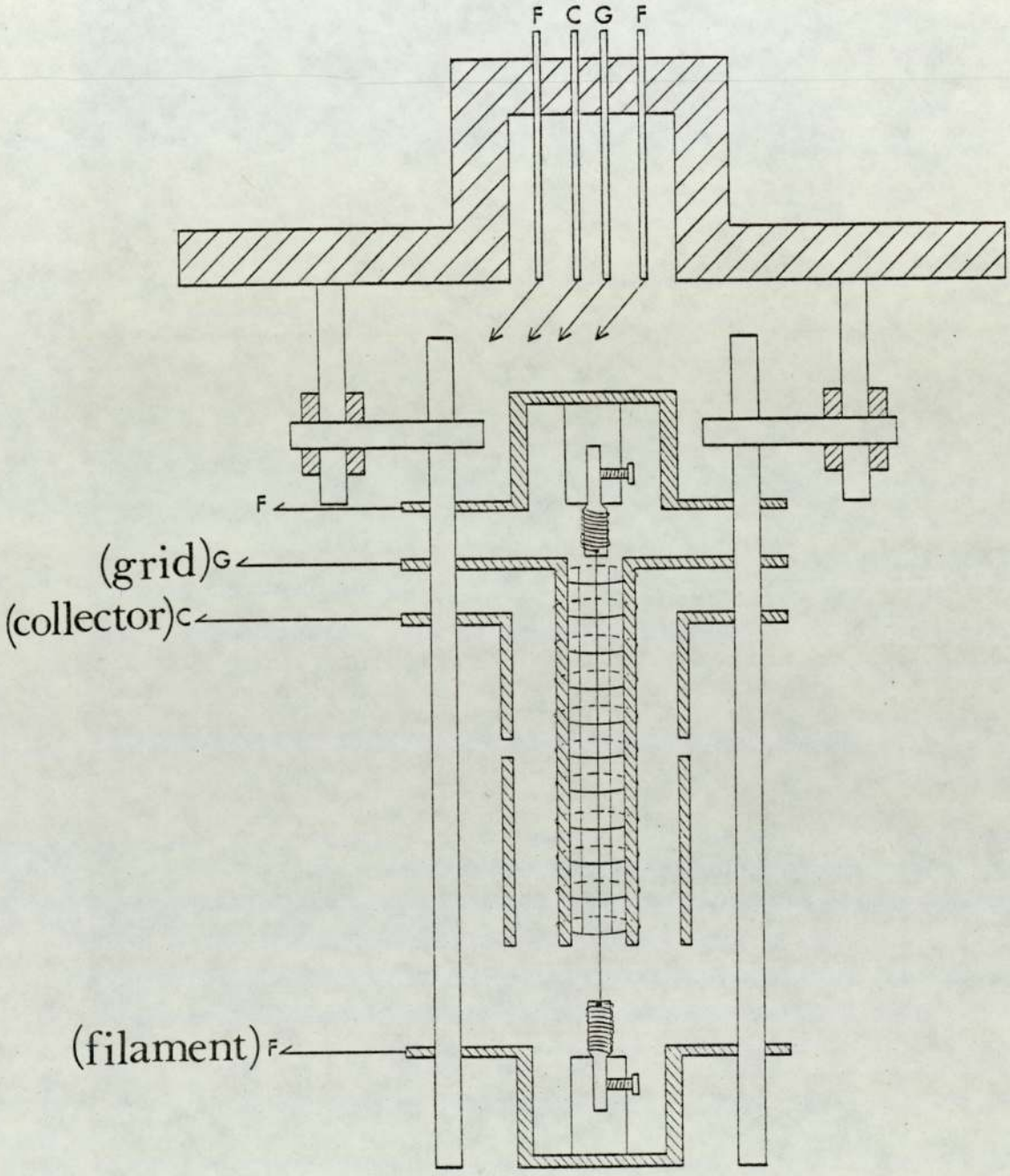

Figure (4.2) The Negative Surface Ionization Source.

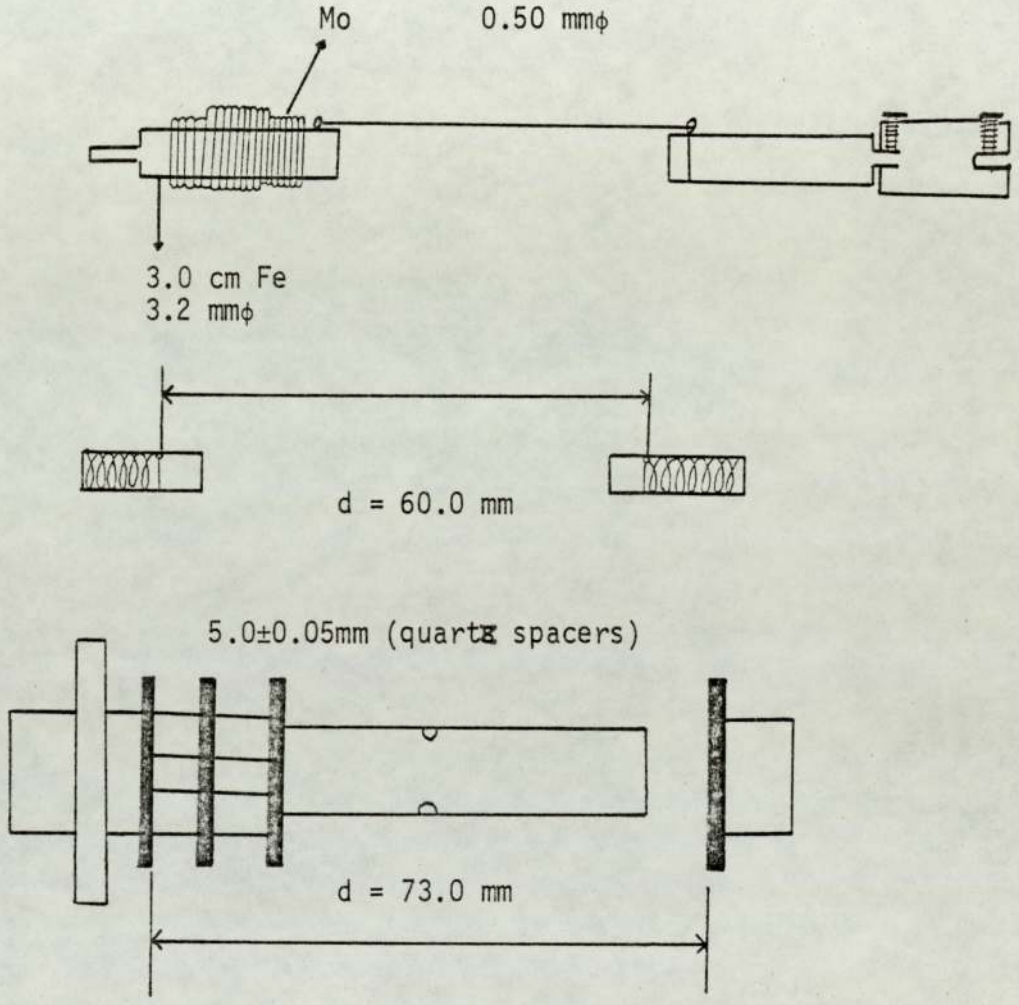

Figure (4.3) Details of the filament assembly.

The filament then was heated (under vacuum) to very high temperatures (about 2500^{o}K) without subjecting it to breakdown at this stage. The filament, of course, twisted out of alignment, but this was not important at this first stage.

Later, after the filament had polycrystalised, it was stretched to the exact "experimental" length. A D.C. stabilised power supply, variable between 0-200 volts, was used to supply the ion accelerating potential.

Another D.C.power supply which was capable of supplying a current up to 2.5 amps was used for the filament. The temperature at the highest heating current was found to be about 2500^{o}K. Figure (4.4) shows the negative surface ionization accelerating voltage.

In most of the experiments carried out, the values shown in this figure were adopted, these were reached after several experiments to satisfy the best experimental conditions; that is to be high enough to overcome the space-charge effect (saturated electronic current) and to obtain maximum transmission efficiency Figure (4.5).

This was achieved by scanning at zero mass (electrons) and recording the highest electronic current passing through the quadrupole analyser and reaching the Faraday cup.

4.2.2. Temperature Measurement

The temperature of the centre of the filament was measured by means of a disappearing filament optical pyrometer (Leeds and Northrup).

The measurements made with the pyrometer were always found

Fig. (4.4) Negative surface ionization accelerating voltage.

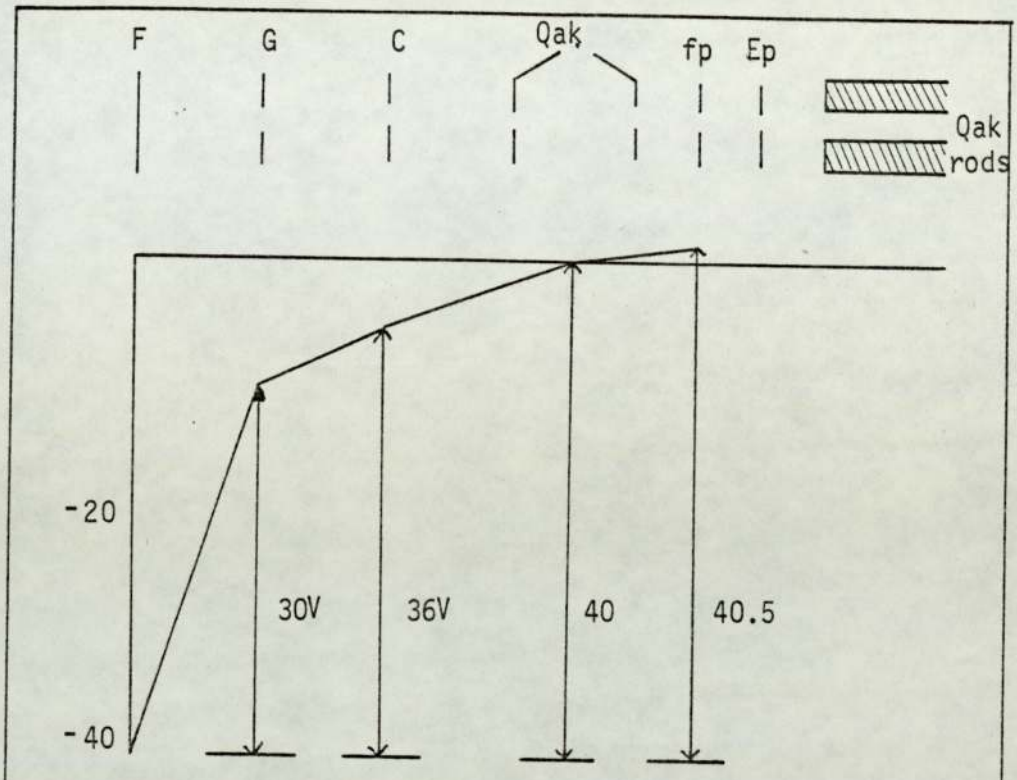

Filament potential (F) = VQ + I.E

Grid potential (G) = VQ - Va + I.E

Qak potential (Qak) = $V_{(zero)}$ + I.E

Collector potential (C) = VQ - Vc = I.E

Key:-

F	filament	G	Grid
C	collector		
Qak	ionization chamber		
fp	focusing plate		
Ep	earth plate		

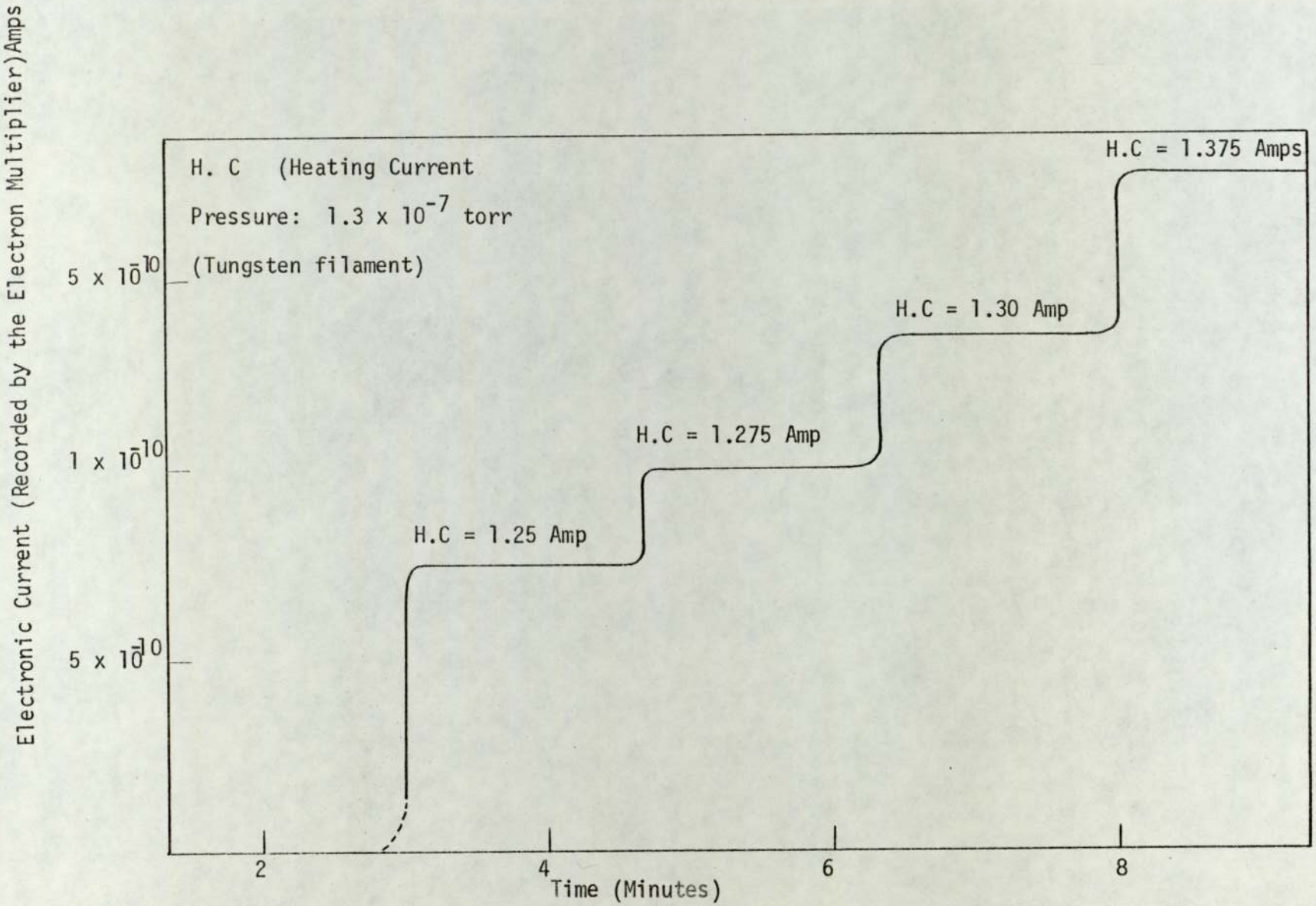

Figure (4.5) Transmission of electrons through quadrupole rods.

to be reproducible within $10^{o}K$ for any temperature.

The observed temperatures were corrected to allow for emissivity effects and also absorption by the glass window through which the filament was observed. The correction was achieved by use of the following equation[86]

$$\frac{1}{T} - \frac{1}{S_\lambda} = \frac{\lambda}{C_2} \ln (\varepsilon_{\lambda,t} \cdot A) \qquad \ldots (4.1)$$

where T is the true temperature

S_λ is the optical temperature measured at wavelength λ

C_2 is a constant (1.43879 ± 0.00019 cm.K)

A_λ is the absorption coefficient (0.92)

$\varepsilon_{\lambda t}$ is the emissivity coefficient at a particular wavelength and temperature.

Graphs of $S(^{o}C)$ (Pyrometer temperature) against $(T\ ^{o}K)$ (True temperature) for tantalum, platinum, and tungsten are shown in Figures (4.6), (4.7) and (4.8).

As the filament temperature was measured from the central portion, any heat losses due to conduction from the ends may be neglected, and therefore at equilibrium the rate of heat loss by radiation is equal to the rate of supply.

According to Stefan's law (assuming the filament is a perfect black body)

$$E = \sigma T^4 \qquad \ldots (4.2)$$

where T is the temperature in ^{o}K, and σ is the Stefan's constant

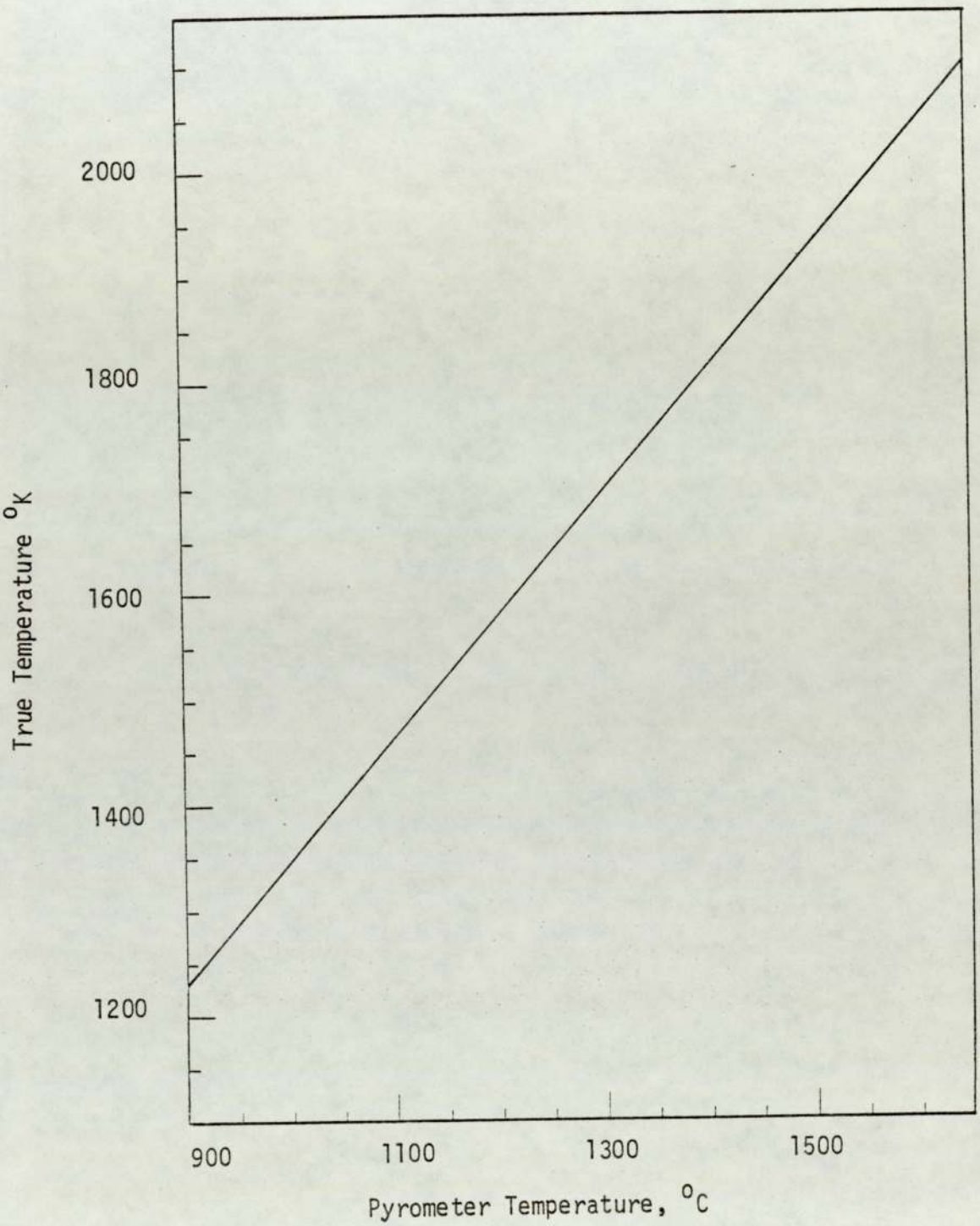

Figure (4.6) Emissivity and Temperature Correction for Tantalum Ta

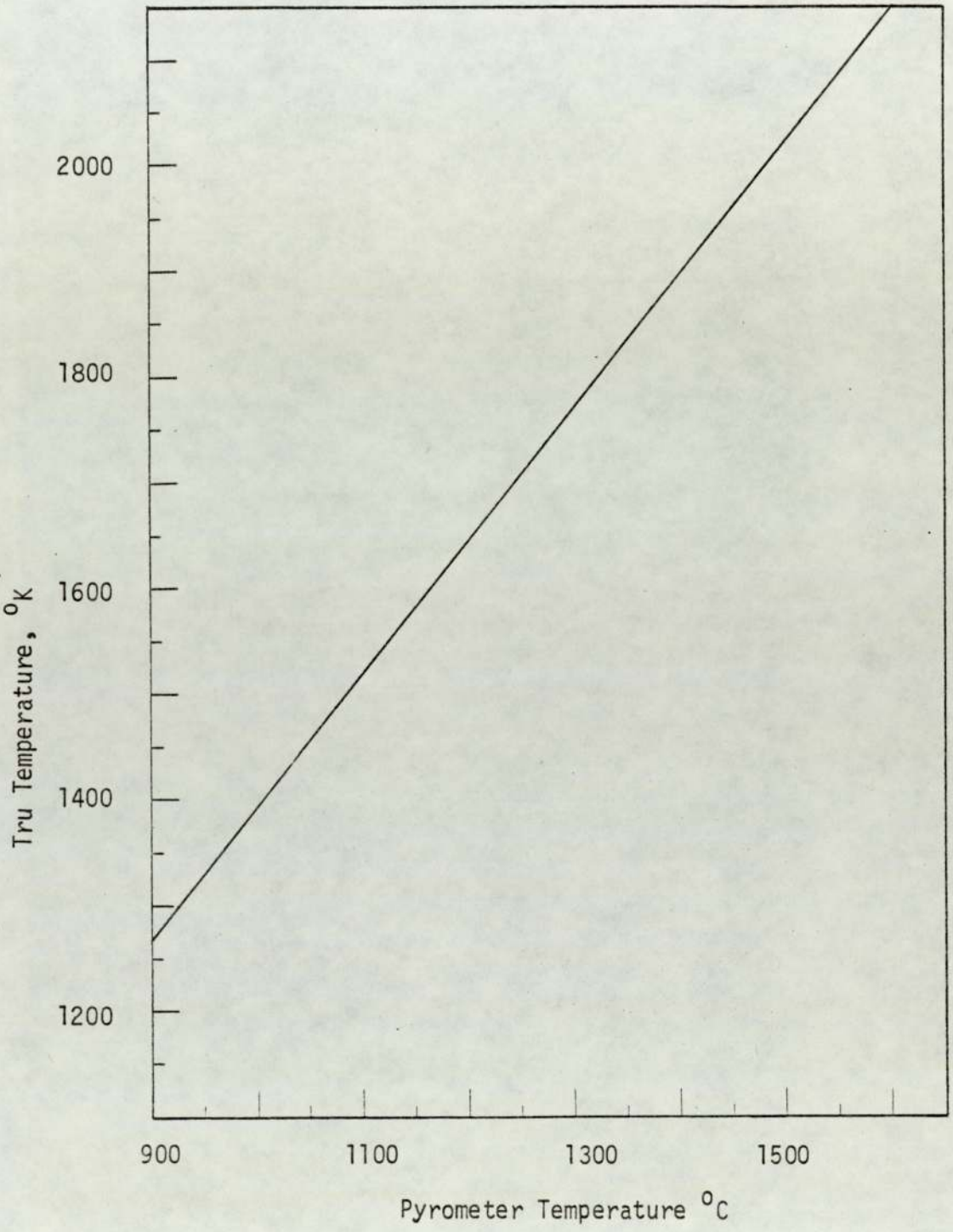

Figure (4.7) Emissivity and absorption temperature correction for platinum Pt

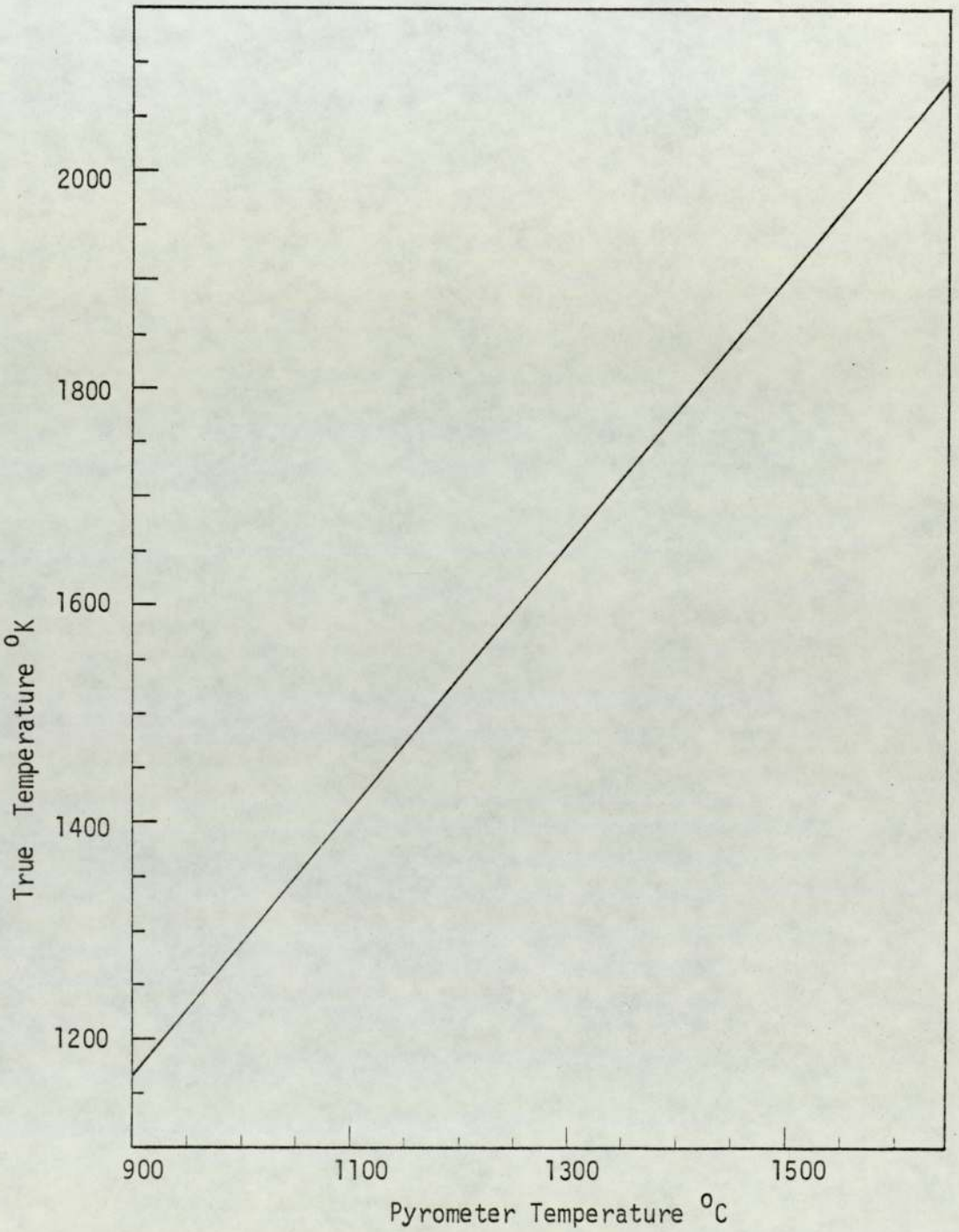

Figure (4.8) Emissivity and absorption temperature correction for tungsten W

Thus $E = \sigma T^4 = j_f^2 R$ ... (4.3)

where j_f is the filament current and R is the resistance (assumed constant over the temperature range studied). (Heat supplied to the filament and resistance is equal to heat loss by radiation)

or $j_f = KT^2$ ... (4.4)

Plotting j_f against T^2 will give a straight line over a range of temperatures for which the above mentioned assumptions are true Figure (4.9).

In order to avoid difficulties in using the optical pyrometer for temperature measurements where there is a discontinuous change in the emissivity of the filament surface, Page and Gaines[4] developed a method using the electron emission directly.

The basic equation for this method may be derived as follows: Richardson's equation may be rewritten as

$$\log j_e = A - \frac{x}{RT} \quad \ldots (4.5)$$

$$\text{or} \quad \frac{1}{T} = \frac{A}{R} - \frac{R}{X} \log j_e \quad \ldots (4.6)$$

where T is the temperature in ^oK, and x is the work function in eV. The general expression used to evaluate the apparent electron affinity from the ion (j_i) and electron (j_e) currents at a pressure P is

$$\log \frac{j_e P}{j_i} = B - \frac{E'}{RT} \quad \ldots (4.7)$$

Figure (4.9) Filament Current as a function T^2 (Tungsten)

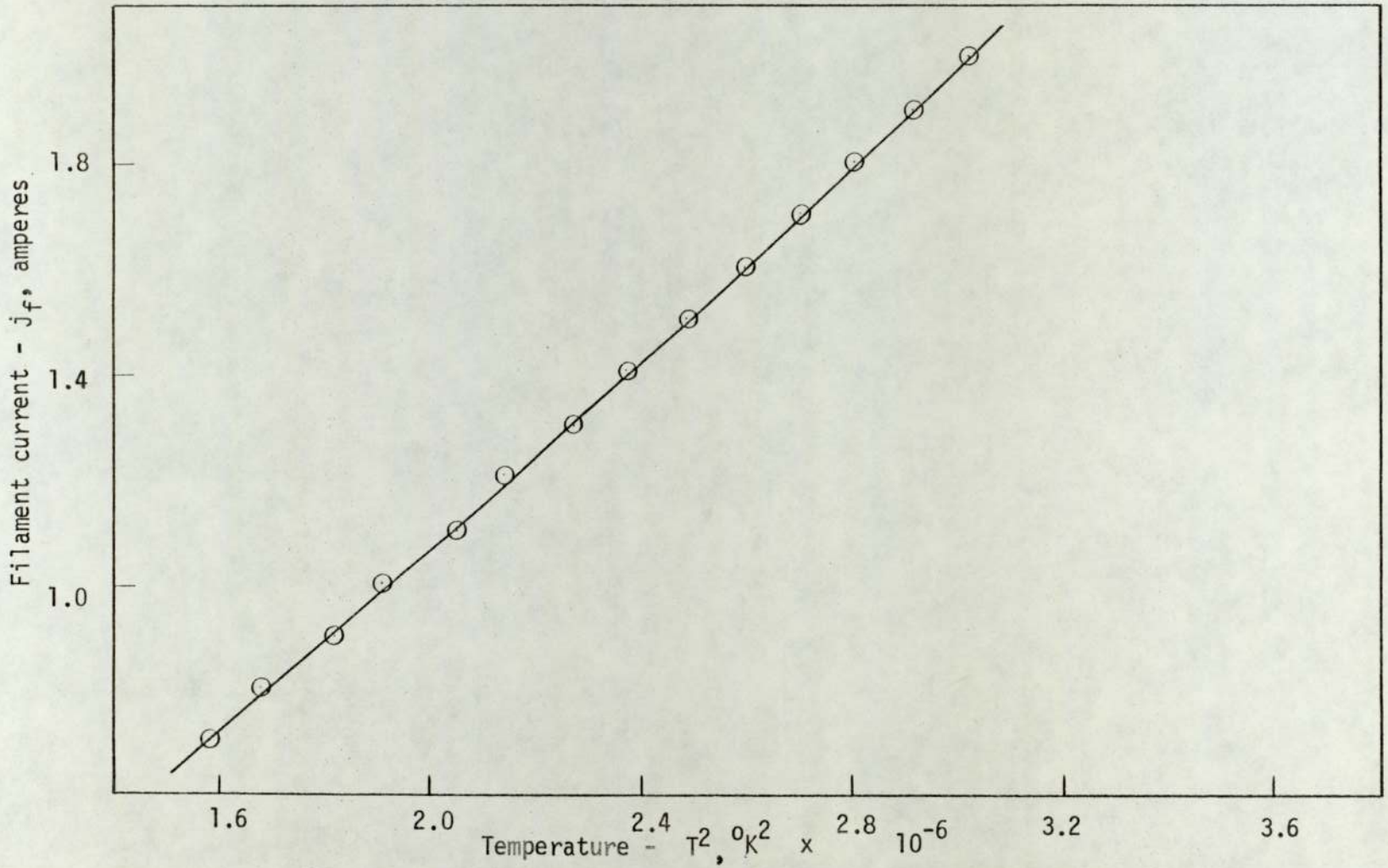

$$= B - \frac{E'}{R}\left(\frac{AR}{X} - \frac{R}{X}\log j_e\right) \quad \ldots (4.8)$$

$$= C + \frac{E'}{X}\log j_e \quad \ldots (4.9)$$

So that a plot of log $j_e P/j_i$ against log j_e yields a straight line of slope + E'/X or it may be shown that a plot of log $j_i P$ against log j_e is a straight line of slope X - E'/X.

4.3 The Mass Filter System

The heart of the instrument is the quadrupole filter and associated R.F/D.C circuitry. It consists of four stainless steel rods, 5" in length and 0.25" in diameter, aligned axially and symmetrically about an inscribed circle 0.215" diameter.

Paul and co-workers[87] Method: in this method ions are injected along the axis of quadrupole radio-frequency electric field. This field is produced between four parallel rods of hyperbolic section to which the radio frequency potential and the superimposed D.C potential are applied (in practice the field was approximated by the use of cylindrical rods). The quadrupole theory is adequately covered in the literature and the theoretical treatment of the ideal quadrupole mass filter is beyond the scope of this study.

As mentioned earlier the mass separation is basically accomplished by application of precisely regulated R.F and D.C voltage levels superimposed on the four quadrupole rods Fig (4.10) Opposite pairs of rods are connected together and R.F/D.C voltages

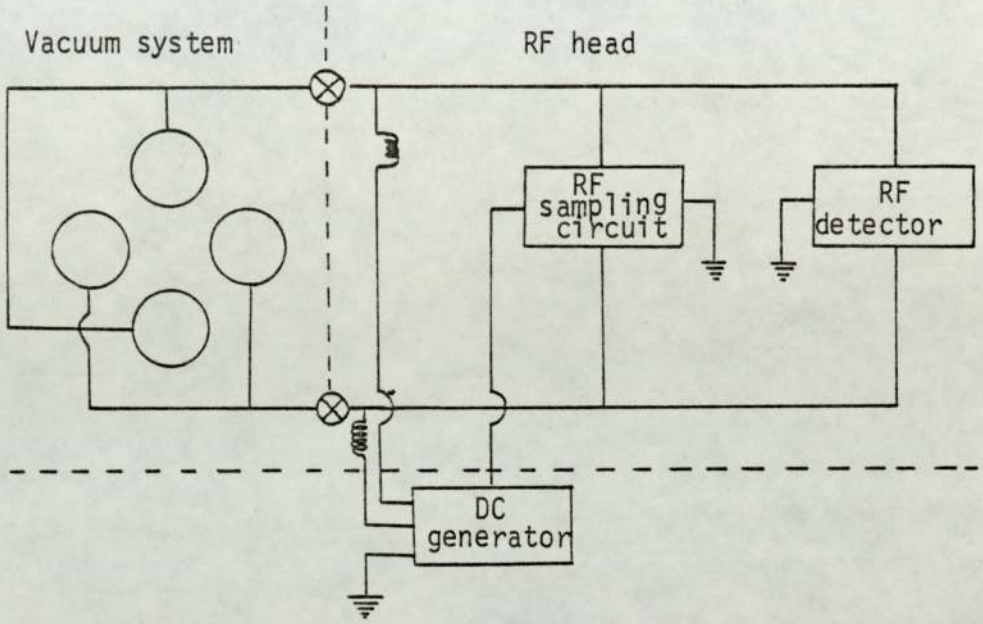

Figure (4.10) RF/DC Voltages applied to filter rods

of opposite signs are applied to the pairs, giving zero field at the centre of the filter and on the axes between the rods.

The RF signals excite oscillations of the ions about the zero field regions, and the D.C level regulates the amplitude of these oscillations.

For a given RF level, increasing the D.C component drives the ion oscillations into a more critical region and the ion transmission becomes increasingly mass dependent, giving enhanced separation of the ions of adjacent molecular weights at the expense of the transmission efficiency (resolution increased at the expense of sensitivity).

One advantage of using the mass filter "quadrupole" is its capability of working at moderately high pressures, other advantages include its sensitivity, adequate resolving power and the possibility of baking the system to expel any ion which might dominate the ion emission.

4.3 The Detector System

As there was no access to the Electron Multiplier's last dynode in the analysed feedthrough flange, it was not possible to use the electron multiplier for negative ion detection (the last dynode of the multiplier was grounded inside the mass analyser).

The electron multiplier was used as a routine check to make sure that the various parts of the mass spectrometer were functioning properly (the positive ionization source was employed).

Throughout our work a D.C amplifier was used,it was capable

of measuring currents up to 10^{-16} amps, it had a range of 10^{-7} to 10^{-16} amps, in decade steps. Unfortunately the long time constant, approximately 30 seconds in the lower current range, precluded its use in obtaining mass spectra by means of the automatic scanning system.

Later, during the investigation a digital electrometer (mode 616) was used. The mode 616 digital electrometer is an automatic ranging multipurpose electrometer which can be used to measure currents from $\pm 10^{-15}$ ampere to 200 milli ampere. It has certain characteristics which enable reliable measurements of very small currents with fast response.

A Faraday "cup" type was used, it consists of a partially screened electrode, at which ionic species may neutralize their charge and be detected.

The ion current arriving at the Faraday "cup" was measured by connecting it, by means of a screened cable, to the D.C. amplifier.

4.4 The Vacuum System

Fig(4.11) shows the layout of the overall arrangement of the vacuum line, the full details of the apparatus can be found in the accompanying key.

The source, the quadrupole mass filter and the detector sections were enclosed by stainless steel vacuum chambers joined by copper gaskets.

The ultimate vacuum attained in the mass spectrometer was about 2×10^{-8} torr, this was possible after out gassing by baking to about $150^{\circ}C$ for more than eight hours.

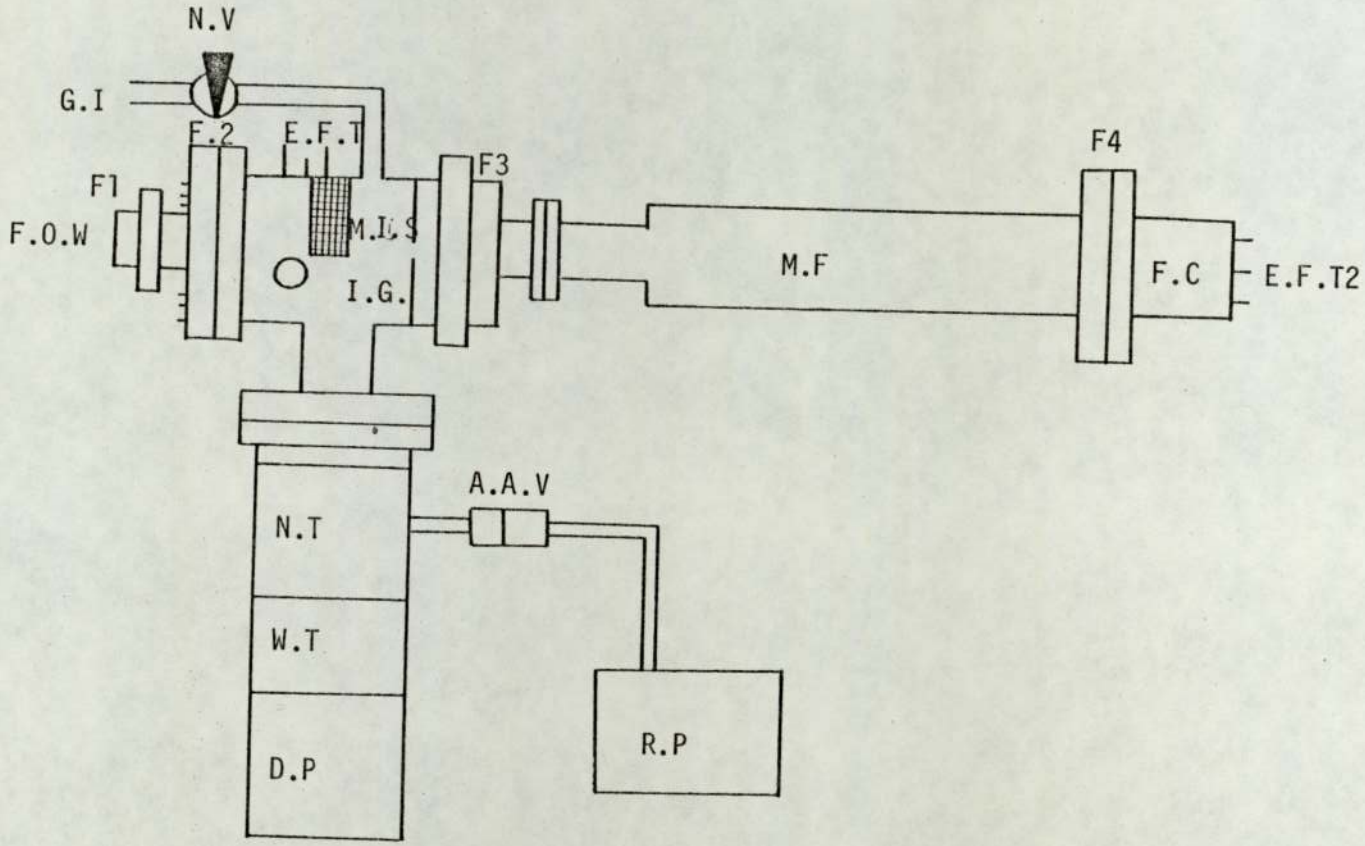

Figure (4.11) Vacuum System Arrangement

Key to the System Arrangement of Figure (4.1)

A.A.V.	Air admittance value
D.F.	Diffusion pumps
E.F.T. (1,2)	Electric feed through
Fl,	Rotable flange
$F_{2,3,4}$	Flange sealed with copper gaskets
F.O.W	Filament observation window
G.I.	Gas inlet
I.G.	Ionization gauge
M.F.	Mass filter
N.T.	Nitrogen trap
N.I.S.	Negative Surface Ionization Source
N.V.	Needle valve
R.P.	Rotary pump
W.C.	Water cooled baffle

This vacuum was obtained by an oil diffusion pump which operates against a baking pressure of 10^{-2} torr which is supplied by a rotary mechanical pump.

Metal (copper) gaskets were used for joining the various components of the apparatus which were made of stainless steel, this makes the whole system above the diffusion pump bakable.

A liquid nitrogen trap, together with water cooled baffles prevent any organic vapours (in measurable quantities) from reaching the ionization source chamber.

A bakable window flange made out of steel was used to allow the filament temperature to be determined by an optical pyrometer.

A lead gate valve was employed to separate the ionization chamber from the diffusion pump, it was always closed for a few minutes before the pumps were switched off, to keep the vacuum in the mass filter chamber at less than 10^{-4} torr, in order to prevent any damage to the electron multiplier of the mass filter while the instrument was not in use.

4.5 The Sample Introduction System

The sampling system is shown in Figure (4.12). The samples were always purified by trap to trap distillation followed by extensive outgassing by means of the Freeze-Thaw technique.

Different modifications to this sampling system were employed depending on the substrate under study, and whether it was liquid or gas, or a highly volatile solid.

A needle valve type was used to admit the sample vapour into the ionization chamber.

The whole sample introduction system was made out of pyrex

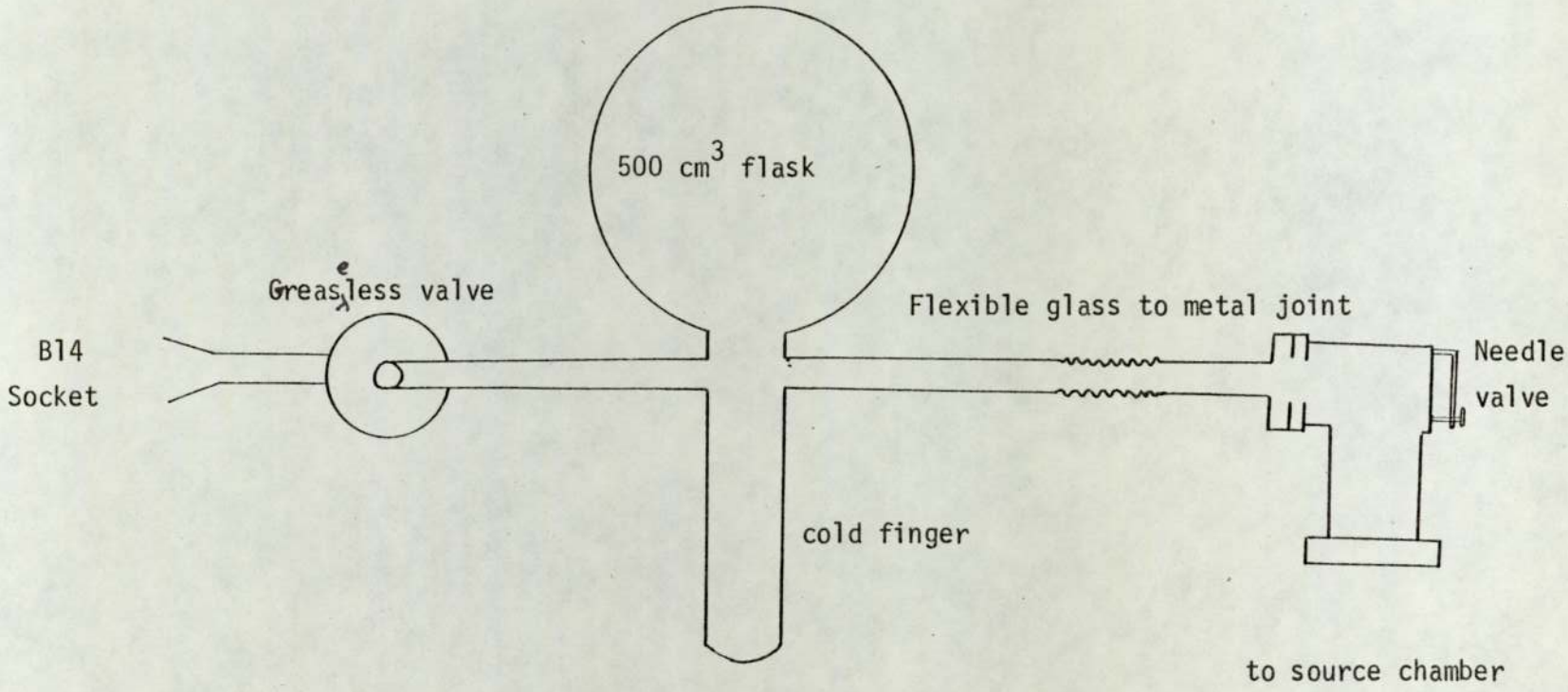

Figure (4.12) The sampling system

to enable it to withstand high pressure and temperature during the outgassing process.

A flexible stainless steel-glass flange was used in the needle valve-sampling system joint.

4.6 Negative-ion Mass Spectrometry

4.6.1 Introduction

In the last few years studies involving positive ion mass spectra have been applied to a great variety of organic compounds [137,138,139]. However, very little has been published with respect to negative ion mass spectrometry. There also appears to be discrepancies in the published experimental results, which demonstrate the need for further work.

The studies of gaseous negative ions which were carried out prior to 1960 have been reviewed by Melton[140], work since that time is described in several books[141] and review articles[142,143, 144,145]. The latest comprehensive review was that of Dillard[146].

Since 1965 there has been a continuing interest in the development of negative ion mass spectrometry as an aid to structure determination.

4.6.2 Modes of Negative Ion Formation

Interaction of electrons with neutral molecules leads to the formation of negative ions. Depending on the energy of the electron and the nature of the molecule, one of three basically different processes will occur. For a diatomic molecule AB these processes are conventionally classified as follows:

a) Resonance capture

$$AB + e \longrightarrow AB^- \qquad \ldots (4.10)$$

b) Ion pair formation

$$AB + e \longrightarrow A^- + B^+ + e \qquad \ldots (4.11)$$

$$AB + e \longrightarrow A^+ + B^- + e \qquad \ldots (4.12)$$

c) Dissociative Resonance Capture

$$AB + e \longrightarrow A^- + B \qquad \ldots (4.13)$$

$$AB + e \longrightarrow A + B^- \qquad \ldots (4.14)$$

In this scheme A and B may be either an atom or a molecule and processes (a) and (b) may involve the breaking of one or several bonds. Process (a) produces a molecular negative ion and occurs near 0 eV, process (c) may be observed in the energy range 0 to about 15 eV, while ion pair production (b) occurs above about 10 eV.

A qualitative picture of these processes and the distribution of energy in the products can be obtained by considering transitions between the potential energy curves representing the ground state of the molecule AB and the molecular ion AB^-.

Potential energy curves representing the various types of

processes are shown in Figures (4.13 - 4.15).

The Franck - Condon principle is used in conjunction with these curves. Thus the speed of the incident electron is considered large compared with the vibrating nuclei of the molecule, hence in electronic transitions the time for the transition was negligible compared with the nuclear vibration period, so that the nuclear separation does not change significantly.

In the potential energy diagrams the transition may be represented by a vertical line. The shaded regions are known as the Franck-Condon regions and the most probable transition occurs from the centre of this region.

The curves in Figure (4.13a) show the simplest type of non-dissociative electron capture process. Electron capture into discrete states of AB^- occurs between energies in the range E_1 and E_2 and since the nuclear separation in AB^- is usually greater than in AB, the AB^- is formed in a vibrationally excited state; it is represented as AB^-*. If the vibrationally excited molecular ion does not emit a photon or undergo collisional stabilisation, the electron will be ejected by auto-detachment (Auger electron):

$$AB^-* \longrightarrow AB^* + e \qquad \ldots (4.15)$$

In Figure (4.13b) another possible process for temporary negative ion formation is given.

This process is described as one where vibrational excitation of the neutral molecule leads to subsequent capture of the incident electron. However, because of the low energy of the electron, long interaction times may occur between the electron and the molecule. This means that the nuclei may change from their normal configuration to a position on the negative ion curve.

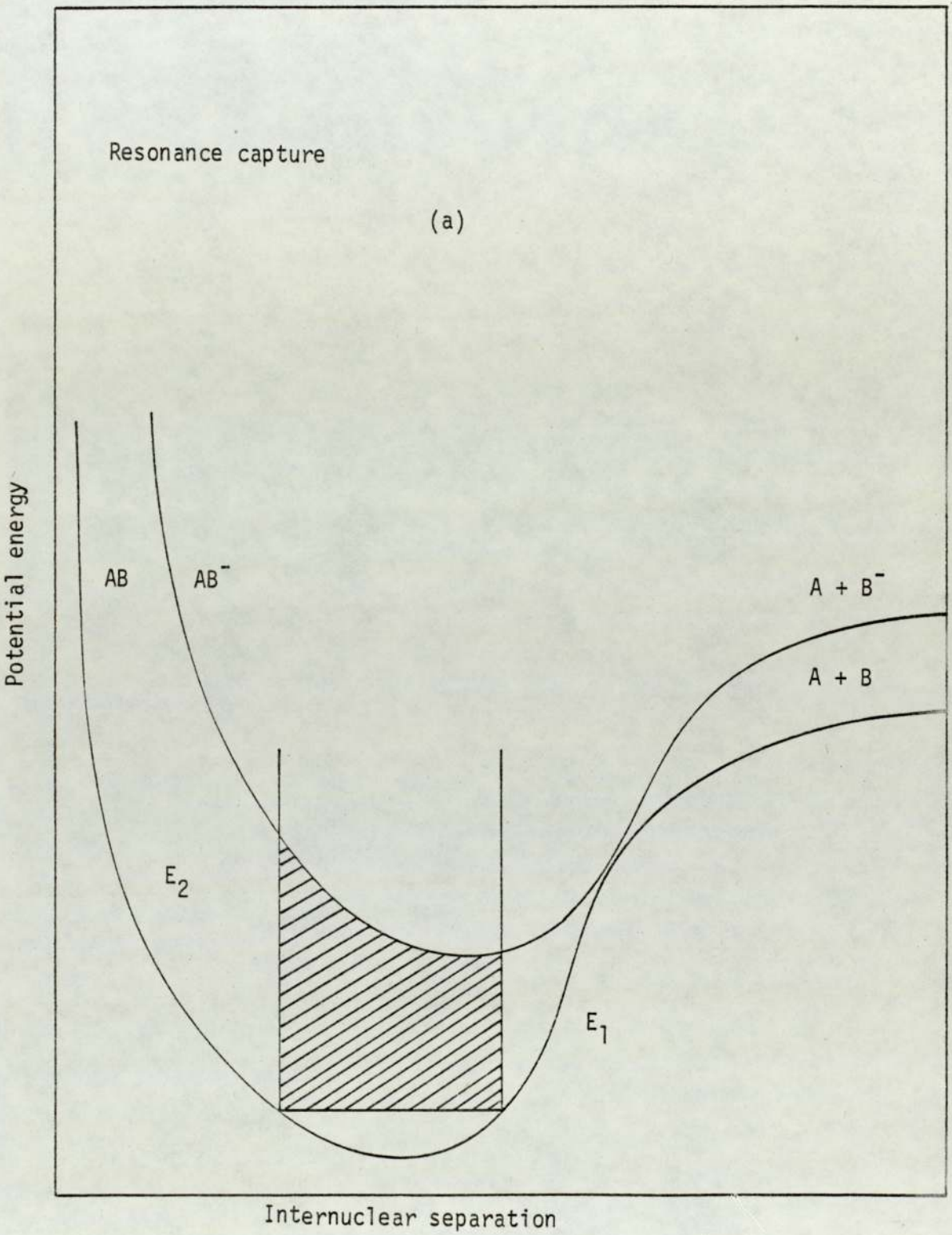

Figure (4.13) Potential energy curves showing formation of negative ion from a diatomic molecule by resonance capture

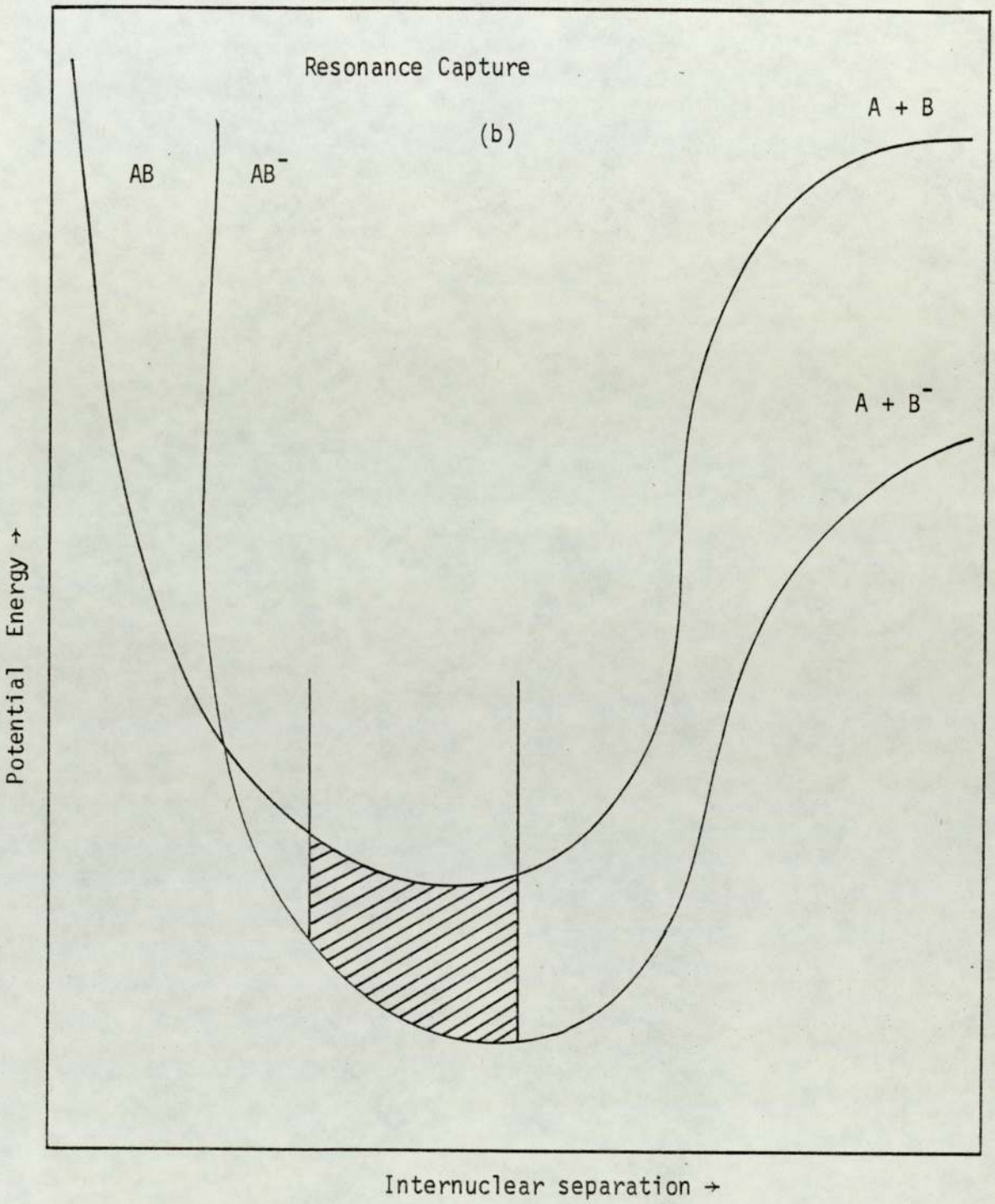

Figure (4.13) Potential energy curves showing formation of negative ion from a diatomic molecule by resonance capture

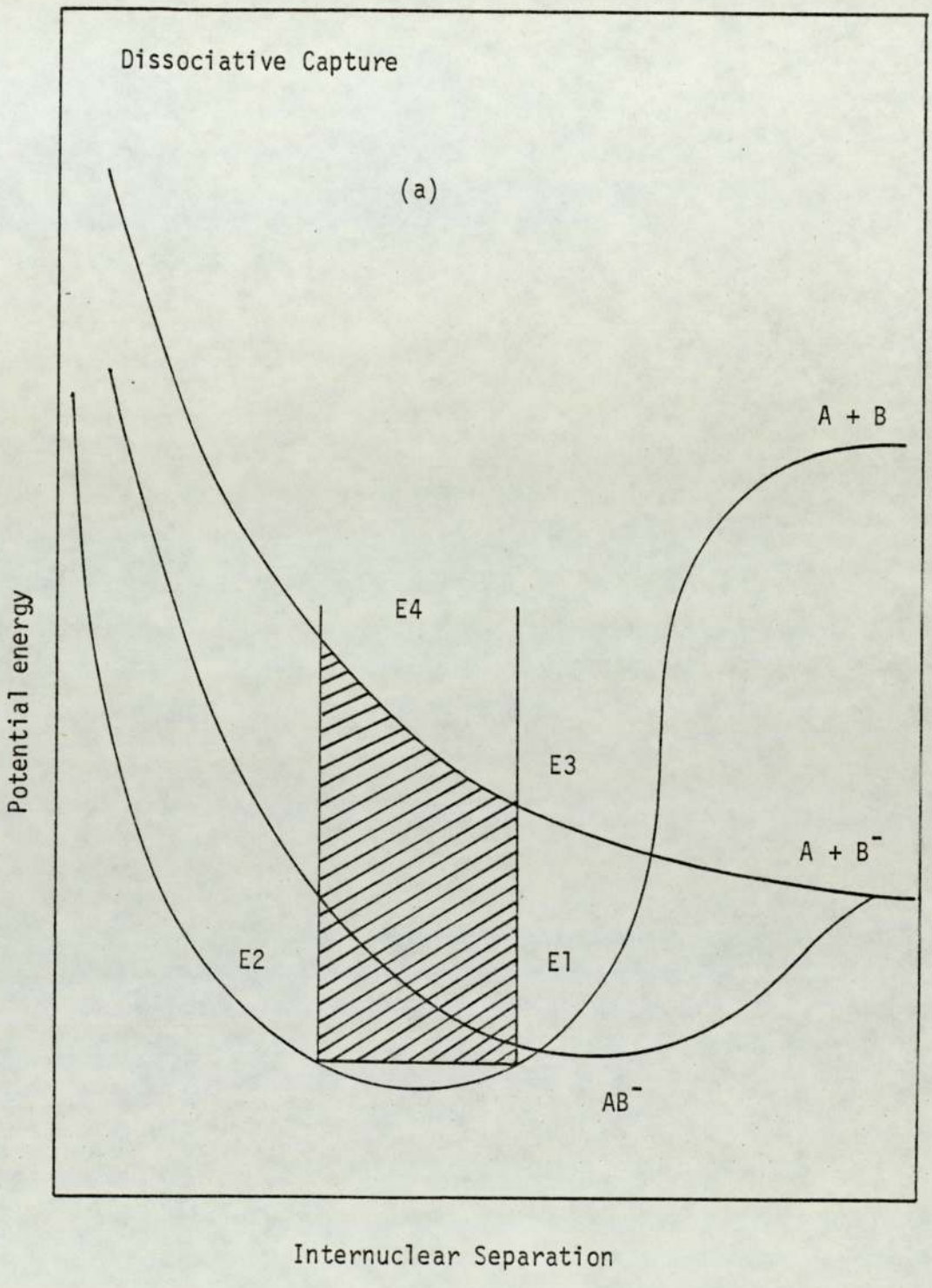

Figure (4.14) Potential energy curves showing the formation of a negative ion from a diatomic molecule by dissociative resonance capture.

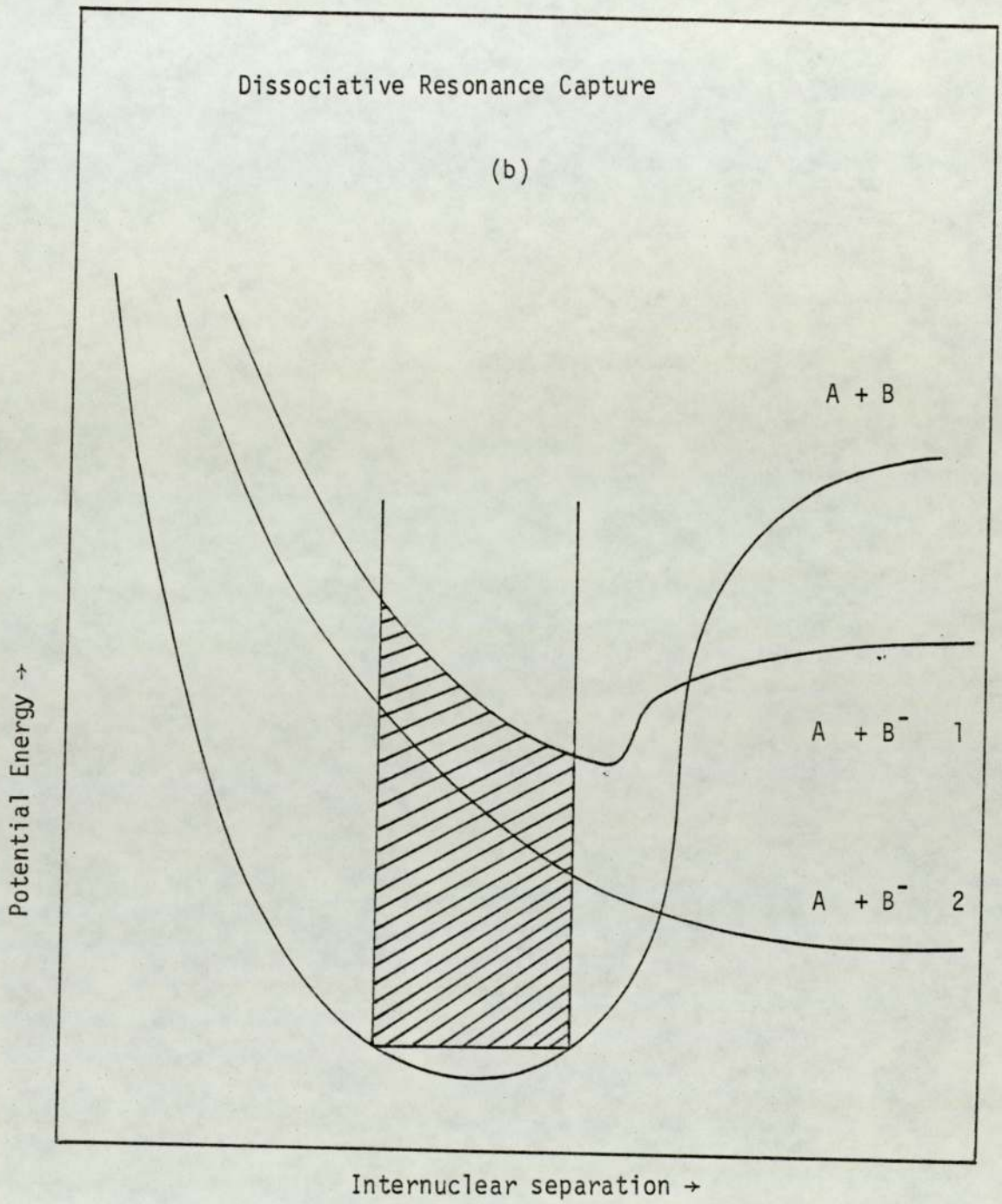

Figure (4.14) Potential energy curves showing the formation of a negative ion from a diatomic molecule by dissociative resonance capture

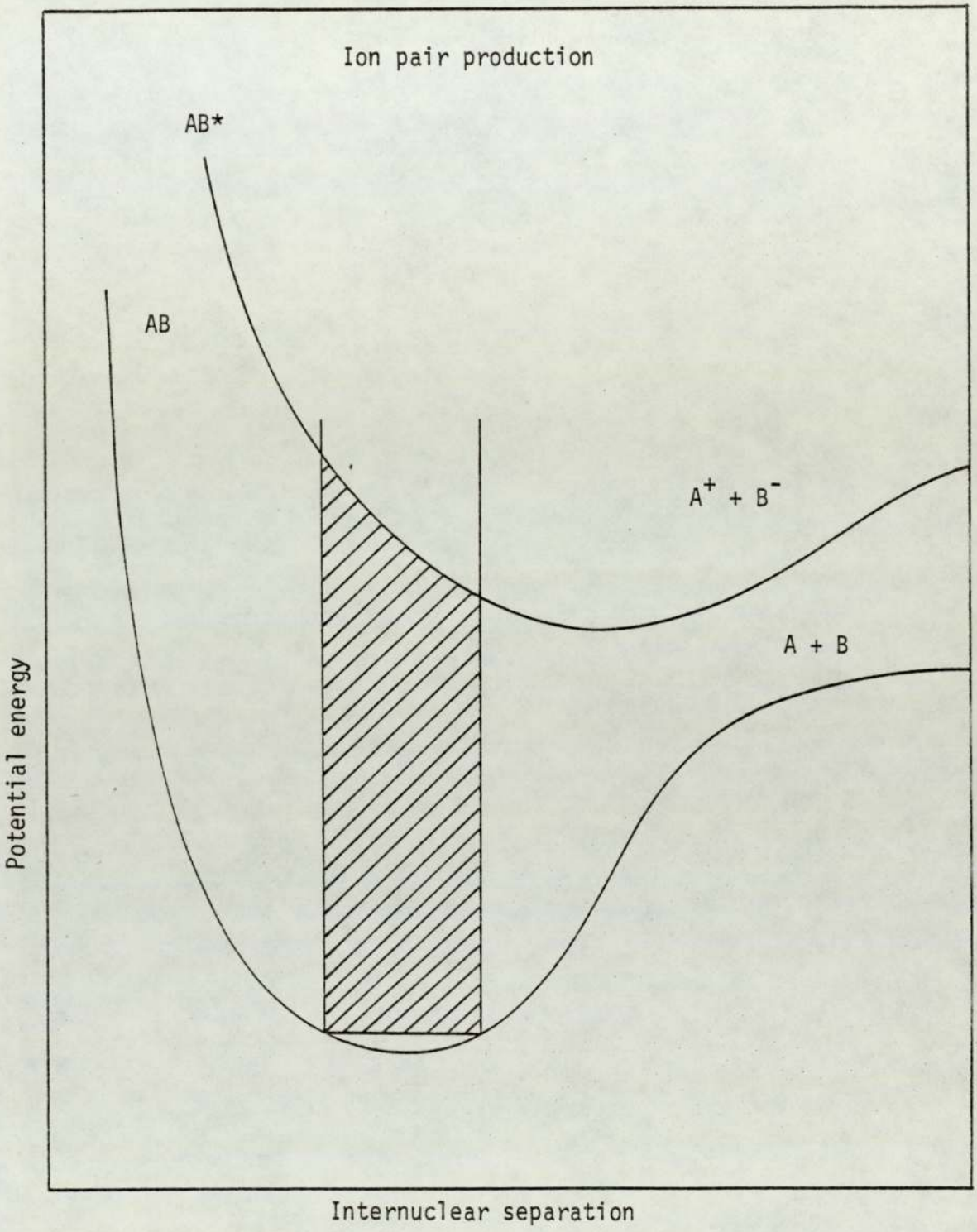

Figure (4.15) Potential energy curves showing the formation of negative ion formation from a diatomic molecule by ion pair production

The potential energy curves in Figure (4.14a) show dissociative transitions through the region of both the attractive and repulsive state of AB^-. Franck-Condon transitions to the attractive state will lead to dissociative capture for electron energies between E_1 and E_2 if levels above the dissociation limit of AB^- are populated. Dissociative attachment will occur for energies between E_3 and E_4 for the repulsive state.

For dissociative resonance processes where the products are produced from levels above the dissociation limit, A and B^- contain excess translational excitation energy. The translational energy is partitioned between A and B^- according to the conservation of momentum.

Dissociative attachment may occur to a bound state of the negative ion, which then undergoes internal conversion to a repulsive state that gives dissociation ionization as shown in Figure (4.14b) Curve 1 represents the bound state and incident electrons are initially captured into this state. Intramolecular radiationless transitions to curve 2 occur before auto-detachment becomes a significant problem.

The molecule then undergoes dissociation from curve 2 to give $A + B^-$.

The energy at which the fragment ion B^- first appears, the appearance potential AP (B^-), is related to the electron affinity of B, E (B), and the bond dissociation energy, D (A - B), by the following equation

$$D\ (A - B) = AP\ (B^-) + E\ (B) - \sum W \qquad \ldots\ (4.16)$$

where W is the total kinetic and excitation energy which fragment species may have. Because it is difficult in practice to

measure the excess energy terms, equation (4.16) is frequently written

$$D(A - B) < AP(B^-) + E(B) \quad \ldots (4.17$$

Thus the dissociative resonance process can be used to measure the electron affinity of ion products or the bond dissociative energy of AB.

The ion-pair process, reactions (1) and (2), is shown in Figure (4.15) In this case electron impact reactions are not usually attachment reactions because the incident electron is not captured but merely serves to excite the molecule to an electronic level that leads to $A^+ + B^-$ (or $A^- + B^+$).

Ion-pair processes are produced by photo impact as well as electron impact, hence the curves in Figure (4.15) are valid for any type of excitation.

The scattered electron can carry away excess energy and the process can take place over a wide energy range from the threshold. The products may contain excess internal and translational energy in a manner similar to that noted for the dissociative resonance capture case. For ion-pair processes there is a minimum energy at which the reaction will occur to give B^-, usually called the appearance potential AP, given by

$$AP(A^+) = AP(B^-) = D(A - B) + I(B) - E(A) + \sum W \quad \ldots (4.18)$$

where I(B), the ionization potential of B, must be greater than E(A) for the process to be exothermic.

The cross-section of ion pair formation increases approximately linearly from the threshold up to an energy roughly three times

the threshold. The cross-section then steadily decreases with increasing energy, where the reaction cross-section is directly proportional to the rate of ion production.

Although ion-pair processes can give information on electron affinities, bond energies or ionization potential, work has mainly been restricted to electron affinities and bond energies.

Several types of mass spectrometers have been used in relation with negative ion formation.

These include conventional mass spectrometers[146], time of flight instruments[147], spectrometers with high-pressure sources[148] and the ion cyclotron resonance (ICR) spectrometers[149].

It has often been stated[140,143] that the ratio of negative ions to positive ions formed in an ion source is generally of the order $1:10^3$. This factor together with the experimental difficulties in obtaining suitable conditions in the ion source (i.e. the presence of ions produced by different processes at different energies of the electron beam) have been cited as reasons why negative ion mass spectrometry has not been generally accepted as an aid to the structure determination in chemistry.

The best illustration of the use of negative ion mass spectrometry for the structure determination is afforded by the spectra of acetylacetonate type complexes.

MacDonald and Shannon[150] first reported that compounds of the type (1) (M = Co or Cu) produced abundant molecular anions. An introductory study has shown that the negative ion spectra of a number of divalent and trivalent metals with hexafluoroacetylacetonate and trifluoroacetylacetonate ligands are equally informative and often more so than the corresponding positive ion spectra. Such systems are most suitable for negative ion studies, as

either the metal or the ligand may accept the secondary electrons. The positive and negative ion spectra of copper hexafluoroacetylacetonate obtained by Bowie and Williams[151] using an R.M.U.6 instrument operating at 70 eV, are shown in Figure (4.16).

In general, peaks due to molecular anions and the ligand radical anion ($L^{-\cdot}$) predominate. Peaks of small abundance due to fluorine migration are also present.

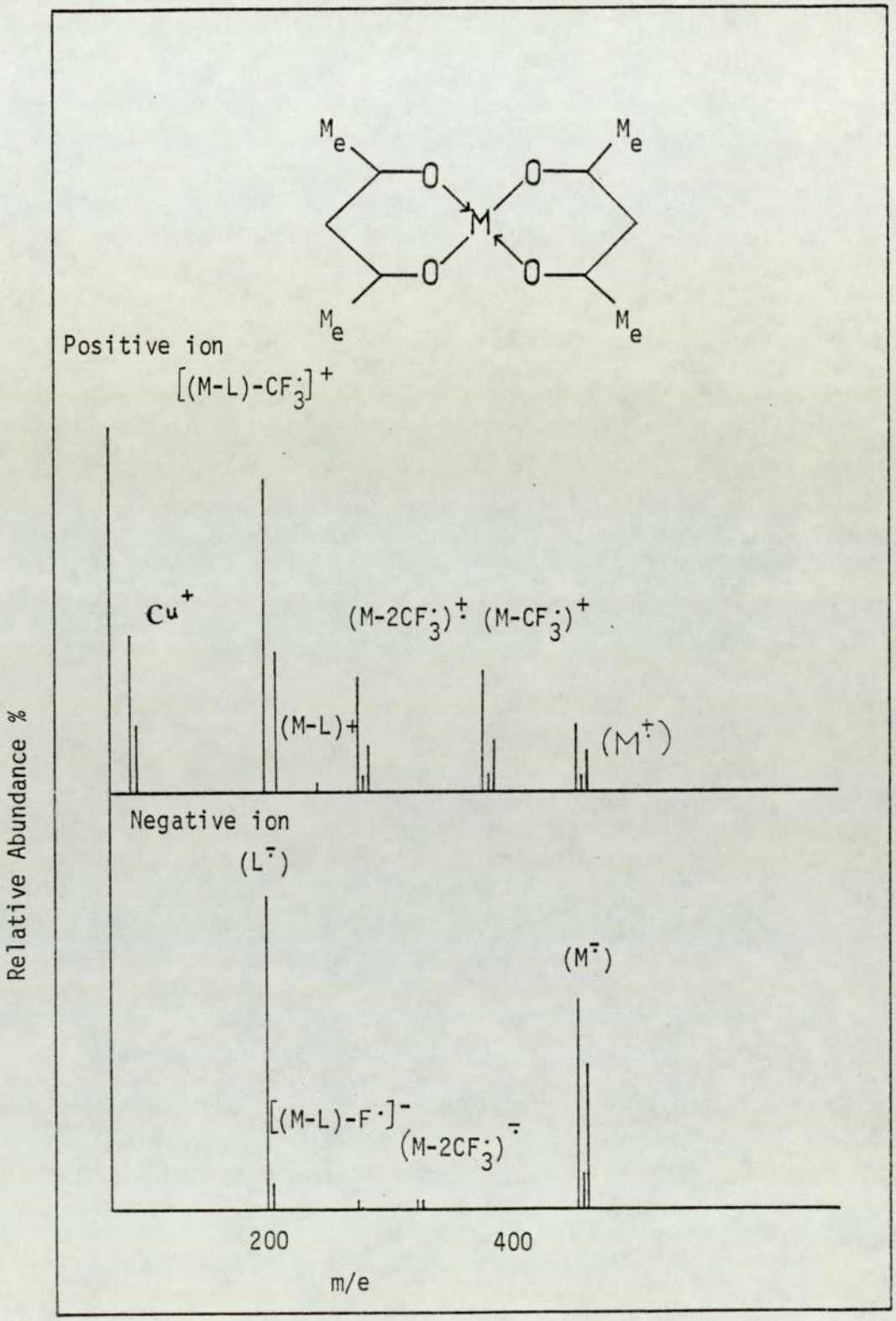

Figure (4.16) Positive and negative ion spectra of copper hexafluoroacetylacetonate

CHAPTER 5

Electron Work Function Measurements

5.1 Introduction

Since the object of this study is to investigate various aspects of negative surface ionization in relation with electron affinity determination, it was desirable to study the electron work function of the filaments being used in this work.

As mentioned earlier, there are several methods available for the experimental determination and theoretical calculation of the work function for a particular material.

In this work, the work function of Ta, W, and Pt filament was measured by the thermionic method.

The surfaces[109] of real emitters are nearly always heterogeneous, this means that their emission and adsorption characteristics are functions of the surface coordinates.

Emitters used in practice are prepared in form of wire, ribbon, or in form of layers deposited on a substrate The structure of such materials is polycrystalline and consequently the surface of the emitters constitutes an irregular "mosaic" of various single crystal faces, which are oriented differently relative to the geometric surface of the specimen.

There is also an adsorption of foreign particles arriving at the surface from the surrounding space as well as from the bulk of the emitter.

It is not possible to obtain ideal homogenous surfaces of macroscopic dimensions, such surfaces constitute a theoretical abstraction.

5.2 The Apparent Electron Work Function[152,153]

The application of thermodynamic and statistical mechanics to the calculation of the saturated current density, j_e, for electrons emitted from a conductor at temperature, T, leads to the well known Richardson - Laue - Dushman equation

$$j_e = AT^2 (1 - \bar{r}e) \exp - x/RT \qquad \ldots (5.1)$$

where A = thermionic constant

$\bar{r}e$ = zero field reflection coefficient

x = work function

If the surface of the emitter is uniform then from equation (5.1) a plot of experimental values of $\ell n\, j_e/T^2$ as a function of (1/T) will give a straight line from which the "apparent" (or Richardson) work function can be calculated.

The key assumption which has been made in the derivation of the well known Richardson - Laue - Dushman equation (5.1) is that the surface of the emitter is uniform (i.e. single crystal).

The surfaces of most experimental emitters are far from uniform; these surfaces consist of patches which have different work functions.

Hence the electron work function measured for "patchy" surfaces is not expected to be"the true work function" but the "experimental electron work function" of that "particular" emitter.

It can be seen that in order to determine the work function by thermionic emission, the temperature of the surface must be varied and if the thermionic emission is used to determine work

function changes there are two factors to consider:

(1) Work function changes can only be measured at temperatures where thermionic emission is measurable and at this temperature many adsorbed films may be destroyed.

(2) If adsorption does occur at the elevated temperatures required for thermionic emission then variation of the temperature may cause the surface coverage to change.

If the surface concentration of adsorbed species is n molecules cm^{-2}, then at equilibrium,

$$n = v\,\tau \qquad \ldots (5.2)$$

where v = bombardment rate from gas phase

τ = mean life time of adsorbed species on surface.

The variation of τ with temperature is normally expressed by the Frenkel equation[154]

$$\tau = \tau_o \exp \frac{(Q)}{RT} \qquad \ldots (5.3)$$

where Q = heat of adsorption

τ = constant (vibration time of adsorbed molecule with surface) $\simeq 10^{-13}$ sec.

Therefore,

$$n = \nu\tau_o \exp \frac{(Q)}{RT} \qquad \ldots (5.4)$$

Interpretation of work function changes found by the temperature dependence of electron emission is therefore not simple but

it is possible providing the above factors are taken into account.

5.3 Experimental

It is of the utmost importance to determine the electron work function of the filaments used in this study before proceeding to any further investigation.

These determinations served as a check on modifications made on the Ion Source and the choice of experimental conditions and also to study the various conditions which affect the electron work function of the filaments.

In this work, tantalum, tungsten and platinum filaments have been used with each sample gas studied by the mass spectrometer.

When a convenient vacuum was reached (about 2×10^{-8} torr), the filament was heated gradually using a D.C power supply to a high temperature ($2500^{o}K$), the filament was left at that high temperature for about an hour, by this time the filament was crystallized.

Afterwards, the electron current measured by an avometer was found to be almost constant at any temperature choosen afterwards. This was taken as sufficient time for the filament to be degassed. The electronic current dependence on temperature was studied in the range of $(1700 - 2000)^{o}K$, (depending on the filament material). The electron with drawing voltage applied to the grid and the anode was enough to overcome the space charge effect (this was confirmed by increasing the grid potential and observing that the electronic current was, almost, constant which means that the electronic current was saturated).

In order to facilitate experimental measurements it was

found convenient to calibrate the temperature of the filament as a function of the current through it (j_f). The optical temperature was measured using a disappearing filament pyrometer (Leeds and Northrup) - type 8630 (6530 $\mathring{A}$ filter), and corrected to the true temperature according to Figure (5.1) to allow for emissivity effects and also absorption by the glass window through which the filament is observed.

A plot of the filament current (j_f) against T, and T^2 are shown in Figure (5.2) and (5.3). It could be seen that the plot of j_f against 1/T is linear over a large temperature range and could be used for several experiments before being checked.

However, to eliminate any sources of error which might be due to temperature measurement (slight changes because of the filament decay at high temperature), the optical temperature of the filament was measured in each experiment together with the heating current.

Throughout the course of the measurements, it has always been possible, after strong pumping and heating, to reach a reproducible state, with a clearly defined temperature dependence of the electronic current.

5.3.1 Platinum filaments

Prior to the work function measurement the new Pt filament was operated continuously for many hours at high temperatures (>2300^{o}K) to ensure complete outgassing of the filament and its support. After this treatment, pressure of $\sim 2 \times 10^{-8}$ torr could be obtained and maintained with the emitter at its usual operating temperature (1300 - 2000^{o}K).

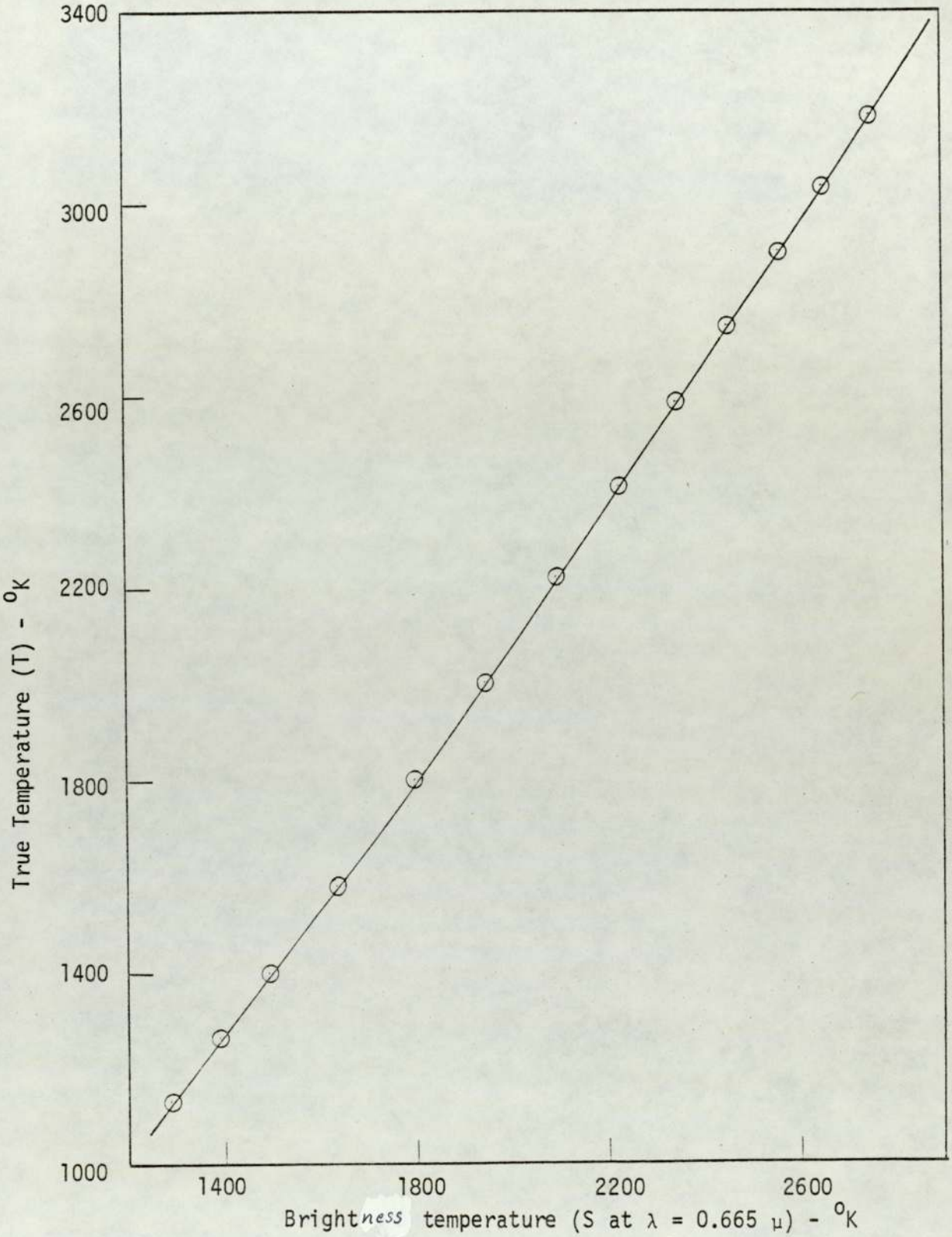

Figure (5.1) True temperature Vs brightness temperature S for the effective wave-length λ = 0.665 μ (Ta)

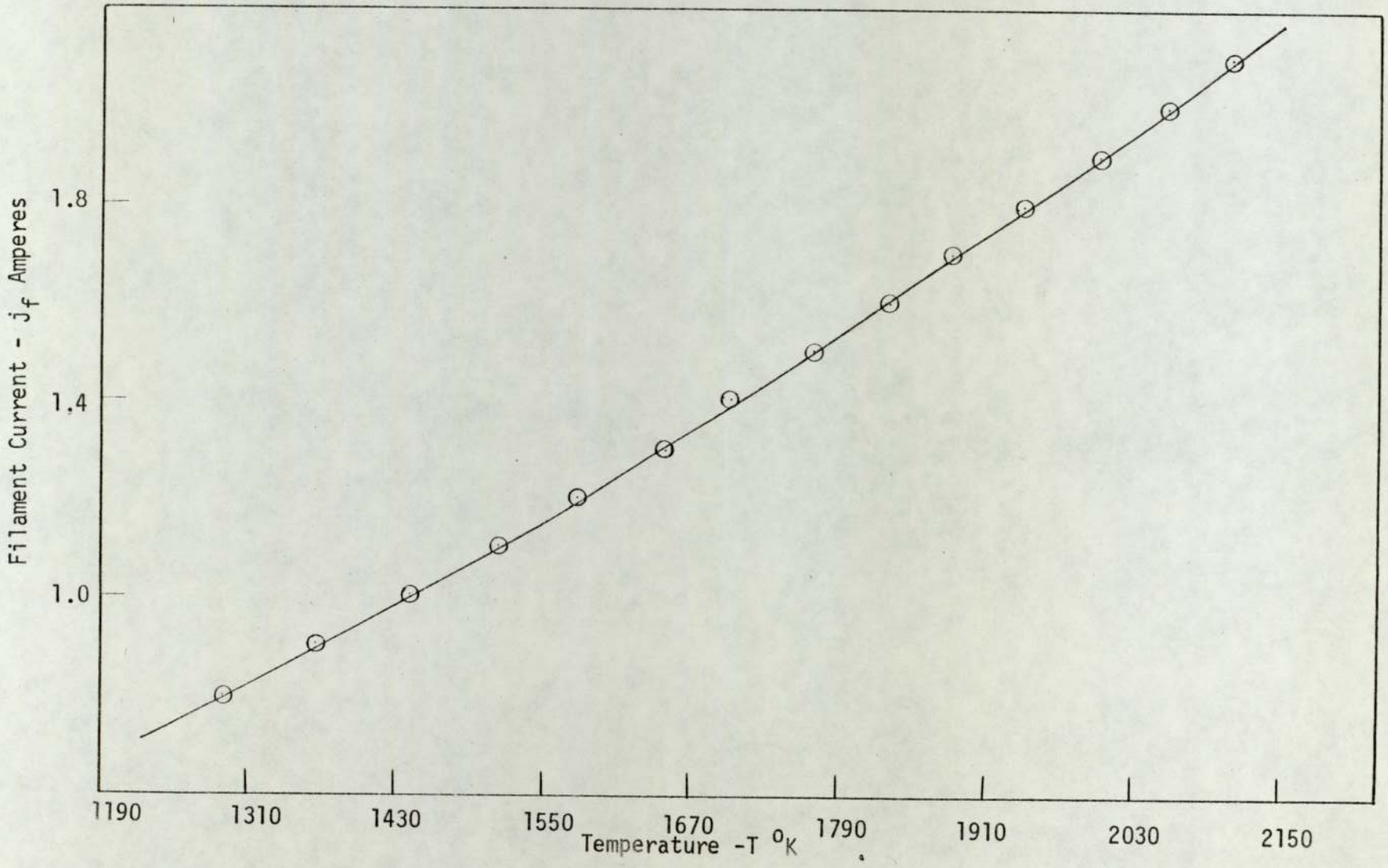

Figure (5.2) Filament current as a function of temperature

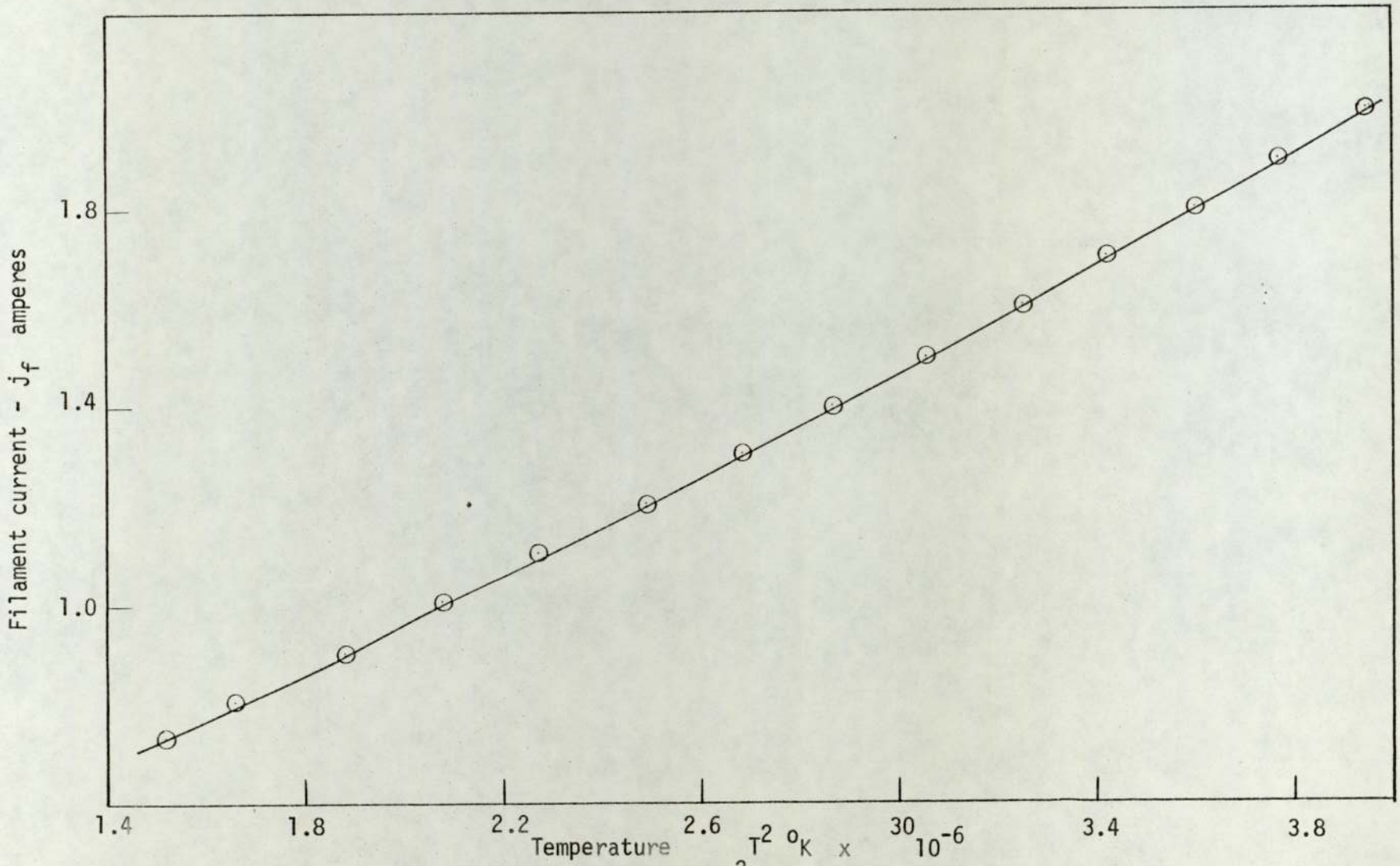

Figure (5.3) Filament current as a function of T^2 (Ta)

Typical log j_e - T^{-1} plots for Pt both clean and with the presence of sample gases are shown in Figures (5.4) and (5.5).

The average (apparent) electron work function of the platinum was found to be (4.55 eV) and the work function was found to remain unchanged in the presence of the sample gases.

This value is in accord with literature values for a poly-crystalline platinum[155] of 4.72 eV.

5.3.2 Tantalum filaments

The above mentioned procedure was adopted to outgass tantalum filaments.

The average (apparent) electron work function of the clean tantalum surface was found to be (3.96 ev) which is in good agreement with the literature value[155] (4.12eV). Exposure to organic materials produced carburised tantalum filaments with a much higher electron work function (5.25 eV) which is in agreement with many literature values of TaC.

It was routine to pass benzene vapours over the hot filament to avoid any changes on the electron work functions during the experiment. Figures (5.6) and (5.7) show a typical plot of log j_e against 1/T for Ta and TaC filaments respectively.

5.3.3 Tungsten filaments

The apparent electron work function for clean tungsten found to be 4.20 eV compared with the recommended literature[155] value of 4.50 eV.

Figure (5.8) shows typical plot of log j_e against 1/T. Lowered work function values were observed in the presence of

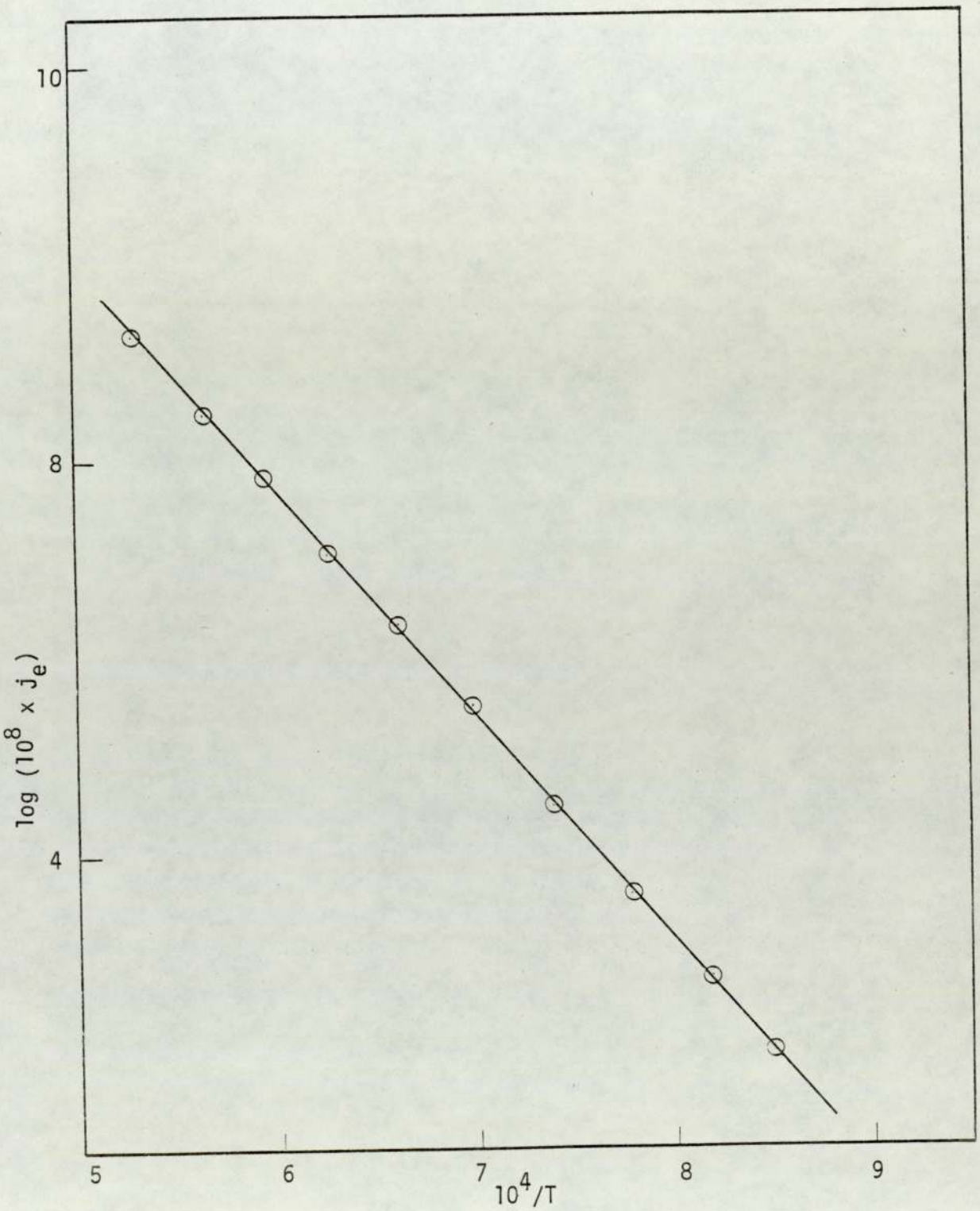

Figure (5.4) Electron work function of "clean" platinum

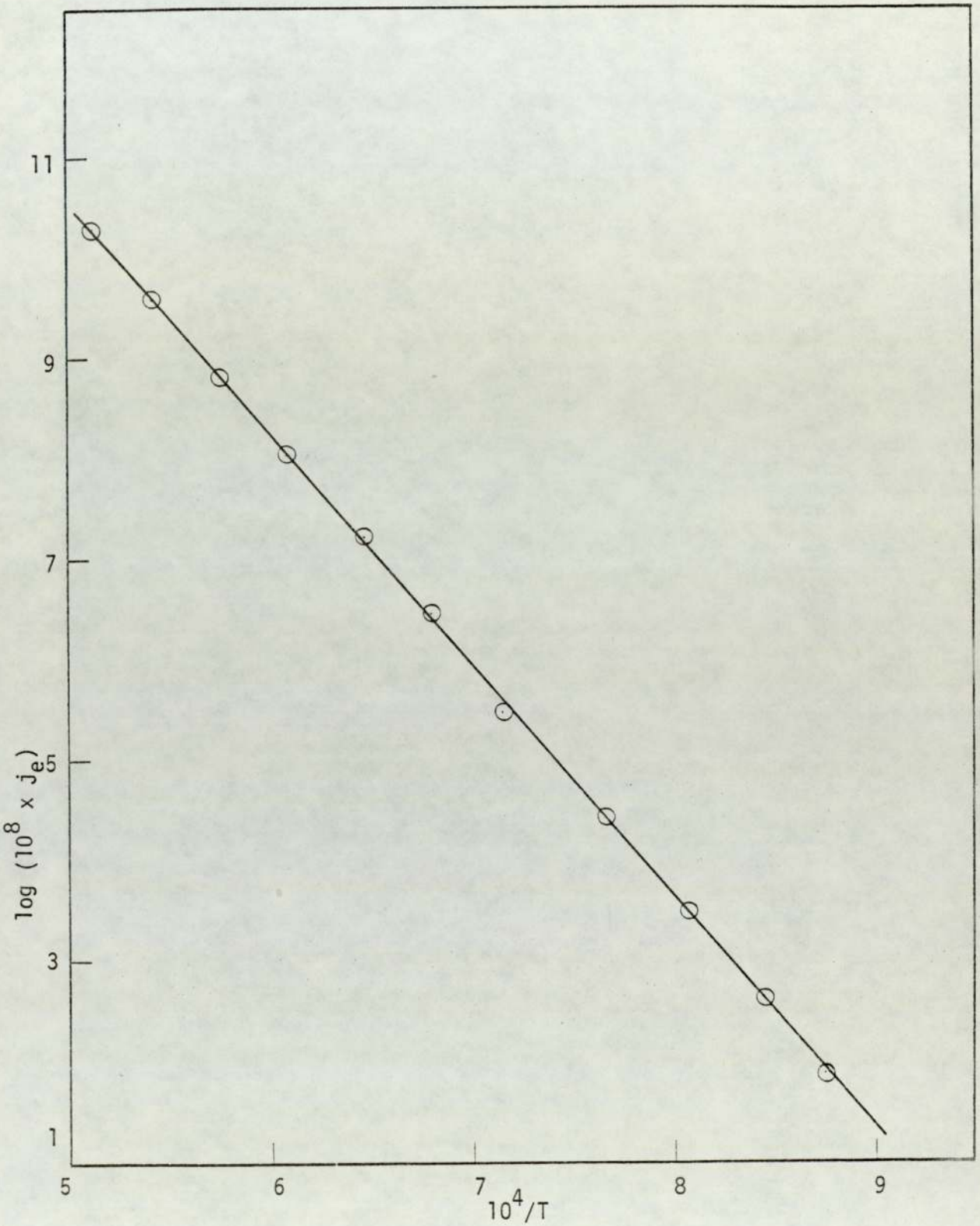

Figure (5.5) Electron work function of platinum in the presence of sample gas

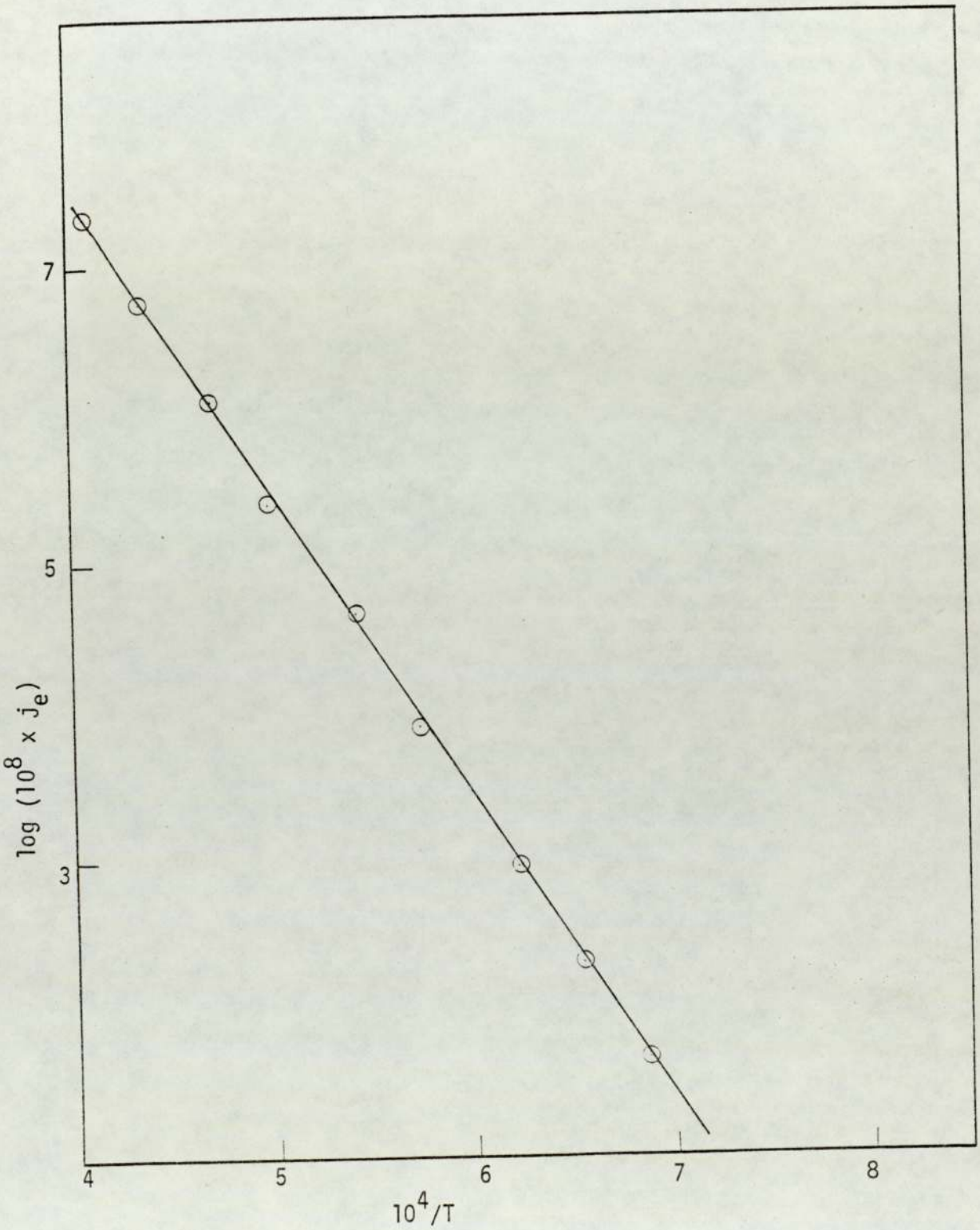

Figure (5.6) Electron work function of tantalum

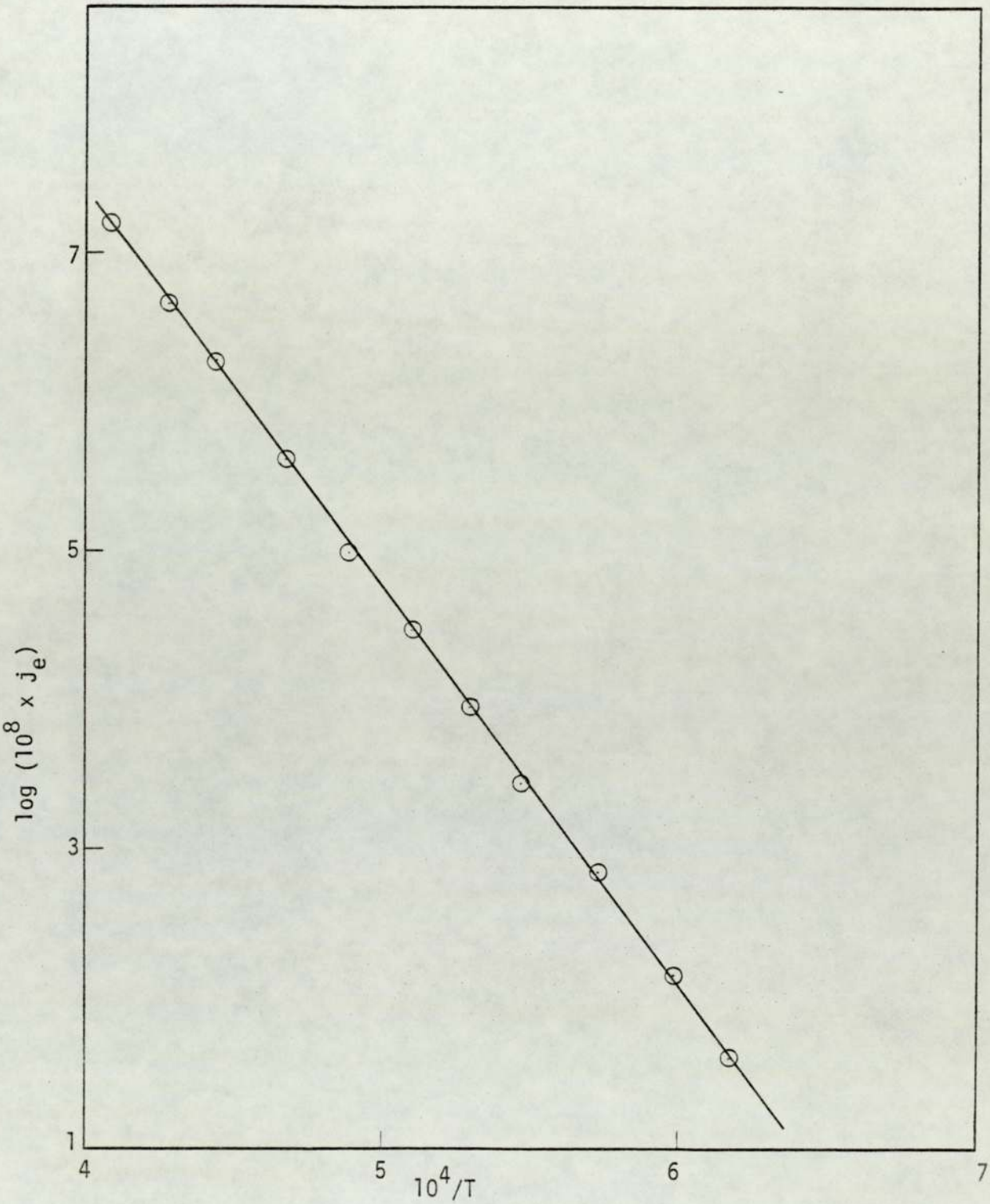

Figure (5.7) Electron work function of Tantalum carbide

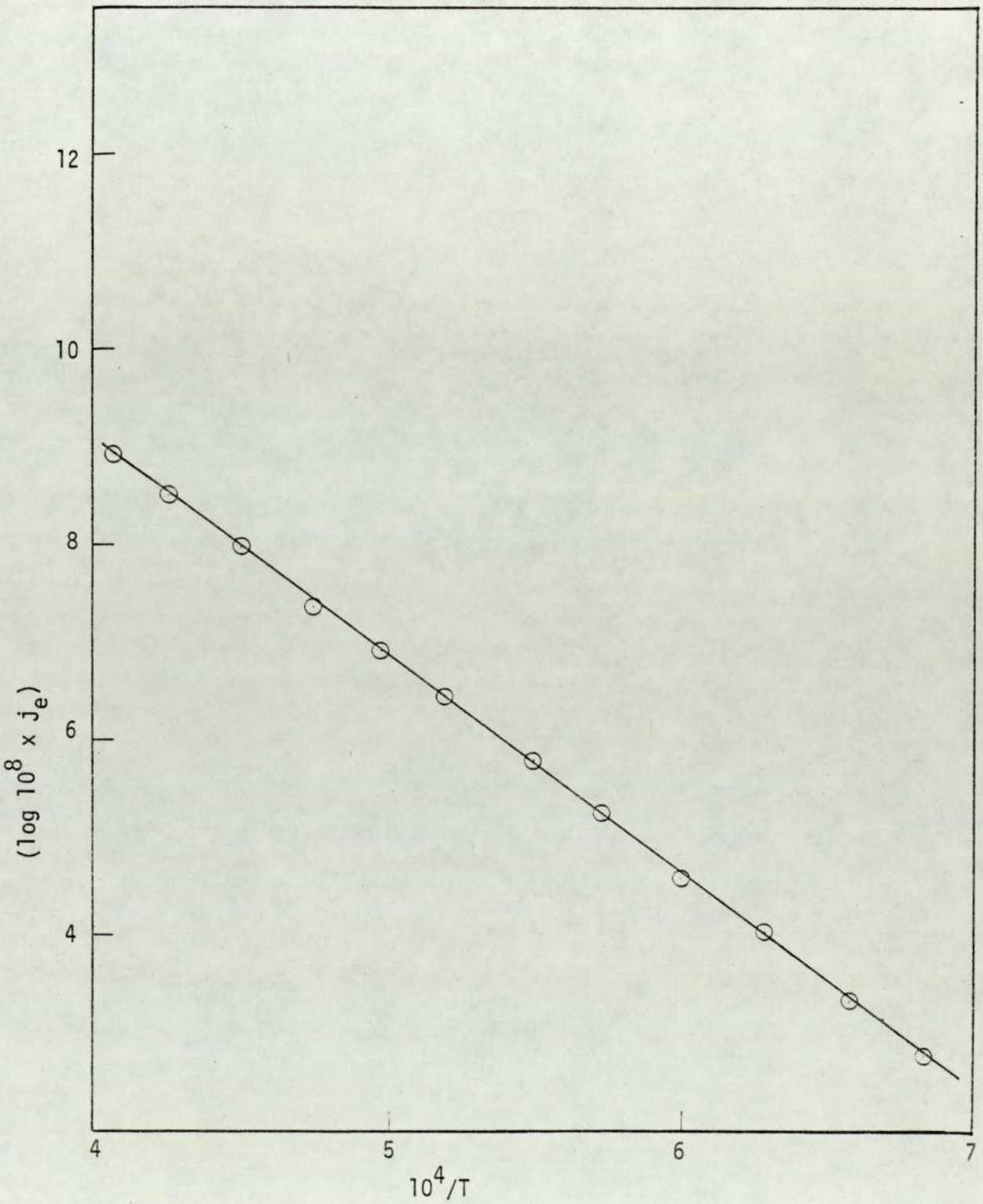

Figure (5.8) Electron work function for tungsten

sample gases. Figure (5.9) shows a plot of log j_e against 1/T for tungsten carbide, the apparent electron work function was found to be 3.8 eV.

The temperature dependence of the electronic current, although reproducible, could not be held to be a fundamental property of the filament material, since it showed a tendency to vary from one batch to another, and to show a slow ageing, but it was nevertheless a well-defined and readily measurable quantity, and one which could be used as the work function of a "particular" filament with confidence.

Usually the variations were slight, being within the experimental error. The experimental work functions obtained in this work were close to the values quoted in the literature, and were used as a test of the proper functioning of the instrument.

The results obtained above are summarised in Table 5.1.

5.4 Measurements of Apparent Electron Affinity

Calculation of $\bar{E}'(T)$

5.4.1 Method of Page and Goode[4]

The apparent electron affinity, $\bar{E}'(T)$, at the mean temperature of the experiment is evaluated from the expression of Page and Goode: at constant pressure

$$\bar{E}'(T) = -R \, d \, \&n \, (j_e/j_i)/d(1/T) \qquad \ldots (5.5)$$

where R is the gas constant.

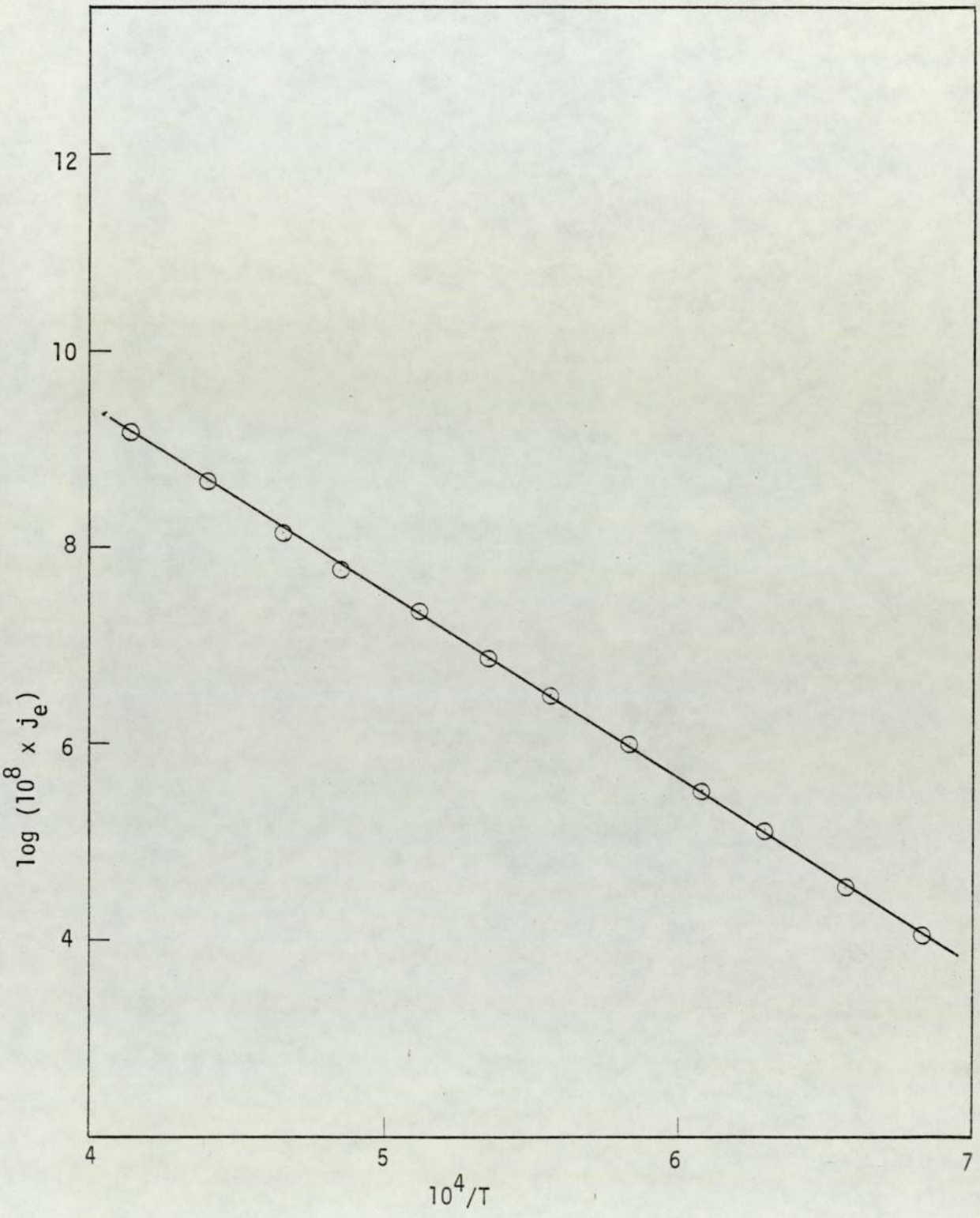

Figure (5.9) Electron work function for tungsten carbide

Table 5.1 Practical Electron Work Function

Filament	Experimental eV	Literature eV
Platinum	4.55	4.72
Tantalum	3.96	4.12
Tantalum Carbide	5.25	3.77
Tungsten	4.20	4.50
Tungsten Carbide	3.80	4.58

5.4.2 Method of Gaines and Page[156]

The apparent electron affinity, $E'(\bar{T})$ at the mean temperature of the experiment is evaluated from the expression of Gaines and Page: at constant pressure

$$x(\bar{T}) - E'(\bar{T})/x(\bar{T}) = d \ln j_i / d \ln j_e \quad \ldots (5.6)$$

where $x(\bar{T})$ is the thermionic work function of the filament, which may be taken from the literature[152,153,157] or derived experimentally.

In the later case the appropriate expression is at constant pressure:

$$x(\bar{T}) = -R \, d \ln j_e / d (1/T) \quad \ldots (5.7)$$

5.5. Transmission of Electrons Through the Mass Filter

The transmission coefficient may be defined as the ratio between the current produced on the filament surface (ionic and electronic) and the current arriving at the detector plate through the quadrupole field. It is of great importance to check the constancy of this value, to make sure of the proper allignment of the filament (that it does not twist upon changing the temperature) and that there is no considerable carbon deposits over the ionization source which might inhibit the ions from reaching the Faraday cup (which might act as a capacitor).

This was achieved by comparing the electronic current at the anode (measured by an avometer) and the electronic current at the

Faraday cylinder (measured by the amplifier). At a given temperature, with the mass filter tuned to pass only electrons (first mass = 0), the electronic current at the anode (j_A) and the Faraday cylinder (j_e) was measured. Measurements were carried out at several temperatures. A graph showing the constancy of the transmission coefficient over a wide range of temperatures is shown in Figure (5.10).

It was noted that when the filament was heated at the beginning of each run there was a slight deviation from the straight line, this is due to desorption of gasses out of the filament surface.

Figure (5.11) shows a plot of log (j_A/j_e) versus 1/T where an almost straight line was obtained, but deviation occurs at high measured currents.

The deviation from a linear behaviour may be accounted for by the presence of a space charge effect within the quadrupole field.

Dawson and Wetten[88] have calculated the maximum ion current which may pass through a quadrupole field. From their results, the maximum electron current expected to pass through the mass filter is about 5×10^{-8} amps. Deviation occurs at measured currents higher than 3×10^{-8} amps, which is in agreement with the expected value.

A high thermionic emission of elctrons was observed, especially when the mass filter was tuned at low mass number, to stop this strong electronic current from arriving at the Faraday cylinder, a handmade magnet of about one Gauss strength (measured by a gauss meter) was placed around the ionization source (outside the instrument).

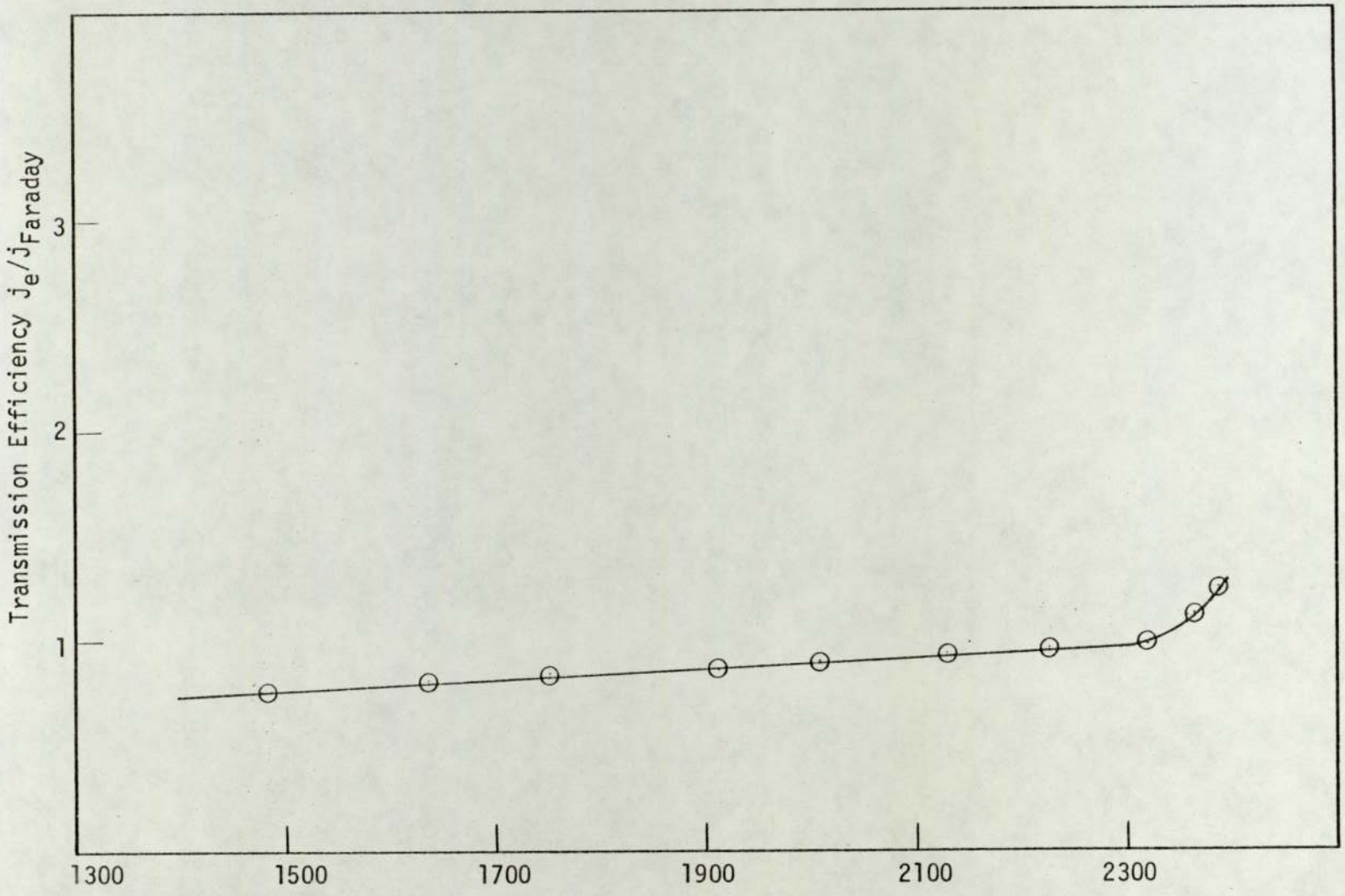

Figure (5.10) Constancy of transmission efficiency

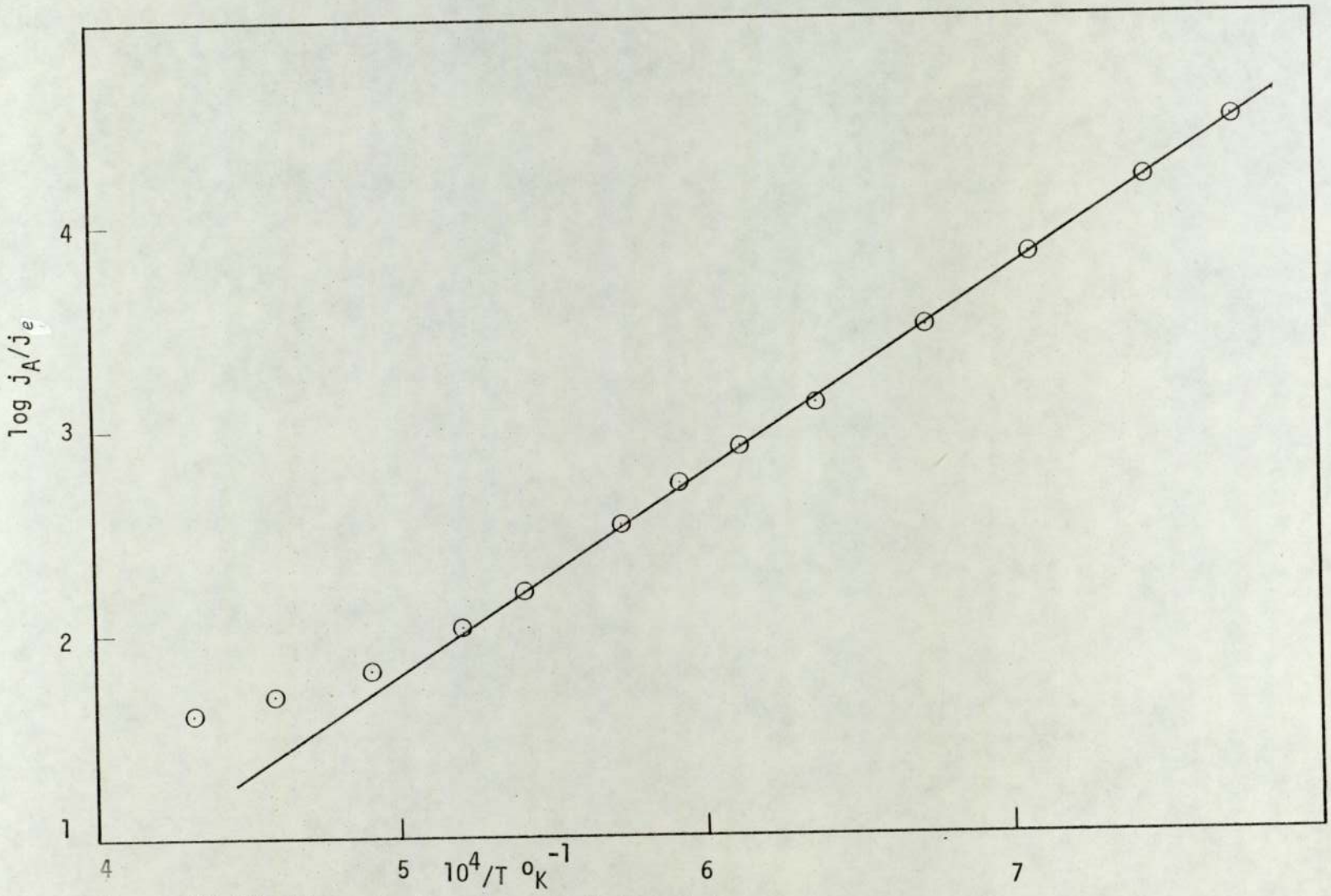

Figure (5.11) Transmission characteristic plot

5.6 Electron Affinity of CCl_4

The most serious problem encountered by Chamberlain[158] was, the observation of both positive and negative ion peaks during his investigation of the ionization of various substituted pyridines, interhalogens, and cyanogen halides, whereas he expected negative ions only. As expected (from such an observation) anomalous results were obtained and were explained quantitatively on the basis of positive ion formation, by negative ion collisions with the sample vapour, in the mass filter.

To investigate the reasons behind the observation of positive ions in the negative ion mass spectra, it was decided to study all the possibilities which might have led to such observations.

One of the possible reasons is the electrical conditions of the ionization source.(The relation between the voltages applied to the filament, grid and the collector (anode), the quadrupole ionization source chamber and the ion focus lens under which the negative ions are accelerated towards the detector.

It was feared that the electron with drawing voltage might have affected the results obtained by Chamberlain and that the electrical conditions might have been favouring the acceleration of any positive ions produced either on filament surface or in the quadrupole field. In order to check this possibility, the negative surface ionization of carbon tetrachloride was studied extensively, and all the conditions which might lead to the formation of positive ions, and consequently their presence in the negative ion mass spectra were investigated.

The first step to prevent any positive ion from reaching the

Faraday cylinder and consequently appear in the mass spectra, was to set up the electrical conditions of the ionization source which favour the drawing of positive ions towards the other side of the quadrupole field, away from the detector.

The second step was to set the detector at a positive potential to ensure that the positive ions (if formed for any reasons within the mass filter region) will not reach the detector.

In the first few experiments aimed at finding the best electrical conditions of the ionization source, positive ions (Cl^+) were noticed, although chlorine is well known for giving very strong negative currents (Cl^-)[159,160].

Upon variation of the electrical conditions several times, at one stage no ions (positive or negative) appeared in the mass spectra, while in another stage the only ions observed were negative ions.

Figure (5.12) shows the best electrical conditions reached after several experiments. This was facilitated by the ion focusing lens which was originally set on negative potential (for positive ion detection) to extract positive ions from the ionization chamber and to focus them in conjunction with the filter end and plate into the quadrupole analyser.

This lens could be varied between 0 and ±60 volt. (Access being obtained by removal of the top panel and adjusting RV1 on PCB2 while the avometer is connected to pin No. 6 of the analyser feedthrough - interace connection).

This lens was kept at slightly positive potential. The results obtained from these preliminary experiments clearly indicated that the drawing potential applied to the various parts

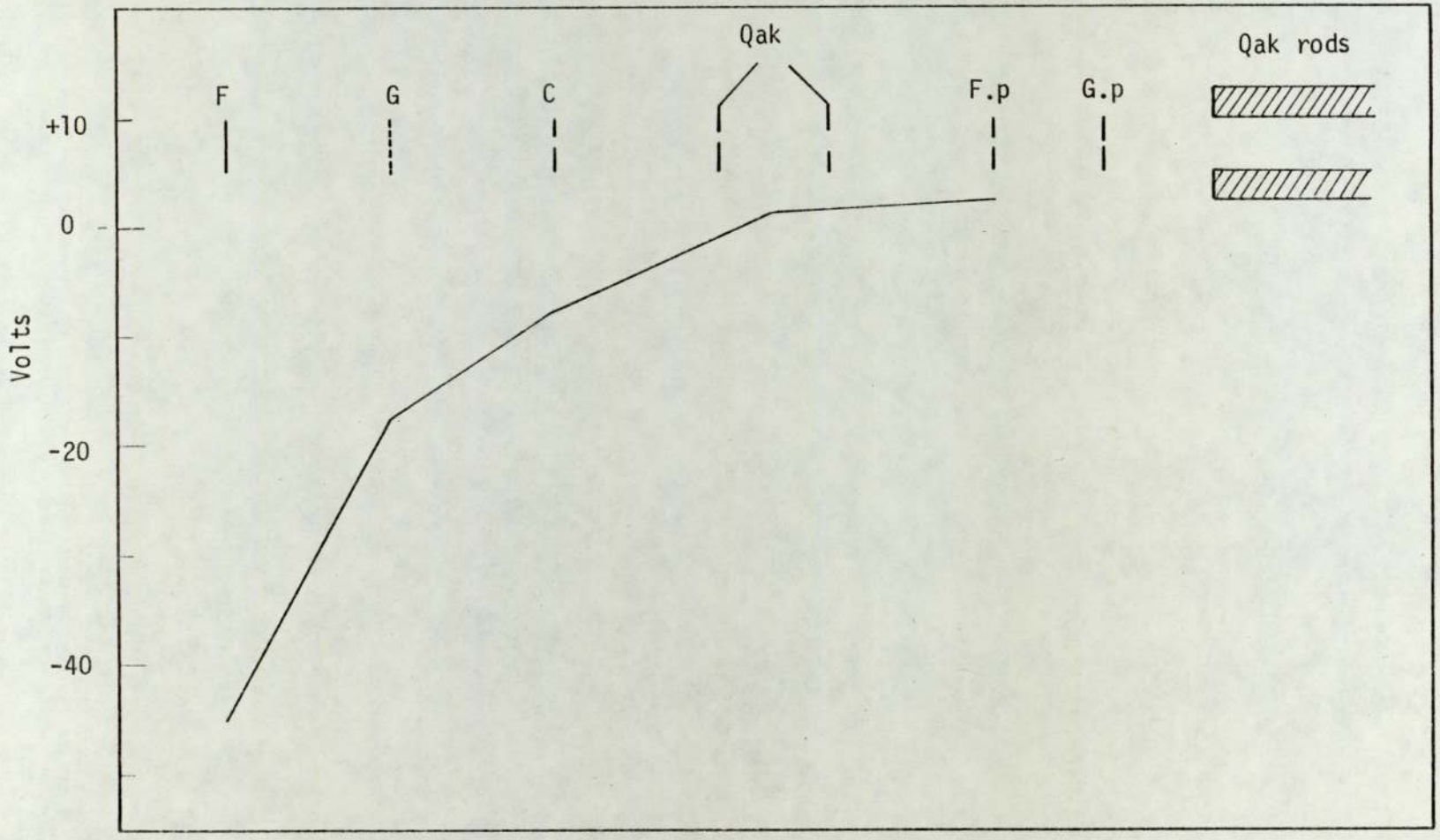

Figure (5.12) Ion accelerating potential

of the ionization source were of great importance, and at this stage were thought to be responsible for the presence of positive ions peaks (other reasons yet to be examined). This is because as mentioned earlier the quadrupole mass spectrometer is insensitive to the sign of the charge on the transmitted ion. Hence for a given set of analyser field settings both positive and negative ions of a particular mass/charge ratio may be transmitted simultaneously through the filter. This is not the case with a magnetic sector instrument.

The filament EMISSION ON/OFF switch (Qak) enables potentials to be applied to the standard ion source lens plates to facilitate the focusing of ions from external regions (our ionization source) through the source into the quadrupole filter.

Further assistance to the transmission of a negative ion through the source is given by reversing the polarity of the ionization chamber and focus plate potentials, this is achieved by selecting the NEGATIVE ion position of the positive/negative ion switch on the rear panel of the control unit.

In the latter switch position the ionization chamber potential (varied by means of the ION ENERGY dial on the control unit front panel) is negative with respect to ground and the ion focus potential is positive with respect to the ground.

5.6.1 Composite Spectra[161]

When a Faraday plate or first dynode monitoring is used at the detector it is possible to accelerate negative ions through the standard ion source while it is operative. In this way three types of spectra may be produced after carefully regulating the parameters involved. These are:

(1) Negative ion spectra from the external source

(2) Gas phase positive ionization spectra

(3) Composite spectra

Both positive and negative ions may be produced at the same mass. This is likely in the case of the more electronegative elements such as F, Cl and O. In these cases the ions will appear at the same point in the spectra and the composite results will involve diminished peaks in one particular sign. An example of this is shown in Figure (5.13).

In the case of more complex molecules (e.g hydrocarbons, fluorinated hydrocarbons etc.) the negative ion spectra tend to complement the positive ion spectra and few diminished peaks appear in the composite spectra Figure (5.14).

5.7 Surface Ionization of Iodine and Bromine

5.7.1 Introduction

The surface ionization of iodine and bromine on various metal filaments has been studied closely and their electron affinities are well known. The following two experiments were carried out as a check on modifications made on the ionization source and the choice of experimental conditions and to make sure that the eletron affinities obtained were independent of the filament material.

5.7.2 Electron Affinity of Iodine

The surface ionization of iodine on various metal filaments

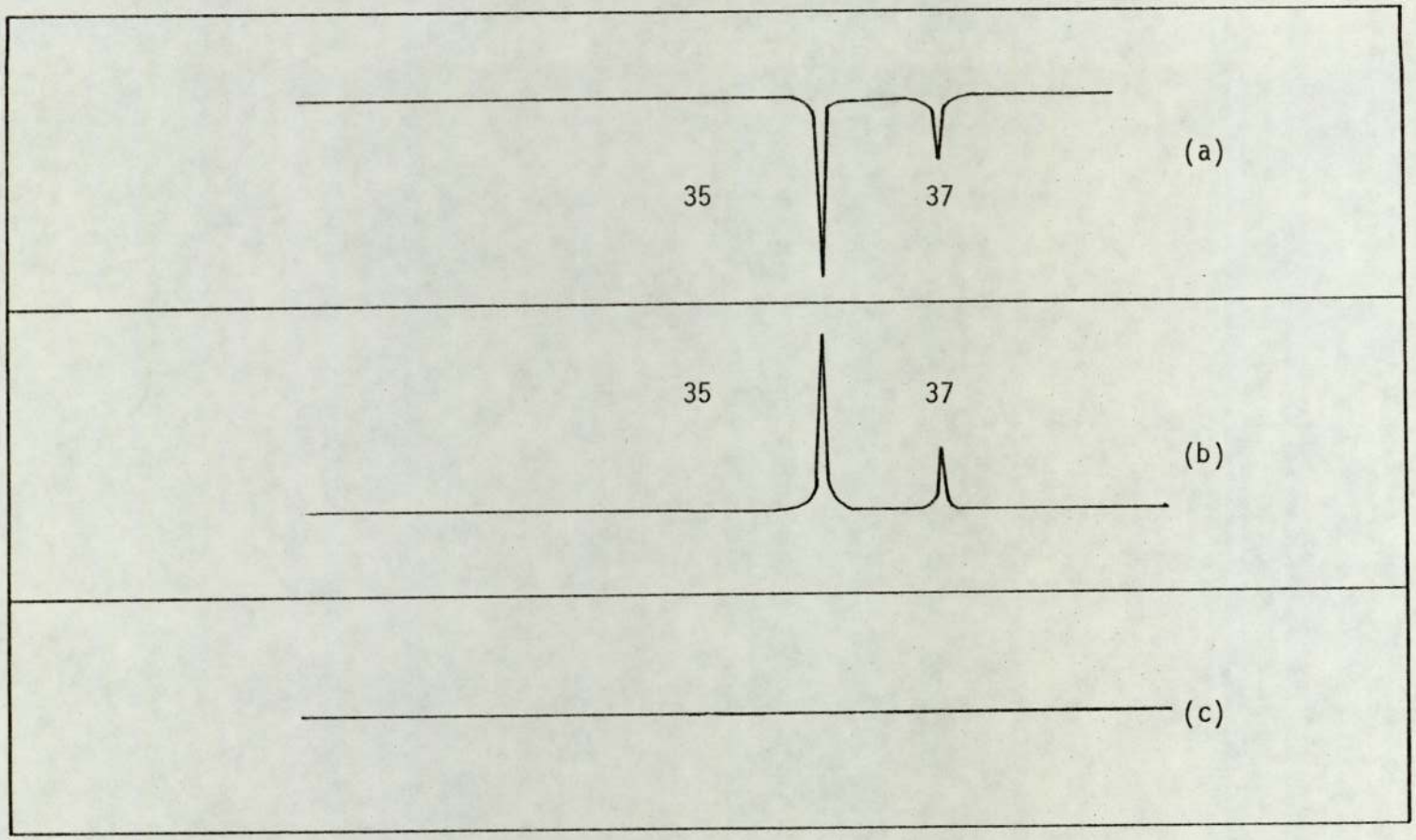

Figure (5.13) (a) Negative ion spectra of Cl_2 on Re

(b) Positive gas phase phase ionization spectra of Cl_2

(c) Balanced NIS' + PGPI spectra of Cl_2 showing diminished peak highest.

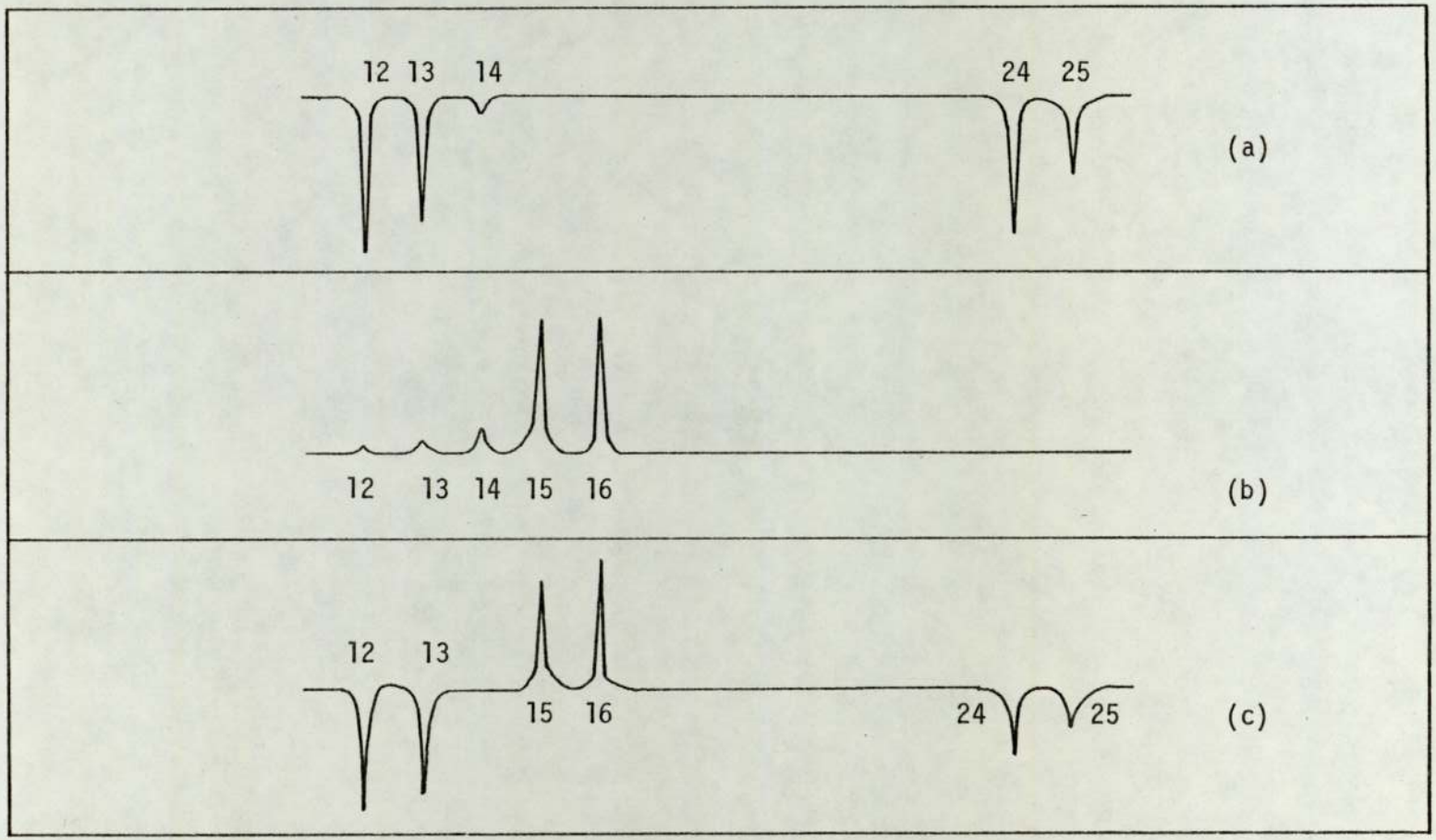

Figure (5.14) (a) NIS spectra of CH_4 on Re (b) Positive gas phase ionization of CH_4
(c) Balanced NIS + PGPI spectra of CH_4

has been studied closely and its electron affinity is well known. In 1935, there were the first two determinations of the electron affinity of iodine by surface ionization, one employing magnetron technique, and the other the space-charge method or shift in the volt-ampere characteristic.

The first, was that of Glockler and Calvin[122] where they obtained a value of 3.24 eV by the space-charge method. The second was that of Sutton and Mayer[72] where a value of 3.14 eV was obtained by the magnetron method. Since then several other methods have been used to determine the electron affinity of iodine, including optical methods[162,163].

As mentioned earlier the temperature dependence of the electron emission from a tantalum filament prior to the admission of iodine gave an apparent work function of 5.25 eV (Tantalum carbide). This value was found to be unchanged by the presence of iodine vapour.

The variation of iodine negative ion (I^{127}) current with temperature was studied by the mass spectrometer. A typical plot of log of the electron to ion (I^-) current ratio against the reciprocal of the filament temperature (log j_e/j_- vs 1/T) is shown in Figure (5.15). The average apparent electron affinity was found to be 3.21 eV which is in good agreement with the photodetachment [162,163] value of (3.05 to 3.10) eV.

5.7.3 Electron Affinity of Bromine

The early determinations of the electron affinity of bromine followed the work done on iodine.

The negative ion mass spectra gave two peaks of equal intensity

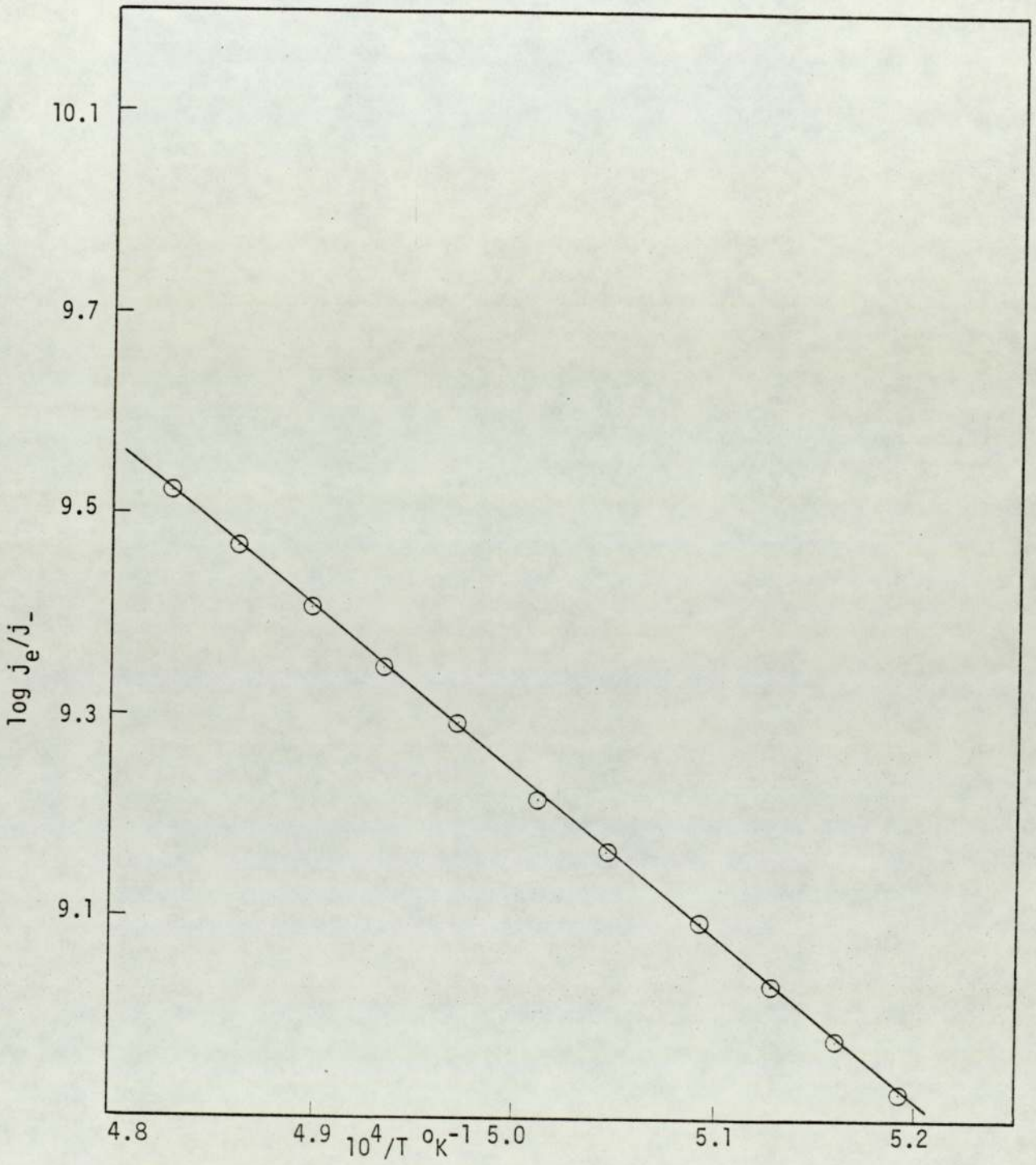

Figure (5.15) log j_e/j_i against reciprocal temperature for I^-

at an m/e value of 79 and 81, which were identified as the two isotopes of bromine (abundance of Br^{79}/Br^{81} is 50.57/49.43). A typical plot of log j_e/j_- (Br^-) against 1/T is shown in Figure (5.16).

The apparent electron affinity of bromine was found to be 3.32 eV which is in good agreement with the literature value[163] 3.36 eV.

The electron work function was found to be unchanged by the presence of bromine vapour.

The values determined for the electron affinities of bromine and iodine were in good agreement within the experimental error, with spectroscopic values.

5.8 Electron Affinity Determination

5.8.1 Introduction

In the light of the growing controversy about the validity of electron affinity determination obtained by the magnetron method, it was decided to study a few compounds some of which have been studied before by the magnetron to test some of the values obtained by this method, and to answer some of the criticism of the surface ionization systems and, consequently, the magnetron, for the determination of the electron affinity of atoms, molecules and radicals.

Chamberlain[158] pointed out that the magnetron method is non-specific and that the deductions drawn about the identity of the charge carriers on energetic grounds may be in error.

Herron et al[136] and Zandberg and Paleev[126] demonstrated that ions predicted to occur in the magnetron were not always observed in

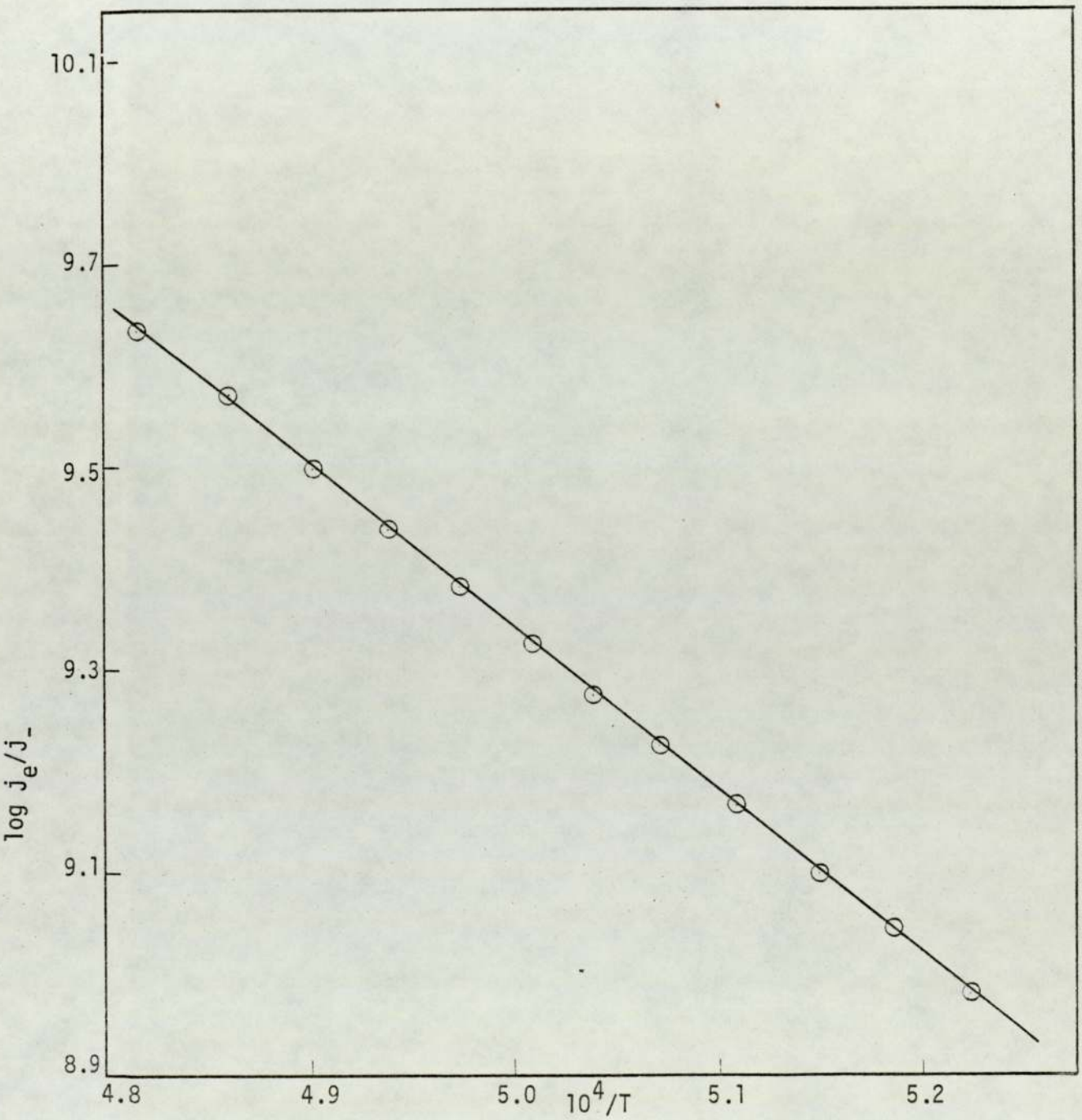

Figure (5.16) log j_e/j_i against reciprocal temperature for Br^-

the mass spectrometer.

Zandberg and Ionov[109] claimed that reliable results can be obtained only by mass spectrometry.

All the compounds mentioned in this work have been studied using the QqK quadrupole mass spectrometer (the details of its construction, and its ionization source have been described earlier).

Carbon etrachloride has a high electric strength, which is often associated with ease of negative ion formation.

Because it has been studied by the magnetron, and it is easy to handle, it was selected to be studied by mass spectrometry.

5.8.2 Carbon Tetrachloride

Negative surface ionization of carbon etrachloride was studied over tantalum, tungsten and platinum filaments.

The variation of electronic and ionic currents, with temperature, at constant pressure was studied. Several experiments were carried out until reproducible results were obtained.

No trial was made to select certain pressure throughout the whole experiments, the only criteria was to work at any pressure below 5×10^{-5} torr and make sure that this pressure remained constant throughout the run. This was achieved by fine adjustment of the needle valve of the sampling system.

It was always made sure that there was enough time, after the sample gas (CCl_4) was admitted in the instrument, to attain equilibrium over the filament surface, this was achieved by frequent checks on the electronic and ionic currents, this time was varied from one hour to several hours without noticeable effect on the results obtained.

The formation of Cl^- ions from CCl_4 has been examined (two peaks were recorded corresponding to Cl^{35} and Cl^{37}). No other ions were found in the mass spectrum over the temperature range studied which was between 1600 and 2000°K, although Cl_2^- and CCl_3^- have been reported[126].

Figure (5.17) shows the variation of ionic and electronic current with temperature (heating current), it is a smooth function of temperature.

Figure (5.18) shows a mass scan of CCl_4 in the negative mode, it could be seen that the ionic current is constant at constant temperature and pressure.

Zandberg and Paleev[126] indicated that when the ratio of the electron (j_e) to ion (j_i) current is not a function of temperature then the process is not surface ionization, the ions do not originate from the filament surface but are formed from a gas phase process.

A plot of j_e/j_i against T is shown in Figure (5.19) it clearly indicates that Cl^- ions are produced by surface ionization.

Then by plotting log j_e/j_i against 1/T Figure (5.20) the apparent electron affinity was found to be 27 K cal mol^{-1}, which agrees very well with the difference between the electron affinity of chlorine (84 K cal mol^{-1}) and the bond energy (68 K cal mol^{-1}).

This result indicates that a valid estimate of the electron affinity of an observed species may be determined from the temperature coefficient of the ratio of the electron to total ion current in the magnetron provided that the mechanism of the ion formation is known.

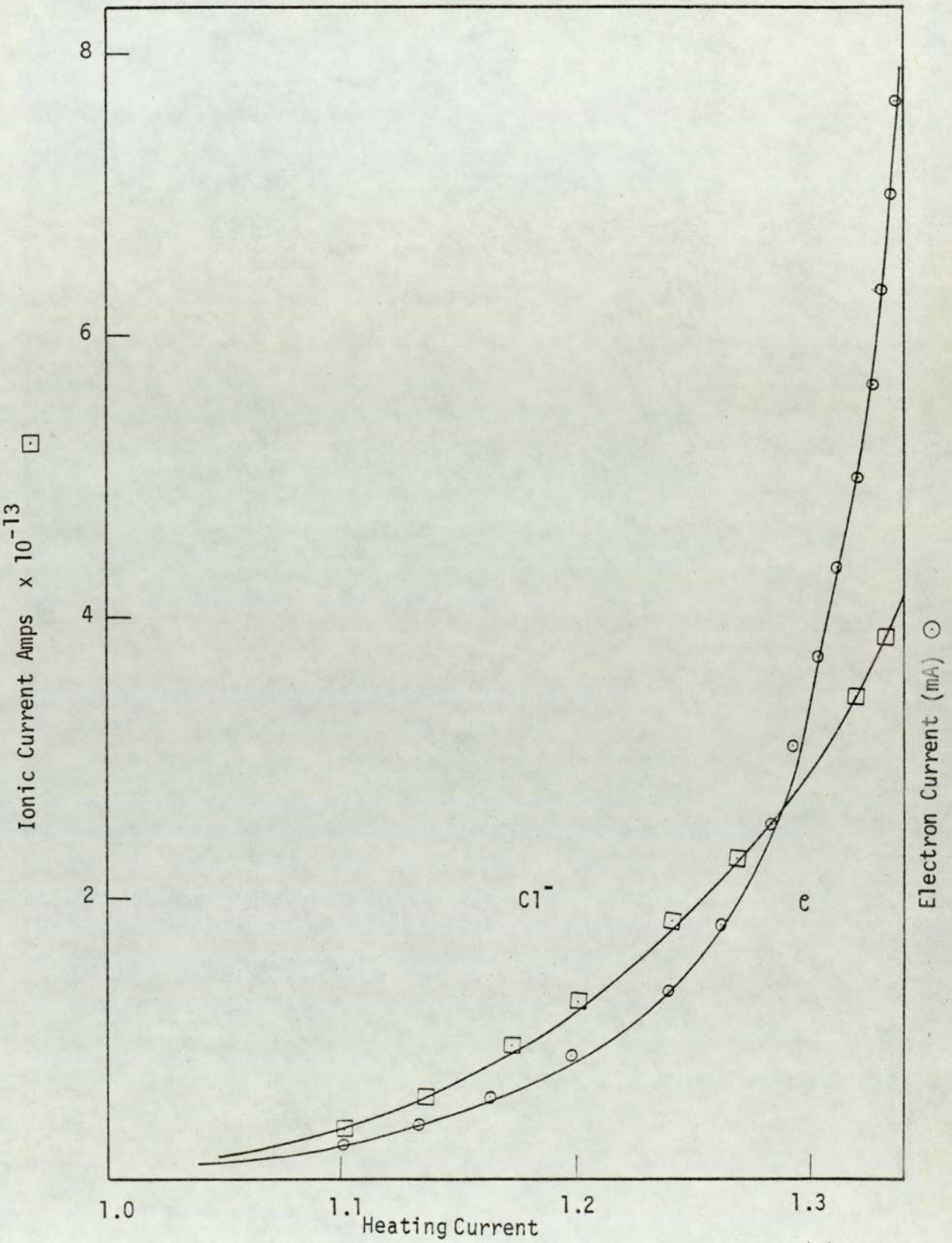

Figure (5.17) The variation of ionic and electronic current with temperature (heating current)

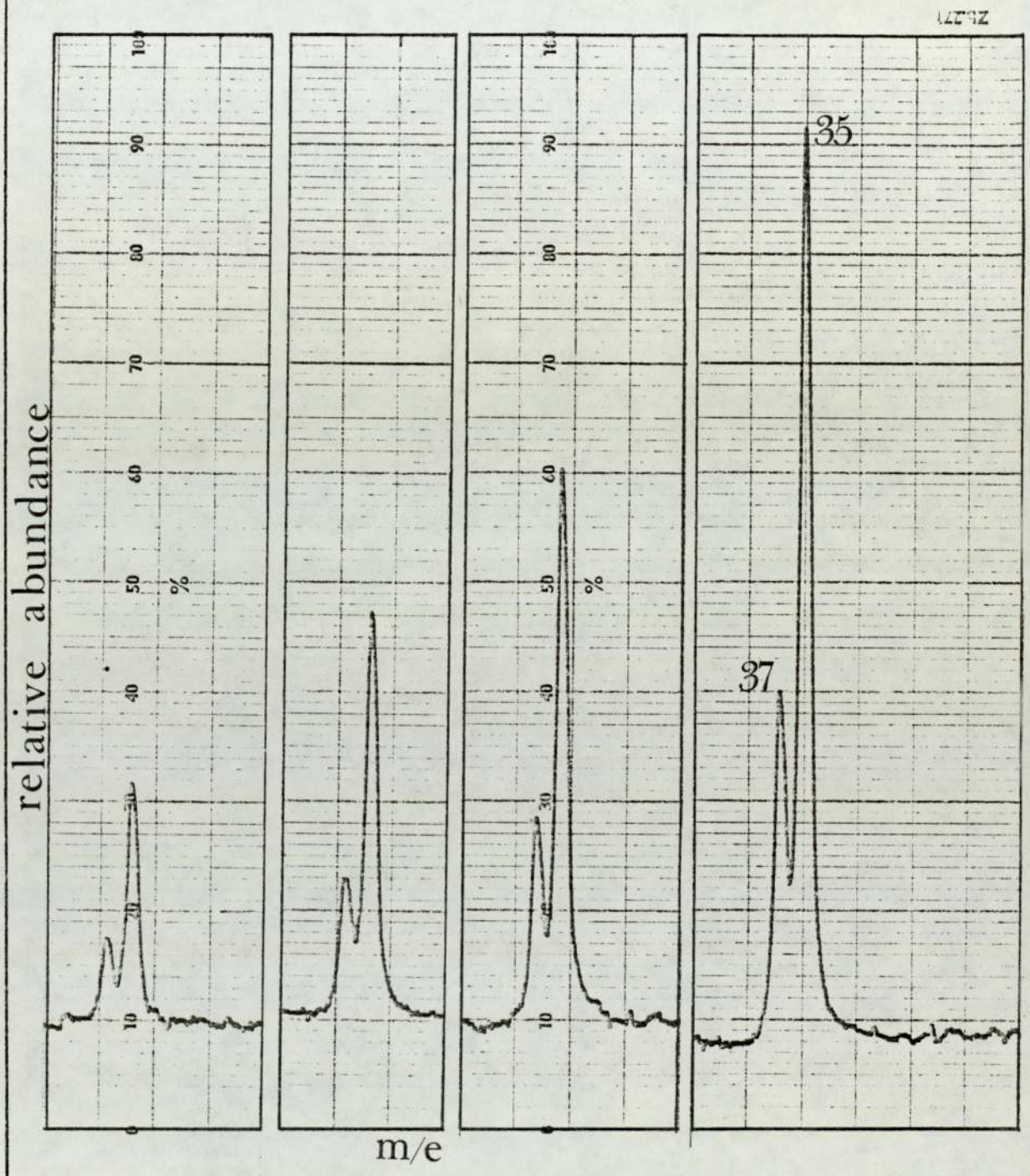

Figure (5.18a) Variation of Ionic current with temperature (Cl^-)

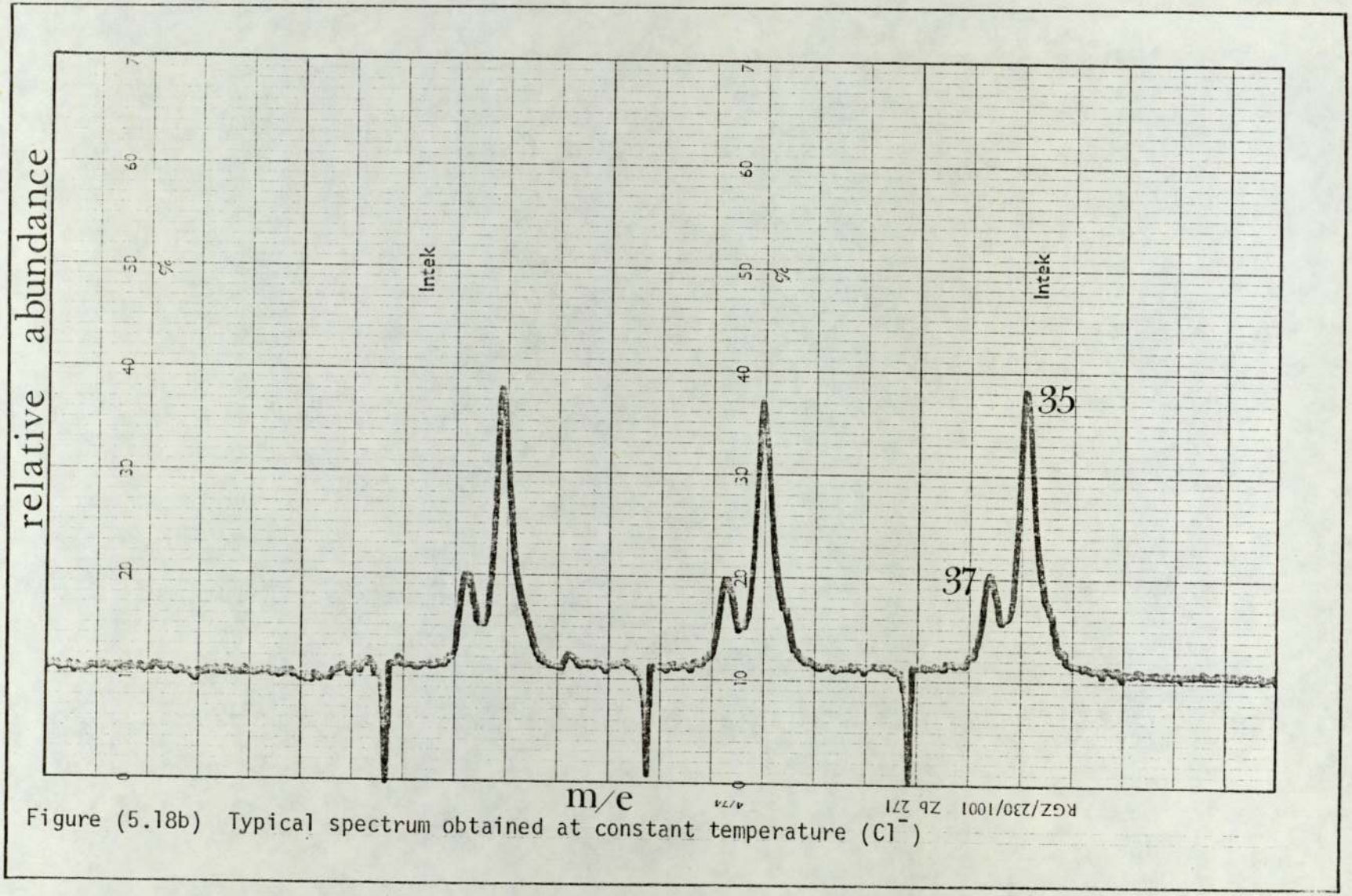

Figure (5.18b) Typical spectrum obtained at constant temperature (Cl^-)

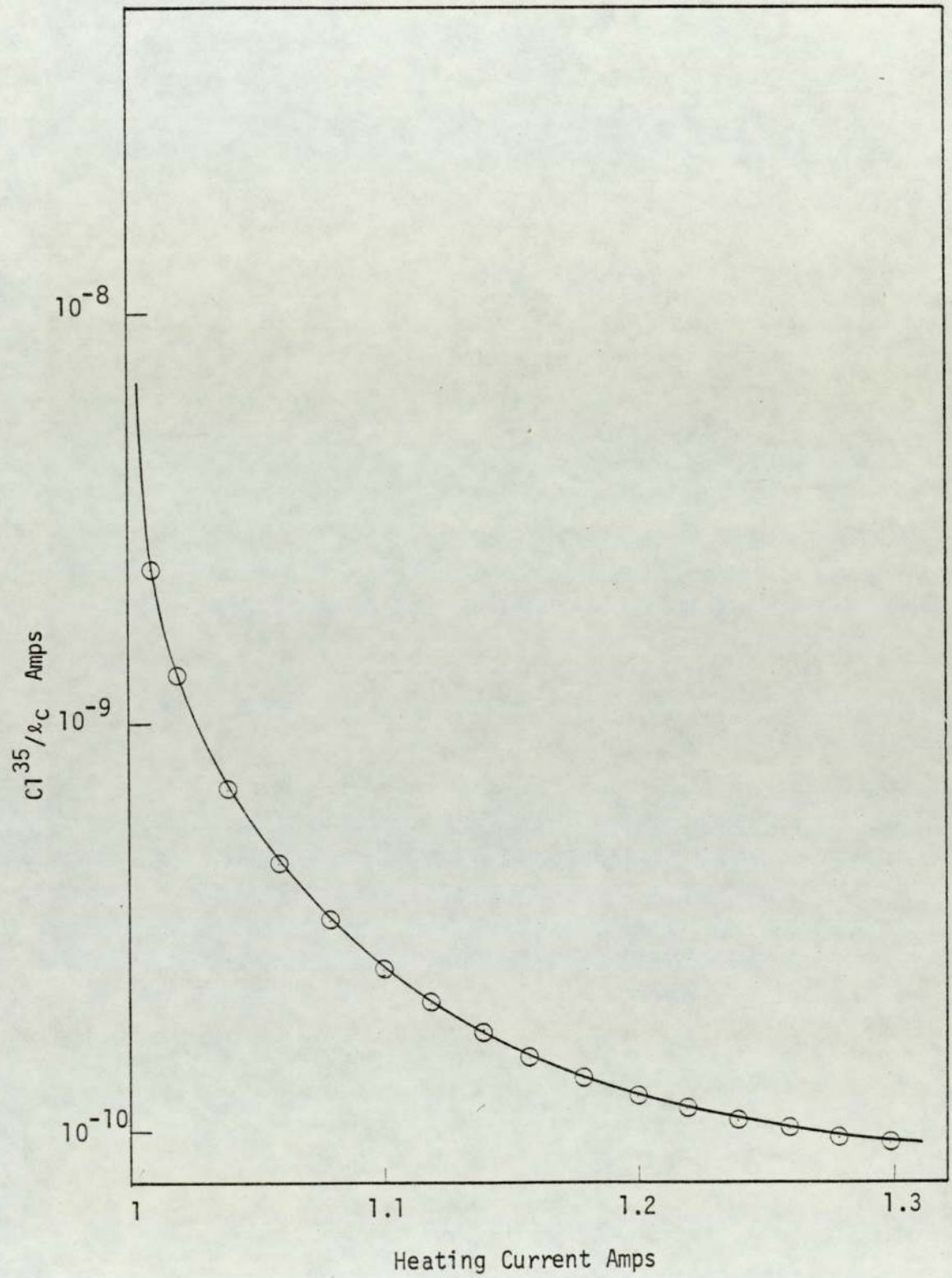

Figure (5.19) Ionic Current/Electronic Current against Heating Current

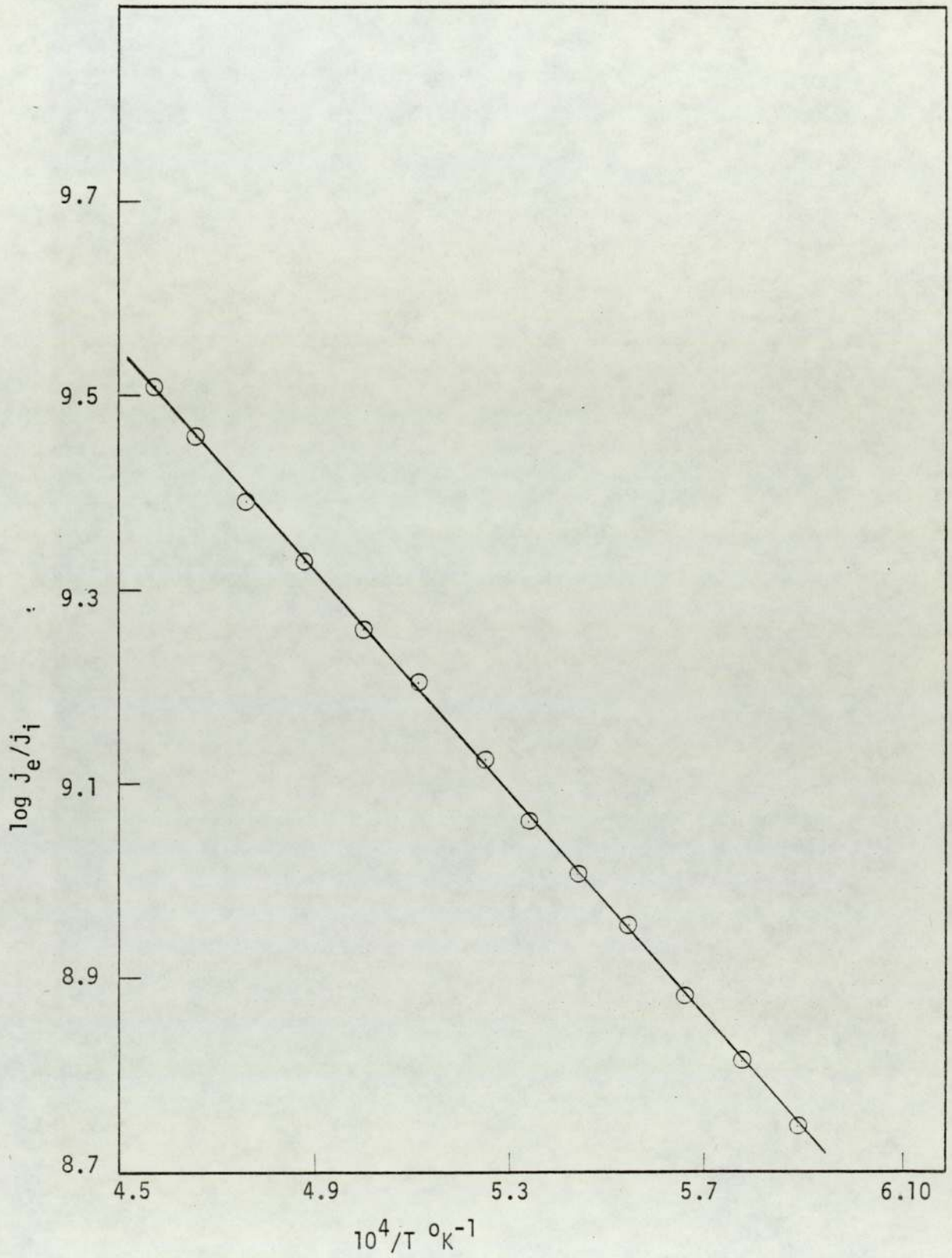

Figure (5.20) log j_e/j_i against 1/T for Cl^-

5.8.3 Sulphur Hexafluoride

Sulphur hexafluoride is of considerable importance as a gaseous dielectric.

Knowledge of the electron affinity of SF_6 is important in the understanding of the electron attachment properties of SF_6 and the thermodynamic properties of SF_6^-.

Kay and Page[164] reported a direct measurement of the electron affinity of SF_6 with the result electron affinity = 1.49 ± 0.2 eV.

Hammond[165] analysed the charge-transfer bands of solutions containing SF_6 and deduced a value of 0.61 eV for the E.A of SF_6.

Chen et al[166] studied the temperature dependence of the rate of electron attachment to SF_6 and deduced that the electron affinity of SF_6 must be greater than $\sim$ 0.7 eV.

Feh senfeld[167] used the observation that thermal energy O_2^- ions charge transfer to SF_6 and that SF_6^- charge transfers to atomic oxygen to establish a lower and upper limit to the electron affinity of SF_6 i.e.

$$0.43 < EA\ (SF_6) < 1.46 \text{ eV}$$

Because of the above mentioned controversy it was decided to study sulphur hexafluoride by surface ionization method.

It was very easy to obtain negative ions in the negative ion mode spectrum.

Ions identified as SF_6^-, SF_5^-, SF_4^-, SF_2^-, F^- were obtained.

Zandberg and Paleev[126] criterion (i.e. the ions formed in the gas phase should have a zero or very low temperature coefficient) was applied to the ions observed Figure (5.21). It is

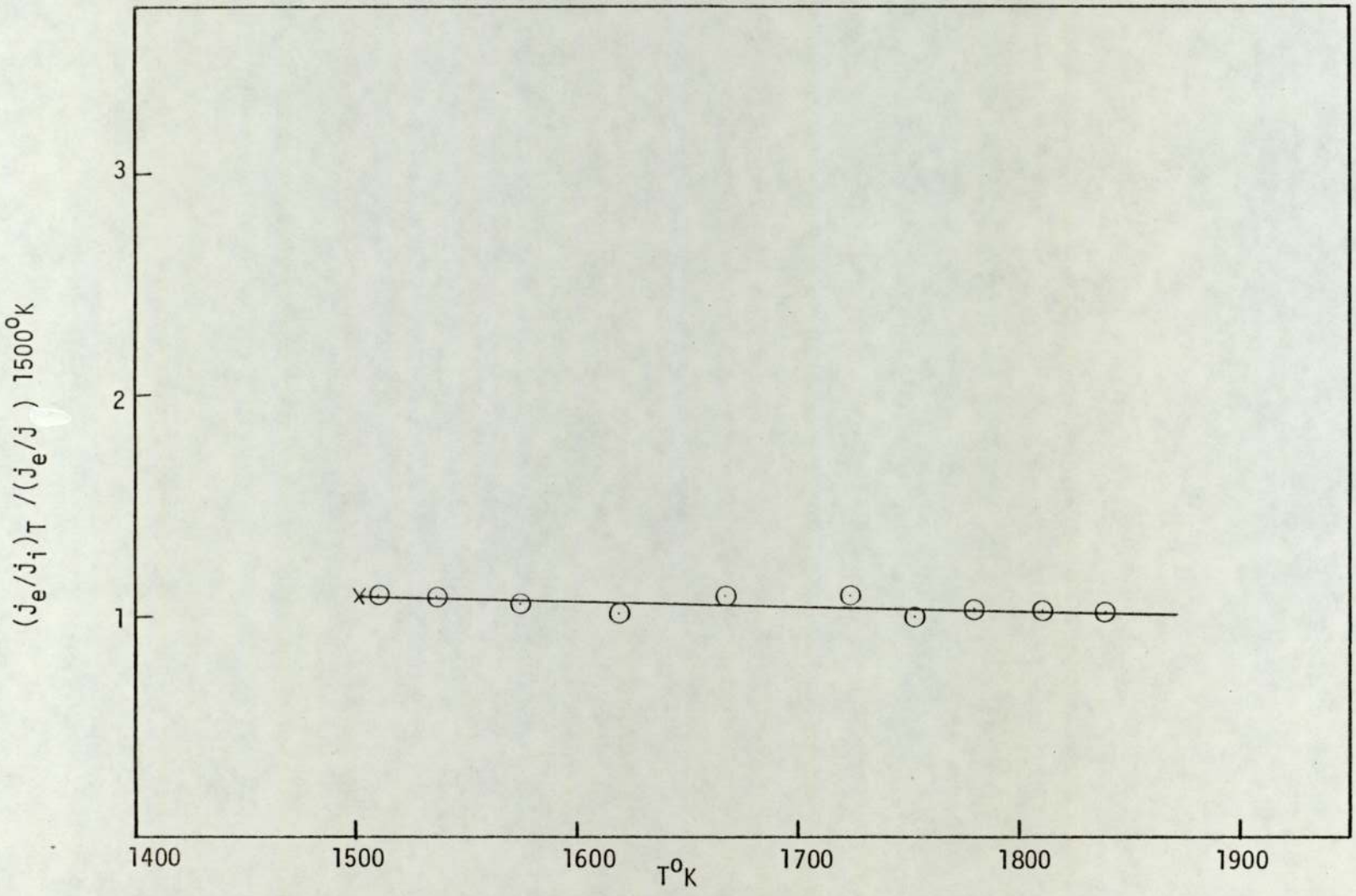

Figure (5.21) Ratio j_e/j_- = f(T) for ionization of SF_6

clear that these ions are not formed by surface ionization.

5.8.4 Uranium Hexafluoride UF_6

The sample was obtained from the British Nuclear Fuels Limited.

The UF_6^- ions observed were believed to have been formed by surface ionization.

Figure (5.22) shows that the ratio of the electronic current j_e to j_i (UF_6^-) is temperature dependent i.e. true surface ionization.

A typical graph of log j_e/j_- against 1/T is shown in Figure (5.23).

The apparent electron affinity obtained is 4.7 eV which is in good agreement with the most recent[168] value of 5.1 eV.

Difficulties due to decomposition of UF_6 on the ionization source were encountered and a green deposit presumably UF_4 was formed on the filament mounts. The work done to gain more information about volatile uranium compounds, especially UF_6, was enhanced by the increasingly technological importance of such compounds and that very little is known about them in ionized gases.

Recently Beauchamp[169] presented a study of endothermic reactions of UF_6^- ions (generated by surface ionization) with various gases.

From the threshold for the reaction

$$UF_6^- + BF_3 \rightarrow BF_4^- + UF_5 \qquad \ldots (5.8)$$

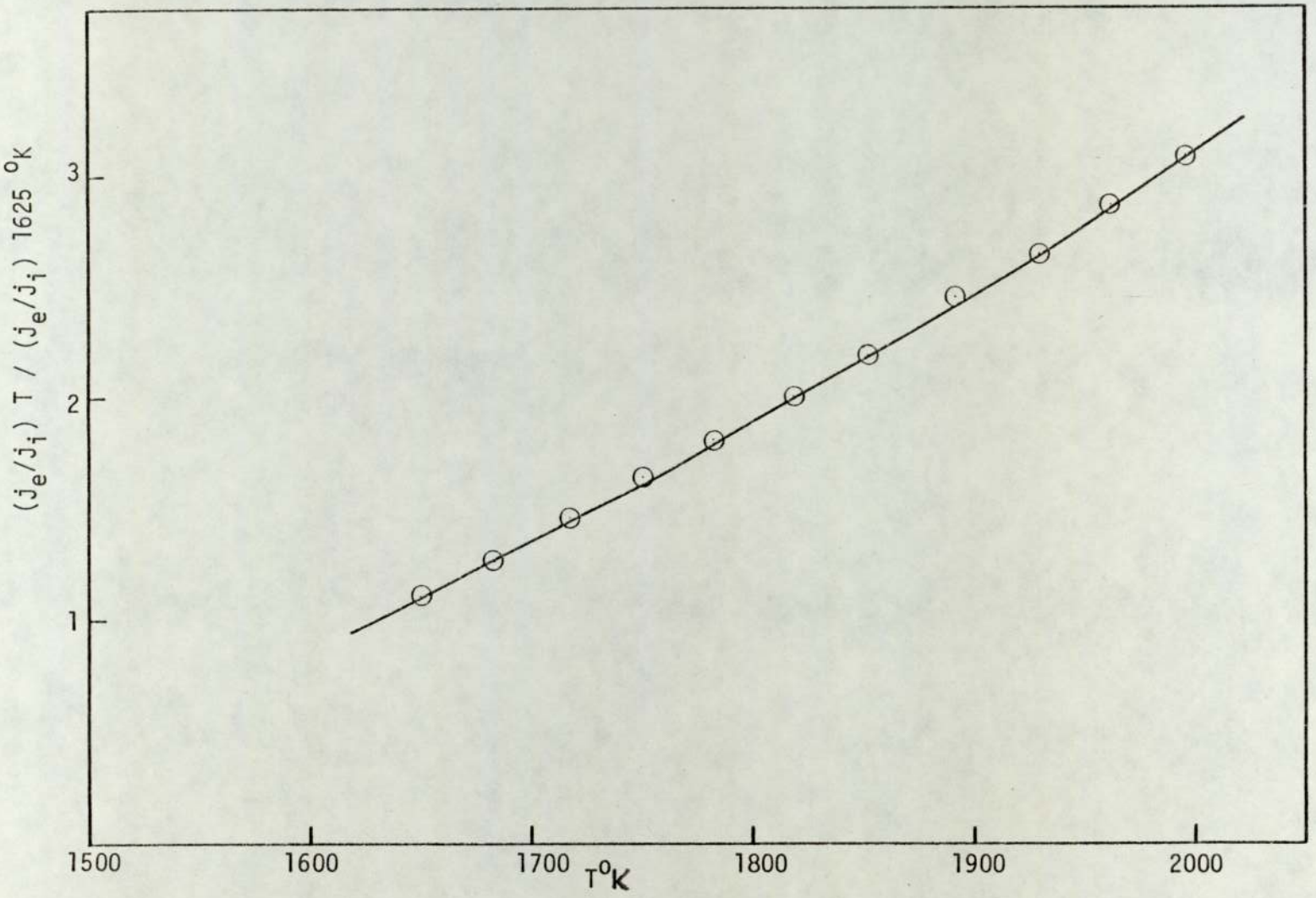

Figure (5.22) Ratio j_e/j_i = f (T) for ionization of UF

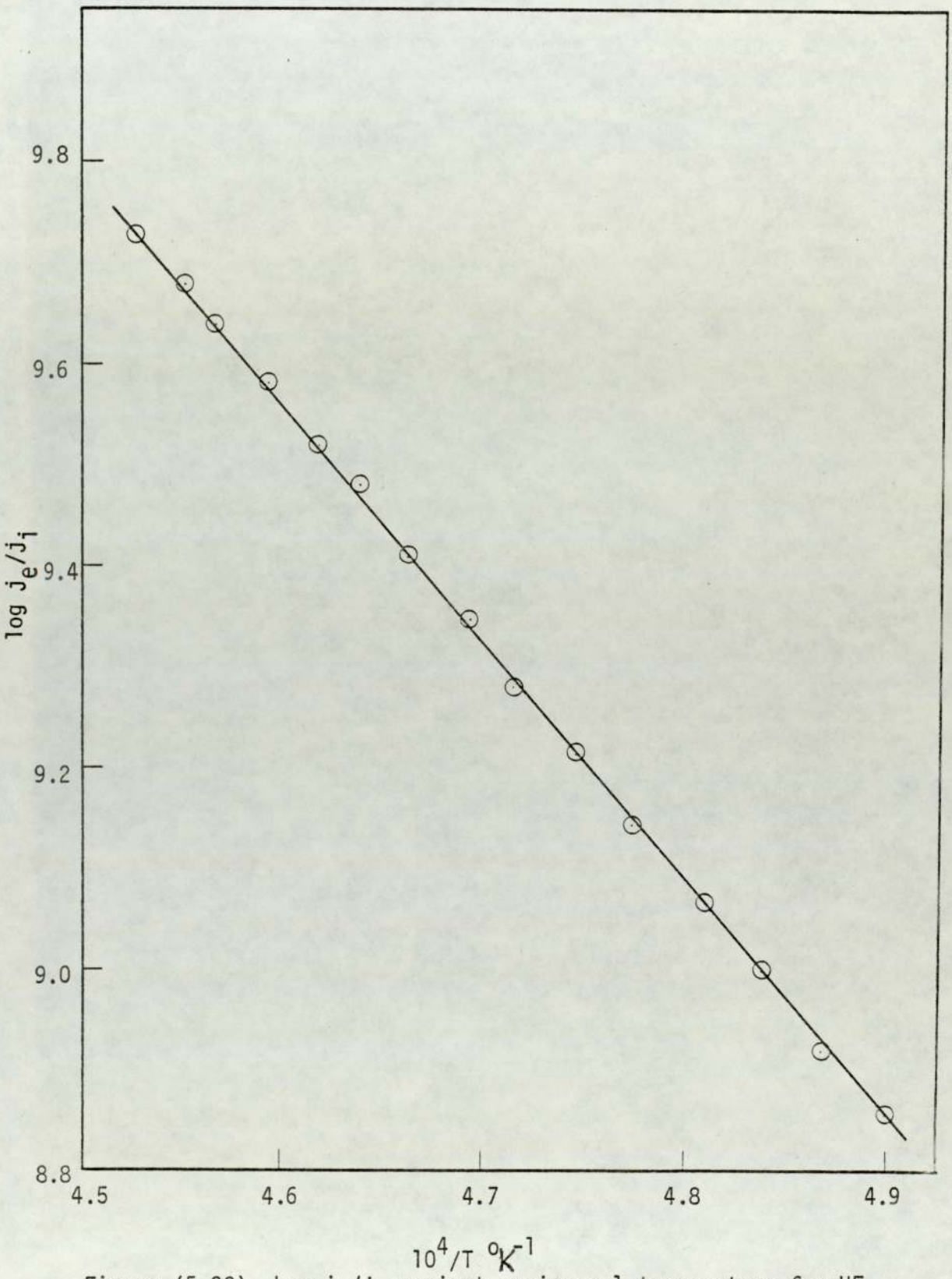

Figure (5.23) Log j_e/j_i against reciprocal temperature for UF_6

a value for the electron affinity of UF_6 was deduced to be 4.9 ± 0.5 eV.

5.8.5 Molybdenum Hexafluoride MoF_6

A high value for an electron affinity of MoF_6 has been reported[170], it was 4.1 eV.

A sample of MoF_6 (obtained from Glasgow University) was used to study surface ionization of MoF_6 over Ta and W filaments.

This study was hampered by the many difficulties encountered by the blue deposits over the ionization source (which turned to greenish blue with yellow spots upon exposure to air) which were very difficult to remove. It was accompanied by a high electronic current (up to 9.8 mA).

The MoF_6 fragmentation products were believed to react with the oil of the diffusion pump, this was noticed by the high pressure (5×10^{-5}) after these experiments while the needle valve was off.

5.8.6 Dimethyl Mercury $Hg(CH_3)_2$

The electron affinity of CH_3 has been reported to be 1.08 eV by the magnetron method.

Page[4] studied the surface ionization of several substrates in connection with electron affinity determination. Among those studied by the magnetron technique was lead tetramethyl, lead tetraethyl and dimethyl mercury. Several experiments aimed at detecting any CH_3^- ions originating from surface ionization were unsuccessful. It was believed that either the CH_3^- negative

ion current was below the detection limit of the amplifier or that the CH_3^- is not produced at all. An up to date literature survey supports the second assumption.

5.8.7 Benzene

Gaines and Page[171] studied benzene, benzil, dibenzyl, toluene, azobenzene, mercury diphenyl, and mercury di-p-tolyl by the magnetron technique in order to determine the electron affinities of the phenyl and benzyl radicals.

The behaviour of benzil and benzene showed that the electron affinity of the phenyl radical is 50.9 K cal mol^{-1} at 0^oK.

The above estimate of the electron affinity of the phenyl radical was based on energetic grounds only, and no positive identification of the phenyl negative ion was achieved.

Several workers since then have studied the negative surface ionization of benzene, by other methods; specifically by mass spectrometry[126,127].

The phenyl negative ion predicted by the magnetron technique, was not shown by mass spectrometry. While studying benzene over tungsten and platinum filaments Herron et al[136] observed the following ions only C_2^-, C_2H^- and CN^- (the latter was ascribed to surface impurities).

Zandberg and Paleev[126] studied benzene over tungsten and graphite (C) filaments (between 2200 - 2400 ^oK on the tungsten filament and $\sim$ 1800^oK on graphite), at a pressure of 1×10^{-5} torr, the only ions they observed were C_2^-, C_2H^-.

Quite recently Joyce[173] studied surface ionization by the magnetron technique and by mass spectrometry. In the case of the magnetron method the apparent electron affinity obtained

(and attributed to the phenyl radical) was 143 Kcal mol^{-1}.

He concluded that the non-zero gradient of the plot of the electron to ion current ratio against the reciprocal of filament temperature shows that the ions formed arise from the surface of the filament rather than as the result of subsidiary processes in the gas phase.

The mass spectr of benzene in the negative mode obtained by Joyce is shown in Figure (5.24).

The surface ionization of benzene was studied over Ta and W filiaments, Several attempts to obtain a negative ion mass spectrum at pressure of about 5×10^{-5} torr failed (though high temperatures were reached).

A trial made at higher pressure, (Figure (5.25)) gave negative ion mass spectrum, this spectrum was accompanied by a high electronic current.

The spectrum indicates clearly that no phenyl ions are present and the only ions observed were at m/e = 24, 25, 49 73 (very small peak). The base peak was at m/e 25 ($HC\equiv C^-$).

The variation of C_2^- and C_2H^- ions currents with temperature was tried, but lots of difficulties encountered inhibited this trial, because the filaments at this high temperature and pressure breaks easily, and the maximum drawing potential applied to the various parts of the ionization source was not enough to overcome space-charge effects. All the above mentioned work indicates clearly the difficulties encountered with the deduction of the reaction type occurring at the filament of the magnetron.

In those cases where the negative ions predicted by the magnetron technique are not observed, it should not be assumed

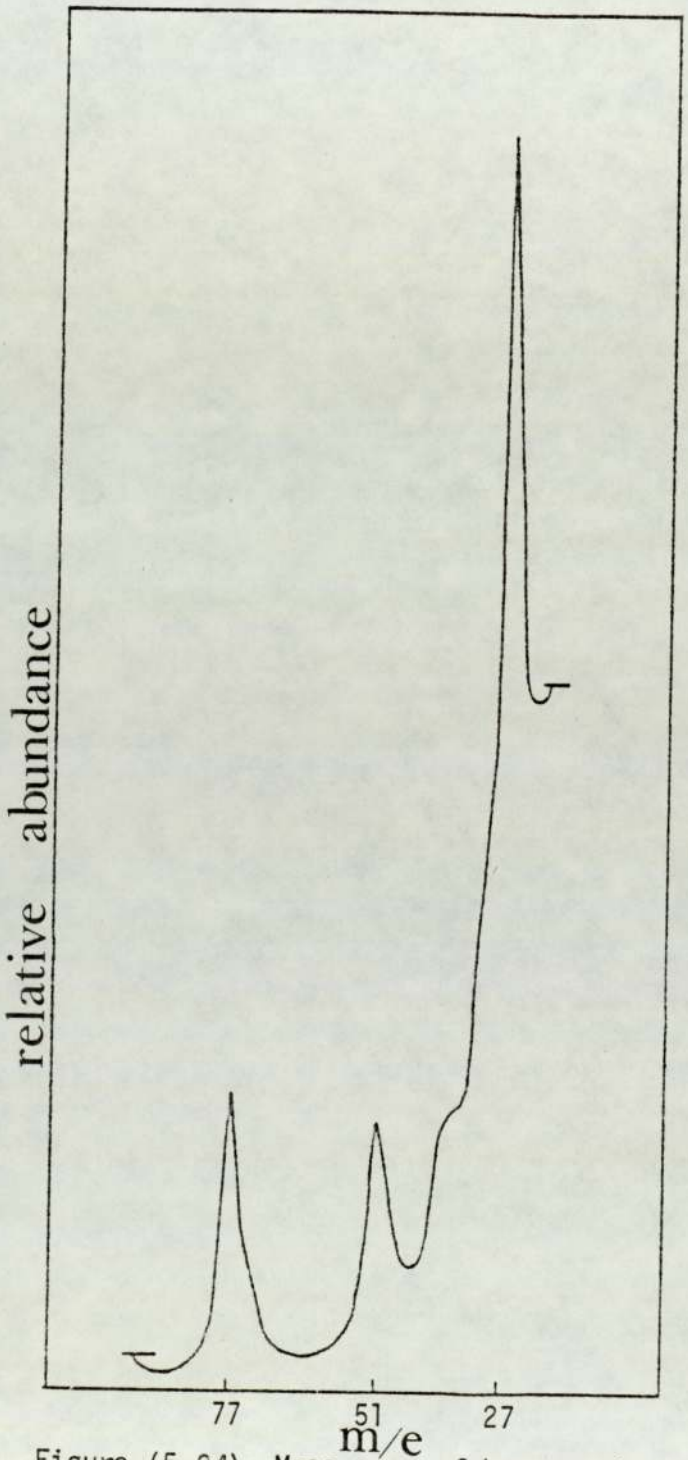

Figure (5.24) Mass scan of benzene in negative ion mode obtained by Joyce.[173]

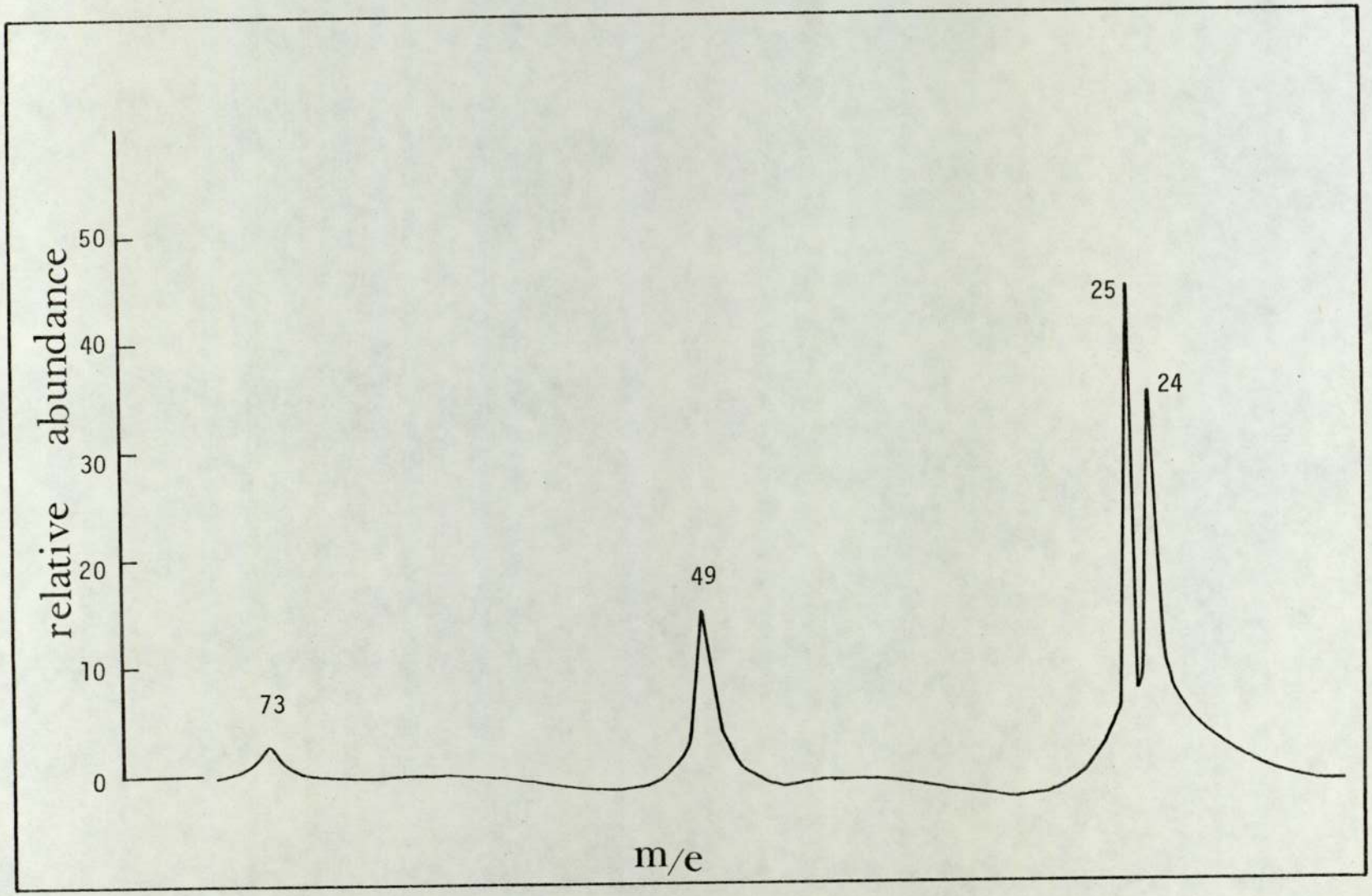

Figure (5.25) Negative surface ionization of benzene at 1.8 x 10^{-4} torr.

that the magnetron method is invalid. The possibility that the magnetron measurements refer to metastable negative ions must not be overlooked. If the negative ion which is first formed, and whose energetics are determined in the magnetron, is a metastable, in that it changes to another negative ion before it is detected, the observed energy will depend on the primary ion, but the mass spectrometer will record only the secondary negative ion; metastable ions are abundant in the negative ion spectra of organometallic[174] and organic compounds[175,176,177].

The negative ion mass spectra of alkylbenzenes substituted benzene, aliphatic acids, esters, nitriles, and ketones have been measured[172]. The spectra were compared with their positive ion counterparts and with other work on negative ion mass spectrometry.

In their study of benzene, toluene, ethylbenzene, n-propylbenzene, o-xylene, and p-xylene, they noticed that the very large fragmentation observed in the negative ion mass spectra with their base peak at m/e 25 ($HC{\equiv}C^-$) was in marked contrast to their positive ion counterparts where the base peak was either the molecular ion or the tropylium ion $C_7H_7^+$ m/e 91.

This difference is readily understood as the production of a negative molecular ion from benzene requires the insertion of an electron into a non bonding orbital, the introduced instability being released by extensive fragmentation. They attributed the most intense peaks (m/e 25, 49, 75, and 79) in the spectra to a series of acetylide anions C_nH^- (n = 2,4,6 and 8). The remaining peaks (m/e 24, 36, 48, 60, 72, 84 and 96) were due to C_n^- (n = 1 to 8) and showed a maximum for even values of n.

Aplin et al[172] results were analogous to those reported[178]

for the negative ion mass spectra of aliphatic hydrocarbons. The very weak M - 1 peak was in contrast with the observations of Ardene who reported both M - 1 and M - 3 peaks for a number of condensed aromatic systems.

It is clear from Figure (5.24) obtained by Joyce[173] that the shift in the base line before and after the measurement is more than the intensity of ions observed which casts some doubts on the reliability of these measurements. The m/e 77 and m/e 51 peaks are suspected as positive ions (or more correctly the difference between negative and positive ion current). The work of Aplin et al[172] supports this (see Figure 5.26)

5.9 General Discussion

The original model of the magnetron assumed that equilibrium was reached at, or very near, the ionising surface. Hotop et al and Hotop and Lineberger[34] said that the recent photodetachment results casts some doubt on the validity of even a relative determination of an electron affinity in surface ionization experiments.

Hotop questioned whether the condition of thermal equilibrium a key assumption for surface ionization, was fulfilled, especially when beams of atoms or complex vapour impinge on heated metal surface and interact with the atoms of the surface for an average time which is difficult to estimate. Zandberg et al[127] answered this criticism by a careful examination of the assumptions and experimental technique of the absolute method of surface ionization for re-determining the electron affinity of iodine, silver and gold.

Their findings led them to conclude that systematic errors

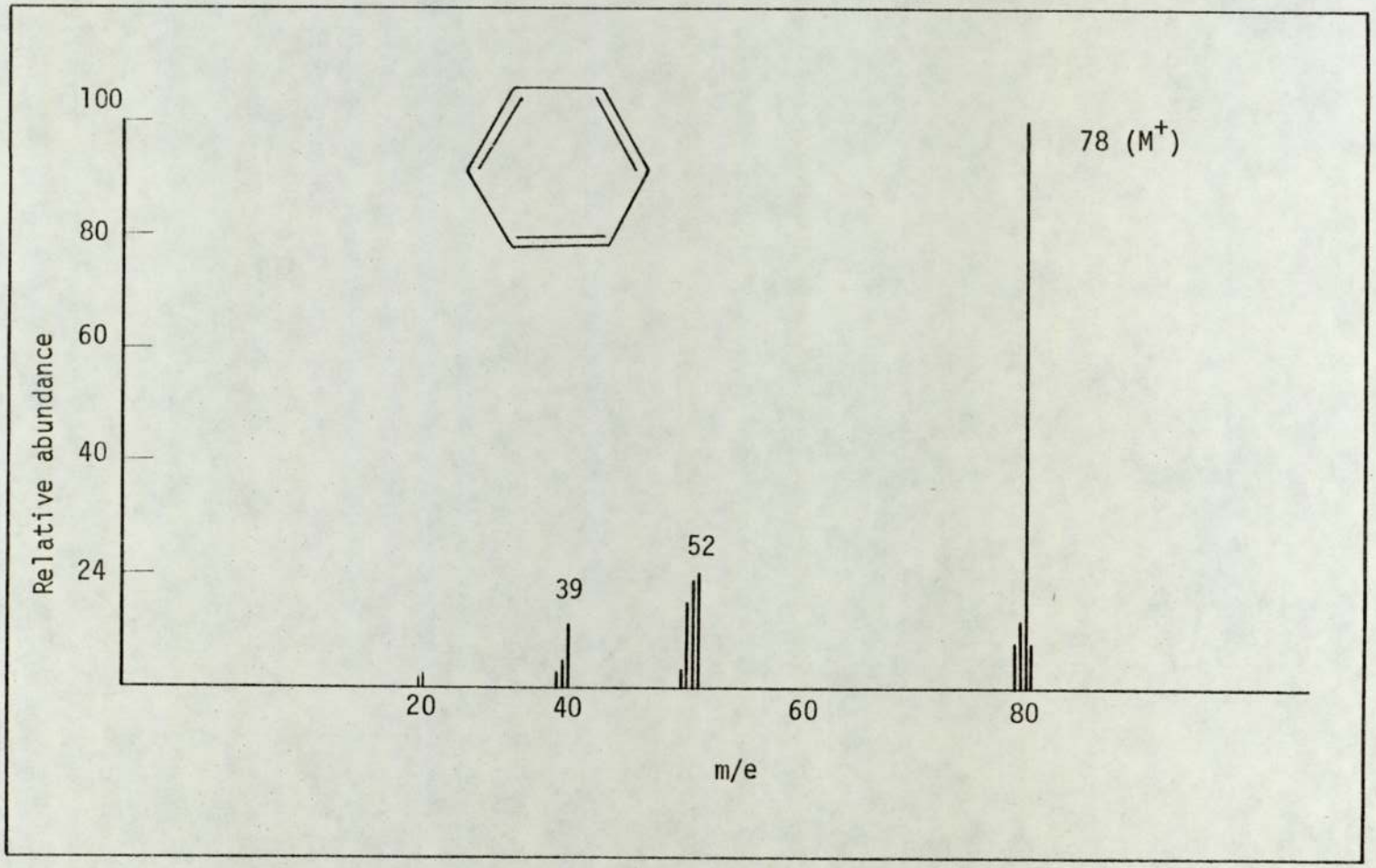

Figure (5.26) Positive ion mass spectr. of benzene

due to use of polycrystalline emitters and the assumptions of the method, do not exceed a few hundredths of a volt.

Page and co-workers[4] have extensively developed the magnetron technique. Page extended the original model of the magnetron to take account of some chemical reactions including the adsorption of molecular fragments on the surface, an extension which could be justified in the examples studied, but which offered too easy an explanation in less straightforward cases.

Herron et al[136] demonstrated that in many cases, the ions detected in a mass spectrometer bore little relation to those postulated as carrying the current.

Zandberg and Paleev[126] have shown that negative ions may also be produced in surface ionization experiments by secondary processes such as dissociative electron capture. Criteria of surface ionization such as, a Maxwellian spread of the ion energies and a non-zero slope of the plot of $\ln j_e/j_- T^2 = f(1/T)$, need to be applied as a check on the source of the ions.

They claimed that many complex organic molecules in surface ionization form mass spectra of negative ions due to bombardment of adsorbed films by positive ions, and that the energy distributions are not homogenous.

This criteria was applied to ions observed in this study before the electron affinities of these ions were determined.

The experimental electron affinities obtained in this work were in good agreement with literature values.

Chamberlain[158] argued that the results of the magnetron are valid provided the pressure of the gas is below 10^{-4} torr. In this work all the results obtained were under pressure of less than 5×10^{-5} torr.

The divergence of the precise measurements of electron affinity by spectroscopic means and the chemical results typified by those obtained by surface ionization in the magnetron has been examined by Page[179].

He questioned not the reliability but the relevance of the "vertical affinities" based on photodetachment. He pointed out that chemical reactions involving negative ions relax into detachment in a slow process during which major molecular re-organisation occurs.

The divergence between the two sets of values increases with complexity of the species examined, there being little disagreement when the ions are monoatomic.

5.10 Conclusion

The mass spectrometer was used to test the magnetron technique (Page kinetic approach) for determining electron affinity. All results obtained were consistent, and in agreement with the literature values, provided the criteria of surface ionization is applied. Thus, a valid estimate of the electron affinity of an observed species may be determined from the temperature coefficient of the ratio of the electron to total ion current in the magnetron provided the mechanism of the rate determining process is known.

REFERENCES

1. Glasstone, "Text Book of Physical Chemistry", MacMillan, London (1948)
2. Moeller, "Inorganic Chemistry", Wiley, New York (1957)
3. Field and Franklin, "Electron Impact Phenomena", Academic Press, New York (1957)
4. Page F. M. and Goode G. C., "Negative Ions and the Magnetron", Wiley, London (1969)
5. Massey, H. S. W, "Negative Ions", Cambridge University Press, London and New York (1950
6. Berkowitz J., Chupka, W. A. and Gutman D., J. Chem. Phys., 55, (2733) (1971)
7. Lovelock J. E., Zlatkis A. and Becker R. S., Nature, 193, (540) (1962)
8. Mullikan R. S., J. Chem. Phys., 3, (573) (1935)
   2, (782) (1934)
9. Christophorou L. G., "Atomic and Molecular Radiation Physics", Wiley, London (1971)
10. Briegleb G., Agnew Chem. Internat. Edit, 3,(617) (1964)
11. Lange, E. Z., Electrochem, 56, (94) (1952)
12. Hedges, R. M. and Masten F. A., J. Chem. Phys., 28, (1220) (1958)
13. Reported in New Scientists, July 1973 63(908)
14. Born, M. Ber. Deut. Phys., Ges, 21, (13) (1919)
15. Born M and Mayer, J. E. Z Physik, 75, (37) (1932)
16. Steiner B., Seman M. L and Branscomb L. M., J. Chem. Phys., 37, (1200) (1962)

17. Berry R. S and Reiman C. W., J. Chem. Phys., 38, (1540) (1963)

18. Cubicciotti D. J., Chem. Phys., 31, (1646) (1959)
33, (1579) (1960)
34, (2189) (1961)

19. Pekeries C. L., Phys. Rev., 126, (147) 1962)

20. Clemnti E and McLean, A. D., Phys. Rev., 133, (419) (1964)

21. Clemnti E., McLean A. D., Raimond D. L and Yoshimine M., Phys. Rev., 133, (1274) (1964)

22. Weiss A. W., Phys. Rev., A3 (126 (1971)

23. Weiss A. W., Phys. Rev., 166, (70) 1968)

24. Sinanoglu O. and Oksuz I, Phys. Rev. etter, 21, (507)(1968)

25. Oksuz I and Sinanoglu O., Phys. Rev., 181, (54)(1964)

26. Shaeefer H. F., Klem R. A and Harris F. E., J. Chem. Phys., 51, (4643) (1969)

27. Shaeefer H. F and Harris F. E., Phys. Rev., 170, (108) (1968)

28. Cade P. E., Proc. Phys., Soc., (London), 91,(842) (1967)

29. Cade P. E., J. Chem. Phys., 74,(2390) (1967)

30. Glockler G., Phys. Rev., 46, (111) (1934)

31. Johnson H. R and Rohrlich F., J. Chem. Phys., 30, (1608)(1959)

32. Edlen B, J. Chem. Phys., 33, (98) (1960)

33. Kaufman M, Astro. Phys. J., 147, (1290) (1963)

34a. Hotop H, Bennet R. A and Lineberger W. C, J. Chem. Phys., 58, (2373) (1973)

34b. Hotop H and Lineberger W. C., J. Chem. Phys., 58, (2379)(1973)

35. Branscomb L. M and Smith S. J, J. Chem. Phys., 25, (598)(1956)

36. Lineberger W. C and Woodward B. W, Phys. Rev. letters, 25, (424) (1967)

37. Kuyatt C. E and Simpson J., Arol, Rev., Sci., Instr., 38, (103) (1967)

38. Wigner E. P., Phys., Rev., 73,(1002) (1948)

39. O'Malley T. F, Phys. Rev., A 137, (1668) (1965)

40. Geltman S., Phys. Rev., 112, (176) (1958)

41. Berry R. S., Chem. Rev., 69, (53) (1969)

42. Berry R. S., MacKie J. C., Taylor R. L and Lynch R., J. Chem. Phys., 43, (3087) (1965)

43. Smyth K. C and Brauman J. I., J. Chem. Phys. 56,(1132) (1965)
56,(4620) (1965)
56,(5993) (1965)

44. Elder F. A and Inghram M. G., J. Chem. Phys., 43, (758)(1965)

45. McCulloh K and Walker J. H., Chem. Phys. Letters, 25, (439) (1974)

46. Compton R. N, Reinhardt P. W and Cooper C. D, J. Chem. Phys. 63, (383)(1975)

47. Baede A. P. M. "Charge Transfer Between Neutrals at Hyper Thermal Energies", in Lawley K P (ed) Advanced Chem. Phys. Vol XXX, Wiley, London (1975)

48. Chupka W. A, Kerkowitz J and Gutman D., J. Chem. Phys. 55, (2724) (1971)

49. Hoijtink G. J and Schooten J., Rec. Trav. Chim. 71,(1089) (1952)

50. Briegleb G, Angew Chem., 76, (362) 1964)

51. Clelland B. J., Chem. Rev., 64, (301) (1964)

52. Mulliken R. S and Person W. B., "Molecular Complexes", Wiley, New York (1968)

53. Briegleb G, "Electron-Donator - Acceptor - Komplexes" Springer - Verlag, Berlin (1961)

54. Szwarz M, "Progress in Physical Organic Chemistry, 6, Interscience Publ., New York (1968)

55. Jaguar G. J, Feld S. L and Szwarz M., J. Phys. Chem., 69, (628) (1965)

56. Cederbaum L. S and Schonhammer K, Phys. Rev. 15, (833)(1977)

57. Patterson T. A., Hotop H, Kasdon A, Norcross D. W and Linenberger W. C., Phys. Rev. Letters, 32, (189) (1974)

58. Kasdan A and W. C Lineberger, Phys. Rev., 10, (1658) (1974)

59. Hotop H, Patterson T. A and Lineberger J. Chem. Phys., 60, (1800) (1974)

60. Kingdon K. H and Langmuir I, Phys. Rev., 21, (380)(1923)

61. Saha M. N., Phil. Mag. 46, (534) (1923)

62. Ionov N. I, "Surface Ionization and its Application", progress in Surface Science, 1, Davison, Pergamon Press, Oxford (1972)

63. Sutton P.P and Mayer J. E., J. Chem. Phys., 2,(145) (1934)

64. Page F. M, Trans. Faraday Soc., 56, (1742) (1960)

65. Dukel'Skii V. M and Ionov N. I, Zh. Eksp. Teoret. Fiz, 10, (1248) (1940)

66. Hendricks J. O, Phipps T. E and Copley M. J, J. Chem. Phys., 5, (868) (1937)

67. Johnson A. A and Phipps T. E, J. Chem. Phys., 7, (1039)(1939)

68. Ionov N. I, Zh. Eksp. Teoret. Fiz, 18,(174) (1948)

69. Bakulina I. N and Ionov N. I, Dokl. Akad. Nauk, USSR, 116, (41) (1957)

70. Bailey T. L, J. Chem. Phys., 28, (792) (1958)

71. Zandberg E. Ya, Kamenev A. G and Paleev V.I, Sov. Phys. Tech. Phys. 16, (1567) 1972.

72. Sutton P. P. and Mayer J. E., J. Chem. Phys. 3,(20) (1935)

73. Khvostenko, V. I and Kukel'skii V. M, Sov. Phys., JETP, 37, (465) (1960)

74. Scheer M. D and Fine J. J, J. Chem. Phys., 50, (4343) (1969)

75. Bakulina I. N and Ionov N. I, Kokl Akad. Nauk, USSR, 105, (680) 1955

76. Bakulina I. N and Ionov N.I, Zh. Fiz. Khim, 38, (2063) (1959)

77. Ionov N. I, Zh. Exsp. Tearet Fiz, 18,(174) (1948)

78. Bakulina I. N and Ionov N. I, Zh. Fiz. Chim., 39, (157) (1965)

79. Bakulina I. N and Ionov N. I, Sov. Phys. Dokl., 9, (217) (1964)

80. Zandberg, E. Ya and Paleev V. I, Sov. Phys. Dokl, 15, (52) (1970)

81. Zandberg E. Ya, Kamenev A. G and Paleev V. I, Sov. Phys., Tech., Phys., 16, (832) (1971)

82. Fine J and Scheer M. D, J. Chem. Phys., 47, (4267) (1967)

83. Scheer M. D, J. Res. Nat. Bar. Std., 74A , (37) (1970)

84. Scheer M. D and Fine J., J. Chem. Phys., 46, (3998) (1967)

85. White F. A, "Mass Spectrometry in Science and Technology", Wiley, New York

86. Martinez, J. M and Majid A. H, J. Appl. Phys., 41, (5322) 1970

87. Paul M and Steinwedel H, J. Appl. Phys., 41, (5322) (1970)

88. Dawson P. H and Whetten N. R, Adv. Elect. Electron, Phys., 27, (59) (1969)

89. Preece, W. H, Proc. Roy. Soc. (London), 38, (219) (1885)

90. Richardson O. W, Proc. Cambridge Phil. Soc., 11, (289) (1902)

91. Wison H. A, Rev. Mol. Phys., 3, (156) (1931)

92. Saha M. N, Phil. Mag., 40, (472) (1920)

93. Kingdon K. H, Phys. Rev., 24, (510) (1924)

94. Scheer M. D and Fine J., J. Chem. Phys., 38, (307) (1963)

95. Moore G. E and Allison H. W, J. Chem. Phys., 23, (1609) (1955)

96. Heyne W. H and Tompkins F. C, Proc. Roy. Soc., London, A293, (19) (1966)

97. Siddigi M. M and Tompkins F. C., Proc. Roy. Soc., London A268, (452) (1962)

98. Kaminsky M, "Atomic and Ionic Impact Phenomena on Metal Surfaces", Springer, Berlin (1955)

99. Oatley C. W, Proc.Roy.Soc.,London, 155, (218) 1936.

100. Gysae B and Wagner S. Z. Phys., 115, (296) (1940)

101. Reiman A. L., "Thermionic Emission", Chapman, London (1934)

102. Becker J. A, "Advances in Catalysis", 7, Academic Press, New York, (1955)

103. Richardson O. W, "The Emission of Electricity from Hot Bodies", Longmans, London (1921)

104. Suhrmann R and Sachtler W. M, Proc. Intern. Symp. Reactivity of Solids , Gothenberg (1952)

105. Gomer R, "Field Emission and Field Ionization", Harvard Univ. Press, Cambridge, Mass. (1961)

106. Mignolet J. C. P, Discussion Faraday Society, 8, (326) (1950)

107. Delchar T. A, Eberhagen A and Tompkins F. C, J. Sci. Instr., 40, (105) (1963)

108. Miller E. R, Ph.D Dissertation, Univ. of Aston in Birmingham (1969)

109. Zandberg E. Ya and Ionov N. I,"Surface Ionization", Izd Nauka Moscow (1969)

110. Farragher A. L, Ph. D, Dissertation, Univ. of Aston in Birmingham, (1966)

111. Vier D. T and Mayer J. E., J. Chem. Phys., 12, (28) (1944)

112. Metlay M and Kimball G. E, J. Chem. Phys., 16, (774)(1948)

113. Page F. M, Trans. Faraday Soc., 57, (359) (1961)

114. Farragher A. L, Page F. M and Wheeler R. C, Discussion, Faraday Soc., 37, (203) (1964)

115. Farragher A. L and Page F. M., Trans., Faraday Soc., 62, (3072) (1966)

116. Ansdell D. A and Page F. M., Trans. Faraday Soc., 58, (1084) (1962)

117. Gaines A. F, Kay J and Page F. M, Trans. Faraday Soc., 62, (874) (1966)

118. McCallum K. Y and Mayer J. E, J. Chem. Physc., 11, (56) (1943)

119. Mitchell J. J and Mayer J. E, J. Chem. Phys., 8, (282) (1940)

120. Glockler G and Calvin M, J. Chem. Phys., 4, (496) (1936)

121. Doty P. M and Mayer J. E, J. Chem. Phys., 12, (323) (1944)

122. Glockler G and Calvin M., J. Chem., Phys., 3, (771) (1935)

123. Ritchie B and Wheeler R. C, J. Phys. Chem., 70, (113)(1966)

124. Glasstone S, Laidler K. J and Eyring H, "The Theory of the Rate Processes", Wiley, London (1960)

125. Goode G. C., Ph. D Dissertation, The Univ. of Aston in Birmingham (1969)

126. Zandberg E. Ya and Paleev V. I, Sov. Phys. Tech. Phys., 17, (665) (1972)

127. Zandberg E. Ya, Kamenev A. G and Paleev V. I, Sov. Phys. Tech. Phys., 19, (385) (1974)

128. Branscomb L. M, Seman N. L and Steiner B, J. Chem. Phys., 37, (1688) (1962)

129. Berry R. S, Reiman C. W and Spokes G. N, J. Chem. Phys., 37, (2278) (1962)

130. Beck A. J, Handbook of Vacuum Physics, 2, (2) (Thermionic Emission) Pergamon Press, Oxford (1966)

131. Ionov N. I, Sov. Phys., J.E.T.P, 18, (96) (1948)

132. Zandberg E. Ya, Ionov N. I, Paleev V. I and Tontegode A. Ya, Sov. Phys. Tech. Phys., 32, (503) (1962)

133. Shelton H, Phys. Rev., 107, (1553) (1957)

134. Ionov N. I and Katataev V. I, Sov. Phys., Tech. Phys., 32, (626) (1962)

135. Zazula Panol Wilhemsoon H., Arkiv. Fysik, 24, (511) (1963)

136. Herron J. T, Rosenstock H. M and Shields W. R, Nature, 206, (611) (1965)

137. Budzikiewicz H, Djerassi C and Williams D. H, "Interpretation of Mass Spectra of Organic Compounds", Holden-Day, Inc. San Francisco, Calif. (1964)

138. Budzikiewicz H. Djerassi C and Williams D H, "Structure Elucidation of Natural Products by Mass Spectrometry", 1, & 2, Holden - Day, Inc., San Francisco, Calif. (1964)

139. Biemann K, "Mass Spectrometry", McGraw-Hill Book Co. Inc., New York, (1962)

140. Melton C. E, "Mass Spectrometry of Organic Ions", Academic Press (1963)

141. Melton C. E, "Principles of Mass Spectrometry and Negative Ions", Marcel -Deckker, New York (1970)

142. Thynne J. C, MacNeil K. A and Caldwell K. J, "Time of Flight Mass Spectrometry", IA Pergammon Press, oxford (1969)

143. Wilson J, "Mass Spectrometry Specialist Reports", 1, Chemical Soc., London (1970)

144. Bowie J. H, Mass Spectrometry Specialist Reports, 2, Chemical Soc., London (1970)

145. Dillard J. G, Chem. Rev, 73, (589)(1973)

146. Bowie J. H and Hant S. G, Int. J. Mass Spectrom, Ion Phys., 13, (319) (1970)

147. Thynne J. C, MacNeil K. A and Caldwell K. J, "Time of Flight Mass Spectrometry", Pergamon, London (1970)

148. Von Ardene M, Z. Angew Phys., 11, (121) (1959)

149. Futrell J. H., "Dynamic Mass Spectrometry, 2, Heyden, London (1971)

150. MacDonald C. G and Shannon J. S, Aust. J. Chem., 19, (1545) (1966)

151. Bowie J. H and Williams B. D, "Mass Spectrometry Specialist Reports", 3, Chem. Soc., London (1977)

152. Kaminsky M, "Atomic and Ionic Impact Phenomena on Metal Surfaces", Springer - verlag Berlin

153. Riviere J. C, "Solid State Surface Sciences, Marcel-Dekker, New York (1969)

154. Robinson W. N,"Physical Principles of Ultra High Vacuum and Equipment", Chapman and Hall, New York (1968)

155. Fomenko V. S, "Handbook of Thermionic Properties", Plenum Press Data Divison, New York (1966)

156. Gaines A. F and Page F. M., Trans. Faraday Soc., 59, (1266) (1963)

157. Hensley E. B, J. Appl. Phys., 32, (301) (1961)

158. Chamberlain A. T, Ph. D Dissertation, The Univ. of Aston in Birmingham (1974)

159. Crowe and Devins, Ann. Rep. Conf. Elect. Insulation, 1, (1955)

160. Works and Lindsay, Ann. Rep. Conf. Elect. Insulation, 5, (1955)

161. Qak Instruction Manual, V. G. Micromass (1976)

162. Morrison J. D, J. Chem. Phys., 33,(821) (1960)

163. Berry R. S and Reinmann G. W, J. Chem. Phys., 38, (1540) (1963)

164. Kay J and Page F. M. Trans. Faraday Soc., 60, (1042)(1964)

165. Hammond P. R, J. Chem. Phys., 55, (3468) (1971)

166. Chen E, George R. D and Wentworth W. E., J. Chem. Phys., 49, (1973) (1968)

167. Fehsenfeld F. C, J. Chem. Phys., 53, (2000) (1970)

168. Dittner P. F and Dats S, J. Chem. Phys., 68, (2451) (1978)

169. Beachamp J. L, J. Chem. Phys, 66, (352)(1977)

170. Compton R. N, J. Chem. Phys, 66, (4478) (1977)

171. Gaines A. F and Page F. M., Trans. Faraday Soc., 59,(1266) (1963)

172. Aplin R. T., Budziekiewcz H and Djerassi, J. Am. Chem. Soc., 87, (3180) (1965)

173. Joyce J. T, Ph. D Dissertation Macquarie Univ., Sydney (1977)

174. Kisar R. W, Sullivan R. E and Lupin M. S, Anal. Chem., 41, (1958) (1969)

175. Bowie J. H and Hart S. G, Int. J. Mass Spectrom. Ion. Phys. 13, (319) (1974)

176. Ho A. C, Bowie J. H and Fry A, J. Chem. Soc. B (530) (1971)

177. Bowie J. H, Org. Mass Spectrom, 5, (945) (1971)

178. Melton C. E and Rudolph P. S, J. Chem. Phys., 31, (1585) (1959)

179. Page F. M. Vacuum 24, (523)(1974)